Copyright Warning & Restrictions

The copyright law of the United States (Title 17, United States Code) governs the making of photocopies or other reproductions of copyrighted material.

Under certain conditions specified in the law, libraries and archives are authorized to furnish a photocopy or other reproduction. One of these specified conditions is that the photocopy or reproduction is not to be "used for any purpose other than private study, scholarship, or research." If a, user makes a request for, or later uses, a photocopy or reproduction for purposes in excess of "fair use" that user may be liable for copyright infringement,

This institution reserves the right to refuse to accept a copying order if, in its judgment, fulfillment of the order would involve violation of copyright law.

Please Note: The author retains the copyright while the New Jersey Institute of Technology reserves the right to distribute this thesis or dissertation

Printing note: If you do not wish to print this page, then select "Pages from: first page # to: last page #" on the print dialog screen

ABSTRACT

EXPERIMENTAL INVESTIGATION OF THE FLUID VELOCITY DISTRIBUTION IN STIRRED TANK REACTORS EQUIPPED WITH RETREAT-BLADE IMPELLERS USING LASER DOPPLER VELOCIMETRY

by
Deepak Rajesh Madhrani

Stirred tank reactors are commonly used in the pharmaceutical industry for synthesis of Active Pharmaceutical Ingredients (API's) and their intermediates. Typically, these vessels are glass-lined and are provided with a single retreat-blade glass-lined impeller and a single baffle. Despite their ubiquitous utilization in the pharmaceutical industry for at least the past 40 years, the mixing characteristics of these systems have not been studied to any great extent, making it difficult to predict mixing performance in any given operation.

In this work, the velocity distribution inside the typical glass-lined vessel/impeller system was experimentally quantified using Laser Doppler Velocimetry (LDV), which is a non-intrusive experimental method used to determine the local velocity distribution (including its fluctuating component) in a fluid placed inside any transparent piece of equipment. Two different reactor configurations were investigated, i.e., a flat-bottom tank and a hemispherical-bottom tank. In each case, two baffling configurations were studied, i.e., a partially baffled tank with a single beaver-tail baffle (the most common baffled configuration used in the pharmaceutical industry), and an unbaffled system. The three velocity components (tangential, axial, and radial) at 13 radial locations on 7 horizontal planes in case of flat-bottom and 5

Horizontal planes in case of hemispherical-bottom tank in the two baffling configurations mentioned above were experimentally determined by LDV.

In the unbaffled flat-bottom reactor case, the tangential component of the velocity appears to dominate over the other velocity components at nearly every location, with tangential velocity typically on the order of 40% to 50% of the impeller tip speed. The radial and axial velocities, especially in the region just below the impeller, were found to be very small, with magnitudes typically smaller than 15% for the axial component and 5% to 10% for the radial component. In general, the presence of a hemispherical bottom did not alter significantly the magnitude of the velocity components except in the lower portion of the tank, where the hemispherical bottom generated a stronger axial and radial recirculation pattern. The velocity distribution in the single-baffle case was found to be only partially different from the unbaffled case, and primarily in the upper portion of the tank, where the baffle is. The velocity distribution in the lower portion of these vessels was not significantly affected by the presence of the baffle.

In conclusion, the dominance of the tangential velocity and the small value of the radial and especially axial velocity in all the system investigated here indicate a poor vertical recirculation of the fluid inside the tank and poor mixing performance of these types of reactors.

EXPERIMENTAL INVESTIGATION OF THE FLUID VELOCITY DISTRIBUTION IN STIRRED TANK REACTORS EQUIPPED WITH RETREAT-BLADE IMPELLERS USING LASER DOPPLER VELOCIMETRY

by
Deepak Rajesh Madhrani

A Thesis
Submitted to the Faculty of
New Jersey Institute of Technology
in Partial Fulfillment of the Requirements for the Degree of
Master of Science in Pharmaceutical Engineering

Otto H. York Department of Chemical Engineering

May 2008

APPROVAL PAGE

EXPERIMENTAL INVESTIGATION OF THE FLUID VELOCITY DISTRIBUTION IN STIRRED TANK REACTORS EQUIPPED WITH RETREAT-BLADE IMPELLERS USING LASER DOPPLER VELOCIMETRY

Deepak Rajesh Madhrani

Dr. Piero M. Armenante, Thesis Advisor — Date
Distinguished Professor of Chemical Engineering, NJIT

Dr. Somenath Mitra, Committee Member — Date
Professor of Chemistry and Environmental Science, NJIT

Dr. Robert B. Barat, Committee Member — Date
Professor of Chemical Engineering, NJIT

BIOGRAPHICAL SKETCH

Author: Deepak Rajesh Madhrani

Degree: Master of Science

Date: May 2008

Undergraduate and Graduate Education:

- Master of Science in Pharmaceutical Engineering,
  New Jersey Institute of Technology, Newark, NJ, 2008

- Bachelor of Science in Chemical Engineering,
  University of Mumbai, Mumbai, India, 2006

Major: Pharmaceutical Engineering

To my beloved family and my late grandmother
"Smt. Padminidevi Assanand Madhrani"

ACKNOWLEDGMENT

I would like to express my deepest appreciation to Dr. Piero. M Armenante, for his continuous support and motivation during the tough times of my research, I wish this motivation towards research continues in future and new innovations in the fields of fluid dynamics arrive at his destiny. Special thanks are given to Dr. Robert B. Barat, Dr. Somenath Mitra for actively participating in my committee.

I would like to specially thank Giuseppe L. Di Benedetto for his continuous support throughout my research and for providing me the simulation data for comparison and to confirm my experimental results. I would also like to thank my other fellow graduate students in the mixing lab: Ankit H. Patel and Micaela Caramellino for their support and suggestions.

I cannot end without thanking my family especially my parents, on whose constant encouragement and love I have come at this stage. I dedicate this thesis to them.

TABLE OF CONTENTS

TABLE OF CONTENTS
(Continued)

LIST OF FIGURES

Figure **Page**

CHAPTER 1

INTRODUCTION

1.1 Background

Stirred tank reactors and vessels are often encountered in chemical and pharmaceutical manufacturing facilities where they are used for a variety of applications. In the pharmaceutical industry, these reactors are routinely employed to synthesize Active Pharmaceutical Ingredients (API's) and their intermediates. These types of reactor are very versatile, and there are many different operations that are performed in these vessels, ranging from mixing, to solid suspension, crystallization, precipitation, multi-phase chemical reactions and many others. Glass lined vessels are the most commonly used type of stirred tank reactors in the pharmaceutical industry, where they are routinely used for the production of small molecules, typically in a batch mode. Glass lining is used to ensure that the reactor can be employed for different types of reaction, and with different reagents and products. The inert glass coating serves to insure that the reaction products do not become contaminated with reaction by-products that could result from a chemical attack on the metal forming the vessel, especially when particularly aggressive reactant are used – a critical requirement for API manufacturing. In addition, glass lining also protects the reactor itself from corrosion. For this to be the case however, not just the reactor walls but also all the internals that could come in contact with the reacting species needs to be glass-lined. This may be appropriate from a chemical compatibility standpoint, but it is not necessarily optimal for the mechanical construction of the system and for the performance characteristics of the reactor, especially from the hydrodynamic

point of view. In fact, the use of glass lining equipment has historically forced the equipment manufacturers to compromise on the design of the impeller and baffling system, which is critical to the hydrodynamics of the system and the ability of the reactor to be an effective mixing device. As a result, glass-lined vessels are typically provided with a single, three-blade, retreat-blade, glass-lined impeller (originally marketed by Pfaudler, although different vendors now exist). Furthermore, glass-lined reactors typically do not have wall baffles, as most other non-glass lined reactors do. Instead, they are often provided with a single glass-lined baffle suspended from the reactor top lid. In addition the mechanical issues associated with a cantilevered baffle, such a baffle cannot be extended to the bottom of the vessel, and its limited size makes it somewhat inadequate to make the system "fully baffled", i.e., to prevent a strong tangential velocity from dominating the fluid flow in the reactor.

Despite their limitations, glass-lined, retreat-blade impeller systems remain the most common type of reactor configuration used. Even more surprising is that only limited information exists on the hydrodynamics of these systems, and that only recently some investigators have started looking at fluid dynamic characteristics of these systems. This information, still very incomplete and typically limited to systems that are not scale-down versions of the industrial reactor, can be found in some recently published work such as that of Campolo et. al. (2002), Dickey et al. (2004), Bakker et al., (2004), Li et al. (2004), Li et al. (2005), Ricard et al. (2005), and Reilly et al. (2007).

From an experimental perspective, one of the most useful tools that can be used to investigate the hydrodynamics of transparent system is Laser Doppler Velocimetry (LDV). LDV is a technique that fluid mechanics researchers have used for a number of

years to make instantaneous measurements of the magnitude and direction of the local velocity at locations inside in fluid flow systems. This technique is non-intrusive and measures the velocity components in all the three directions. With the aid of fiber optics, LDV probes can used to access almost any region inside a vessel.

LDV makes use of the coherent wave nature of laser light. The crossing of two laser beams of the same wavelength produces areas of constructive and destructive interference patterns. The interference pattern, known as a "fringe" pattern is composed of planar layers of high and low intensity light. Velocity measurements are made when particles "seeded" in the flow pass through the fringe pattern created by the intersection of a pair of laser beams. These particles scatter light in all directions when going through the beam crossing. This scattered light is then collected by a stationary detector (receiving optics connected to a photomultiplier). The frequency of the scattered light is Doppler shift and referred to as the Doppler frequency of the flow. This Doppler frequency is proportional to a component of the particles velocity which is perpendicular to the planar fringe pattern produced by the beam crossing. In order to obtain three components of velocity, three sets of fringe patterns need to be produced at the same region in space.

The main advantage of using an LDV technique is that it is non-intrusive and highly accurate since it uses very high frequency response. The major disadvantage of this technique is that sufficient transparency is required between the laser and the target surface, and that the instrument accuracy depends on the alignment of the emitted and reflected beams.

In this work, an LDV-based investigation was conducted to study the hydrodynamics of stirred tank vessels used for pharmaceutical manufacturing processes.

1.2 Objective of This Work

Given the importance of retreat-blade, stirred tank systems in the pharmaceutical industry, the paucity of information available for this kind of systems, and the industrial relevance of mixing and hydrodynamic effects in these systems, the current work is focused on the quantification of the velocity distribution in retreat-blade, glass-lined type, stirred-tank reactors.

Therefore, the objective of this work is to investigate the fluid dynamics of the stirred tank reactors equipped with the retreat blade impeller, with particular attention to the effect, of no-baffling vs. partial baffling conditions, and the type of tank bottom, i.e., flat vs. hemispherical. In this work, the effects of baffling and shape of the vessel bottom on the fluid dynamics in the stirred tank reactors were investigated keeping all other parameters constant throughout the experiments.

The quantification of the fluid dynamics characteristics of these stirred tank reactors is expected to contribute to improve our knowledge of these systems, which is especially important in scale-up, the determination of mixing characteristics of these systems, such as blend time, and the overall optimization of their mixing performance.

CHAPTER 2

EXPERIMENTAL APPARATUS AND METHOD

2.1 Mixing Tank and Agitation System

The model systems studied in this work were cylindrical tanks made of Pyrex glass and provided with either a flat-bottom or a hemispherical-bottom, as shown in Figures 2.1.1 and 2.1.2. The inside diameters of the flat-bottom tank and of the hemispherical-bottom tank were measured to be, respectively, 287mm and 300mm.

The agitation system consisted of a single three-blade, retreat-blade impeller. This is the type of impeller most commonly found in glass-lined reactors used in the pharmaceutical industry. The geometry of the impeller was based on the actual geometry of a full-scale impeller (manufactured by DeDietrich). In order to determine its exact geometry, the actual dimensions of this scaled-down impeller were measured with a caliper, and were found to be as follows: impeller diameter, 219.1 mm; radius of curvature of the blades, 92.08 mm; height of the blade, 25.4 mm; and thickness of the blade, 12.7 mm. The impeller was mounted at the end of a shaft having a diameter of 12.52mm and centrally located inside the tank. The impeller bottom clearance, measured from the bottom of the impeller to the lowest point in the tank (i.e., its center), was always 26.95mm.

The impeller was connected to a 1/4-HP motor (Chemglass, Model CG-2033-11) controlled by an external controller (Chemglass, Model CG-2033-31) which was used here to rotate at a constant agitation speed of 100 rpm. The corresponding impeller tip speed was 1.1 m/s and the impeller Reynolds number was 81,920. The motor-impeller

system was mounted on a bracket above the vessel so that the impeller was centered in the vessel.

Depending on the experiment, each tank was either used unbaffled or was provided with a single, vertical, Beaver-Tail baffle (resembling a profiled cylinder) shown in Figure 2.1.1. The dimensions of the baffle were as follows: diameter of the top section, 15.24mm; length of the top section, 70.64mm; diameter of the middle section, 22.23mm; length of the section, 199.7mm; diameter of the bottom section 20.07mm; length of the bottom section 70.64mm. When the baffle was in place, the baffle clearance off the bottom of tank, measured from the bottom of the baffle to the bottom of the tank at its central location, was 90.23mm. The baffle was placed vertically midway between the centrally mounted impeller shaft and the wall. This corresponded to a distance of 29.60 mm from the wall to the shaft axis for the flat-bottom tank, and 31.64mm for the hemispherical-bottom tank.

In all experiments, the tank was filled with water up to a height equal to the inside tank diameter, i.e., 287 mm in flat-bottom tank and 300mm for the hemispherical-bottom tank. In order to perform an experiment a given tank was placed in a rectangular tank filled with water, i.e., a fluid having a similar index of refraction as of the fluid being mixed in order to improve the optical quality (Figures 2.1.1, 2.1.2, and 2.1.3).

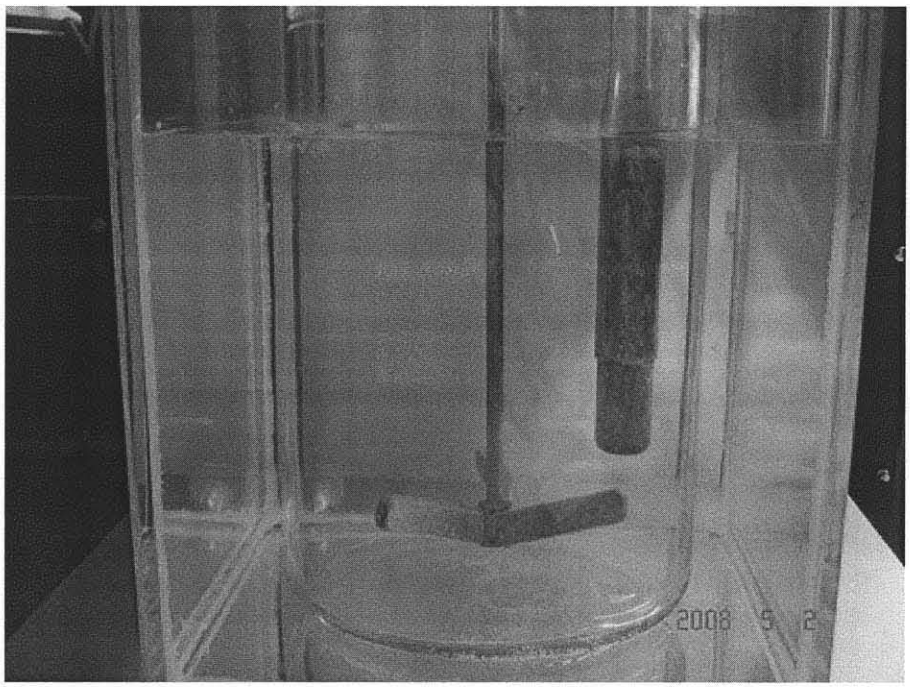

Figure 2.1.1 Cylindrical Flat-bottom Tank equipped with Beaver Tail Baffle and Retreat Blade Impeller.

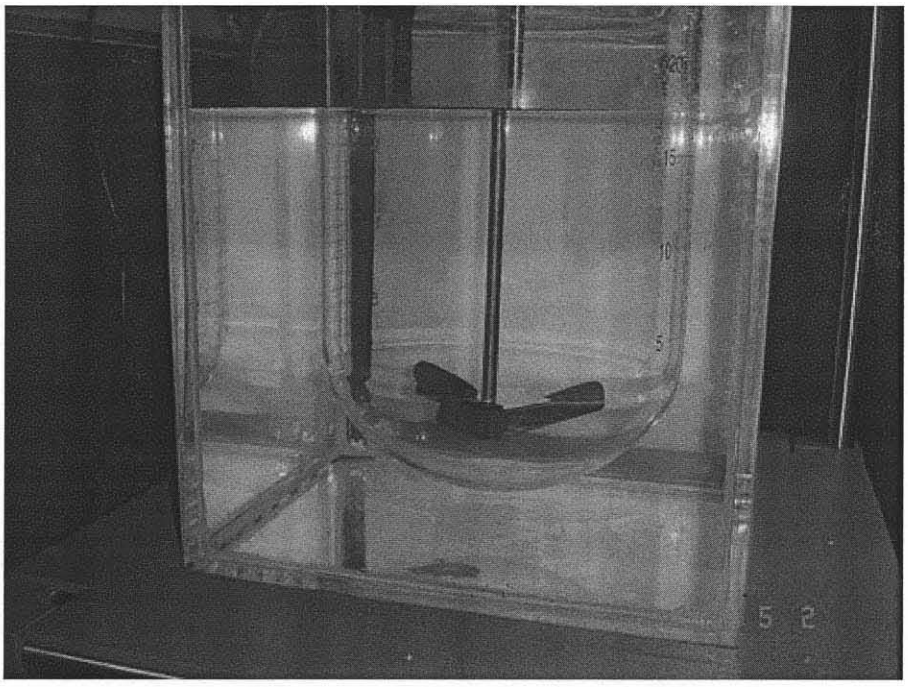

Figure 2.1.2 Cylindrical Hemispherical-bottom Tank equipped with Retreat Blade Impeller.

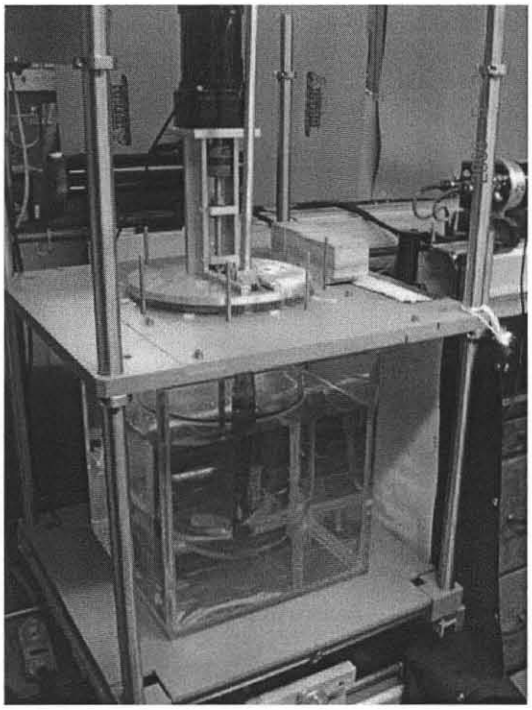

Figure 2.1.3 Motor-Impeller mounted on the Bracket and Traversing system

2.2 Materials Used

The fluid used in this study was always distilled water. In order to be able to perform LDV experiments the liquid in the tank was seeded with small, light-scattering particles that could accurately follow the liquid flow inside the tank. The seed particles were silver coated Glass hollow spheres (S-HGS-10; Dantec Dynamics A/S, Denmark) with mean particle size 10 microns and density 1.4 gm/cc. Because of there small size and density the particles could follow the fluid flow pattern closely.

2.3 Laser Doppler Velocimetry System and Data Acquisition

In this study, a Dantec 55X series LDV apparatus (Dantec Measurement Technology USA, Mahwah, NJ, USA) was used to determine the velocity flow field inside the vessel (Figure 3.1.4). The LDV system comprised a 750 mW argon-ion laser (Ion Laser Technology, Inc.) producing a single multicolored laser beam passing through an optical

filter to generate a monochromatic green beam (wavelength: 512 nm). The resulting beam passed through a beam splitter from which two beams emerged, one of which was passed through a Bragg cell to lower the frequency by 40 MHz and distinguish between positive and negative velocity measurements. The beams then passed through a fiber optic probe equipped with the beam expander system and a final focusing lens with a focal length of 330 mm. This lens made the beams converge so that they intersected each other to form a small control volume in the interrogation region where the velocity was to be measured. In an actual measurement, the beams were made to converge inside the stirred tank vessel. The motor-impeller-vessel assembly was mounted on an x-y-z traversing system that could position the vessel at any desired location in front of the LDV system, thus enabling the velocity to be measured anywhere in the vessel. The light backscattered by the particles was collected by a detector equipped inside the probe and was connected to the photo-multiplier (processor) system. The photo-multiplier system converts the signal and transfers the data to the data acquisition system. Data analysis was performed to generate the local velocity components in the direction parallel to that of the plane of the two laser beams. Appropriate rotation of the laser beam assembly and translation of the vessel-motor assembly yielded the velocity components in all three directions at any location. The time interval for each measurement was typically 60 seconds. In most cases, some 600 to 2500 instantaneous velocity data points were collected at any location and for the selected velocity component, from which the local average velocity could be calculated. The data rate obtained was about 20 to 100 Hz. Higher data rate were obtained in above the impeller region where higher particle densities were obtained.

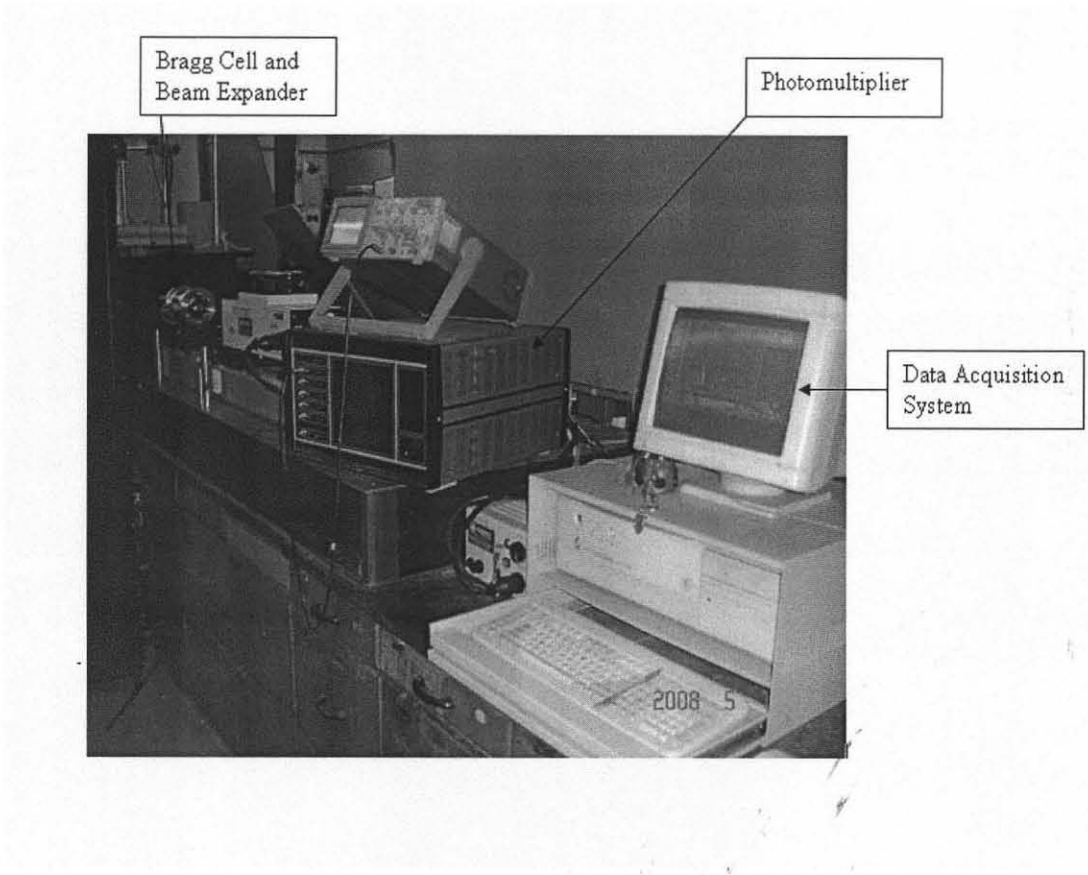

Figure 2.1.4 DANTEC 55X LDV SYSTEM

Iso-surfaces (i.e., horizontal planes intersection the tank) at different vertical (z) positions were selected along the height of the tank where LDV velocity measurements were made. Seven iso-surfaces were selected for the flat-bottom tank and five iso-surfaces were selected for the hemispherical-bottom tank. The iso-surface z=78mm (z/H=0.271) is the plane at which the top edge of the impeller blade lies. The iso-surface z=26mm (z/H0.090) is the plane just below the impeller. The iso-surfaces z=22mm (z/H=0.0766)) and z=24 (z/H=0.0836) are below the impeller, and those at z=96mm (z/H=0.33), z=147mm (z/H=0.49) and z=185mm (z//H=0.644) are above the impeller. For the flat-

bottom tank case, LDV measurements were made on each iso-surface at thirteen evenly spaced radial locations between the shaft and the vessel wall. For the hemispherical-bottom tank case, LDV measurements were made at fourteen evenly spaced radial locations above the impeller. Data were taken in triplicates at each data point, to minimize the error associated and check the reproducibility of the experiment. However because of the hemispherical shape of the vessel bottom and the presence of the impeller blades, fewer locations could be investigated below and at the impeller. At each measurement location, three velocity components (tangential, axial, and radial) were obtained by LDV.

CHAPTER 3

RESULTS

3.1 Velocity Profile for the Unbaffled, Flat-bottom Tank

A total of 13 velocity measurements, each one including all three velocity components, were obtained for the case of the unbaffled, cylindrical flat-bottom tank. All these results are presented in Appendix A.1 (Figures A.1.1.1- A.1.3.4). An example of the typical tangential velocities measured on the iso-surface at z/H=0.644 is shown in Figure 3.1.1. In general, the flow field in this type of tank is dominated by a high tangential velocity component, especially above the impeller. Figure 3.1.1 shows that the tangential velocity on this plane is typically 40 to 50% of the impeller tip speed and it extends for a significant portion the entire iso-surface. The magnitude of the tangential component of the velocity was found to be midways between the shaft and the wall which could be an ideal location for placing a baffle.

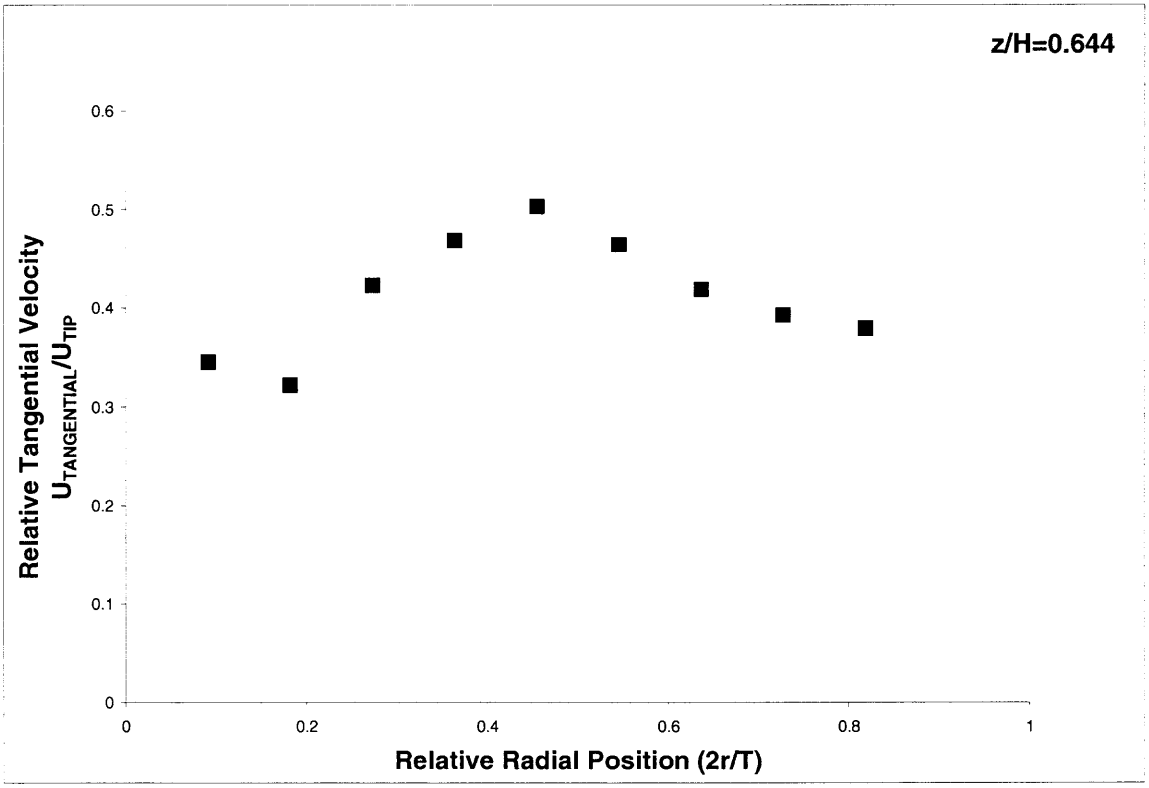

Figure 3.1.1 Experimental tangential velocity data at iso plane z=185mm in the unbaffled cylindrical flat-bottom tank.

By comparison, the axial and radial components of the fluid velocity, also presented in detail in Appendix A.1, were found to be very low. Example of the typical profiles for these velocity components are shown in Figure 3.1.2 and Figure 3.1.3, respectively (in all figures positive axial velocities point upward, and positive radial velocities point outwards, toward the wall). In most cases, the axial components were found to be in the range of 0-10% of the impeller tip speed. In the region above the impeller, the axial component of the velocity was found to be positive between the wall and impeller blade region. In the upper portion of the tank, higher axial velocities were observed near the shaft due to the presence of a vortex. Axial velocities between the center and the wall had higher negative magnitudes, indicating a downward movement of the fluid.

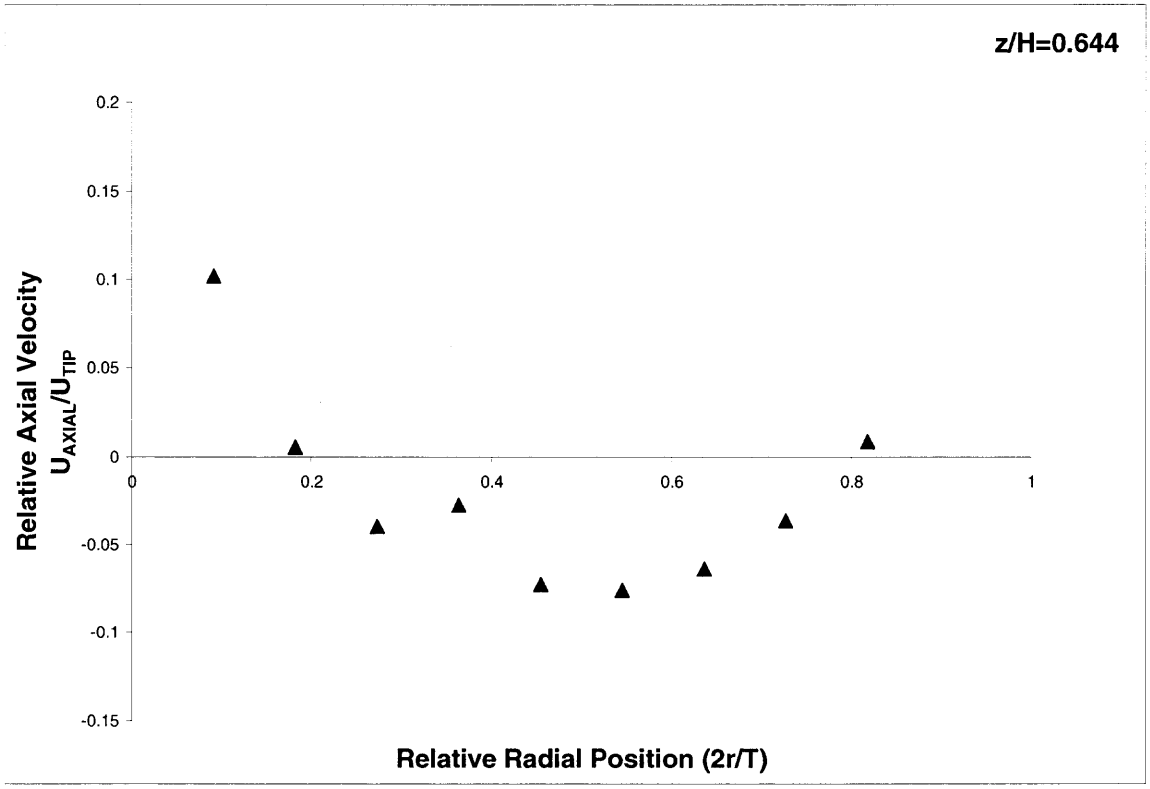

Figure 3.1.2 Experimental axial velocity data at iso-plane z=185mm in the unbaffled cylindrical flat-bottom tank.

The radial velocities measure here ranged from 0 to 5% of the tip speed. Above the impeller region, radial component was almost negative everywhere confirming the moment towards the shaft. In the region below the impeller, the radial velocity components had a positive magnitude, indicating that the fluid moment is towards the wall.

By examining the whole set of velocities presented in Appendix A.1for this case, one can see that the overall flow is largely dominated by the a strong swirling tangential flow which ramps up rapidly from very near zero at the shaft to up to 50% of the tip speed at a radial distance of about 0.4. In the rest of the tank, the tangential flow is nearly constant before dropping at the wall. By contrast, the axial velocities are typically much smaller, indicating poor top-to-bottom recirculation, and the radial velocities are even smaller. The weak axial flow is typically directed downward in the middle of the tank and upward near the wall, as expected.

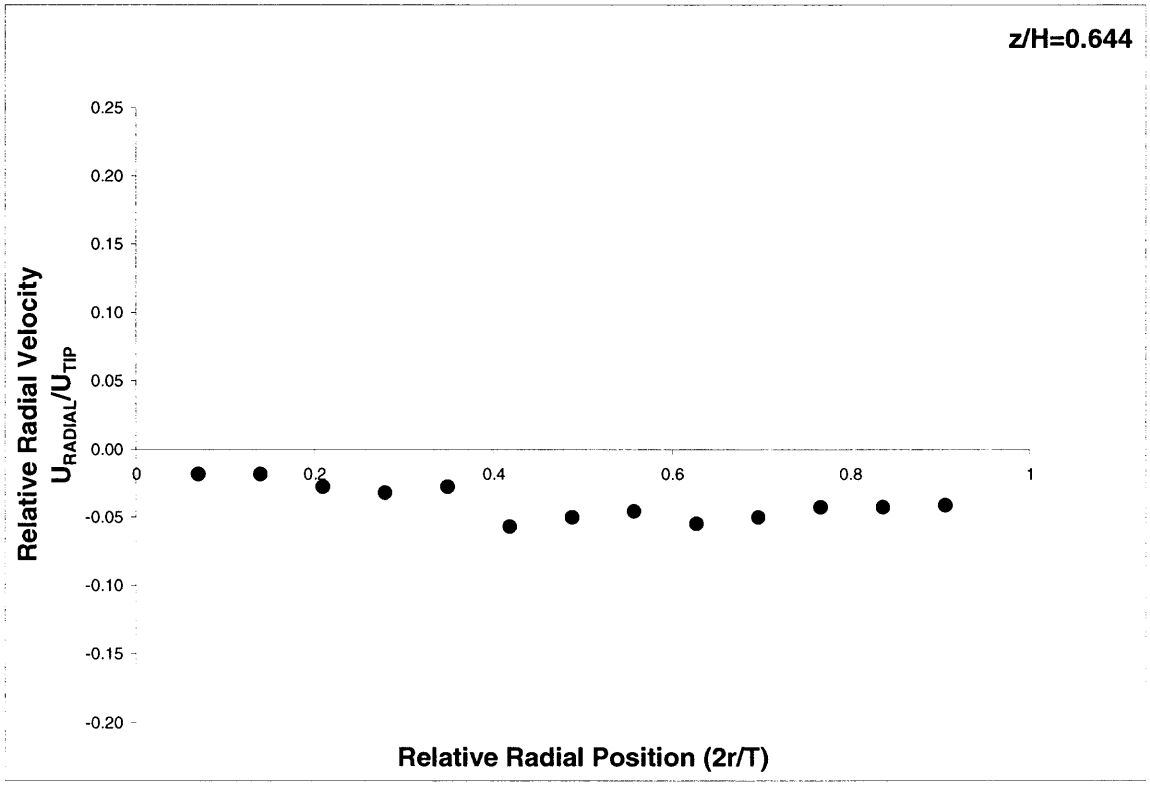

Figure 3.1.3 Experimental radial velocity data at iso plane z=185mm in the unbaffled cylindrical flat-bottom tank

3.2 Velocity Profile for the Baffled, Flat-bottom Tank

The velocity profiles for the case of the baffled, cylindrical, flat-bottom tank are shown in Figures A.2.1.1-A.2.3.4, representing at total of velocity measurements, each one including all three velocity components. A typical example of the velocity profiles is shown in Figures 3.2.1 and 3.2.2. These figure shows that the tangential velocity profile is now typically relatively flat, with velocities on an order of magnitude of about 25-30% of the tip speed, i.e., much smaller than in the unbaffled case. This implies that partial baffling had a significant effect on the tangential component of the velocity, for which the magnitudes were reduced by almost 40% of those obtained in the unbaffled configuration.

In addition, the baffled system showed stronger radial and axial components of the velocity as compared to the unbaffled configuration, with velocity components in the range 0-14% of the tip speed. The higher magnitudes were obtained above the impeller region, near the shaft. These data show a more directional axial flow than in the previous case, with an upward flow near the tank wall, and a downward flow in the central region.

The radial component of the velocity was found to me nearly always negative except in the impeller region. This is consistent with the typical flow produced by a radial impeller in a baffled tank, where the fluid is push radially outwards toward the wall near the impeller blades, and recirculated back toward the center anywhere else in the tank.

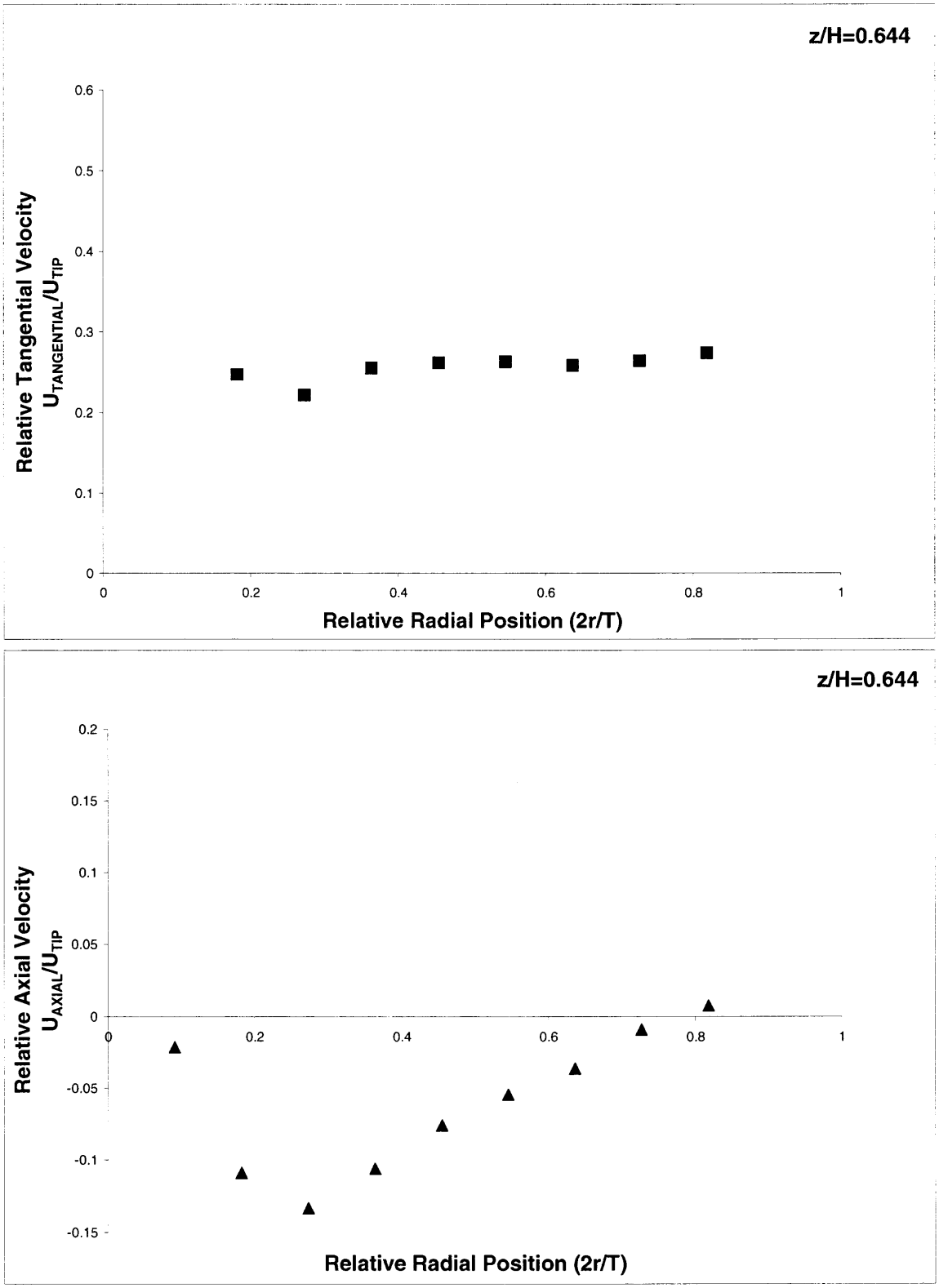

Figure 3.2.1 Experimental tangential and axial velocity data at iso plane z=185mm in the baffled cylindrical flat-bottom tank.

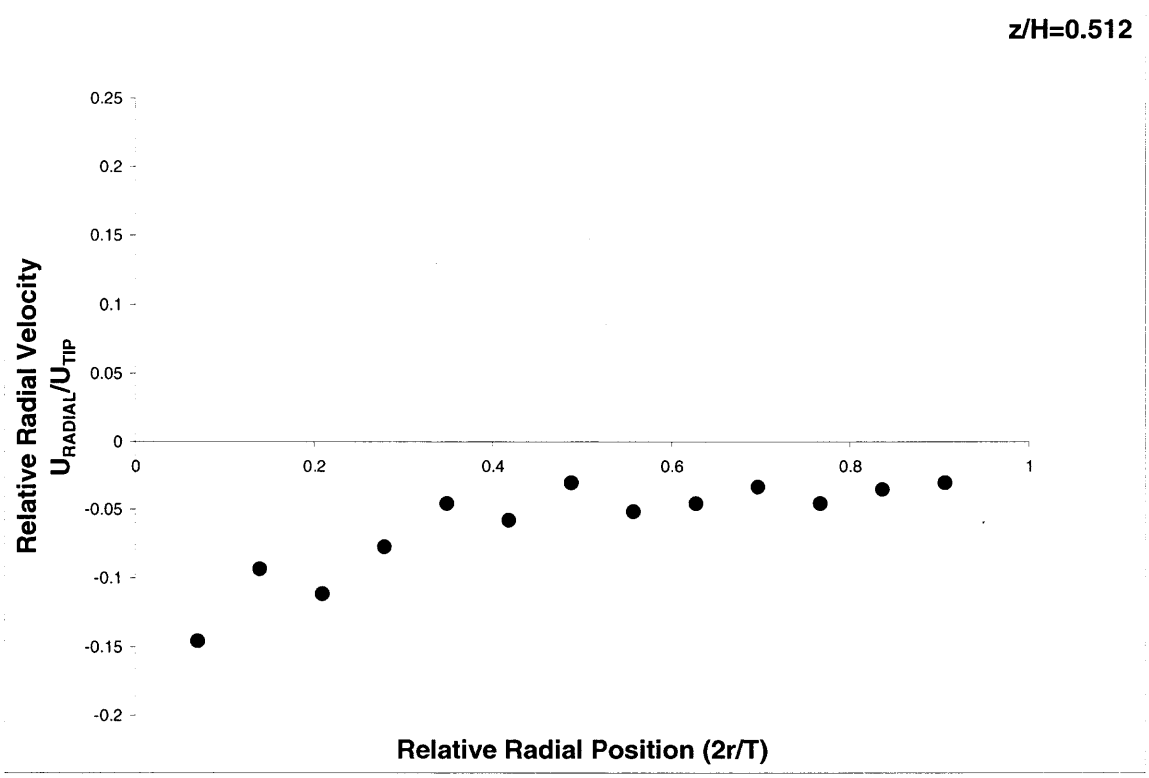

Figure 3.2.2 Experimental radial velocity data at iso plane z=147mm in the baffled cylindrical flat-bottom tank.

3.3 Velocity Profile for the Unbaffled, Hemispherical-Bottom Tank

The velocity profiles for the case of the unbaffled, cylindrical, hemispherical-bottom tank are shown in Figures A.3.1.1-A.3.3.4. Typical examples of the velocity profiles are shown in Figures 3.3.1 and 3.3.2. The velocity profiles obtained for the case of the unbaffled, hemispherical-bottom tank were similar to that of the unbaffled, flat-bottom tank except in the region bellow the impeller.

The tangential component of the velocity observed in this case was clearly strong and had a similar magnitude as that obtained in the case of unbaffled flat-bottom tank. The maximum tangential velocity was obtained at the centre of the shaft and tank wall, which again seems to be the best location for baffling. Above the impeller region, axial component of the velocity of the component of the velocity had higher negative magnitudes between the centre and the wall, which again confirms the downward motion of the fluid.

Below the impeller, the axial component of the fluid velocity was generally very weak except near the wall where a slightly stronger axial velocity in the downward direct was observed. This indicates that this regions is somewhat poorly mixed and possibly segregated from the rest of the tank.

The radial velocities for this configuration were very hard to collect and the results were of poor quality (low data acquisition rate) and showed a poor degree of reproducibility. This is likely the result of the curvature of the tank, especially in the hemispherical portion of the tank, which, in the worst cases, refracted the beams to the point of preventing them from intersecting. Therefore, the data for this velocity component are not shown for this case.

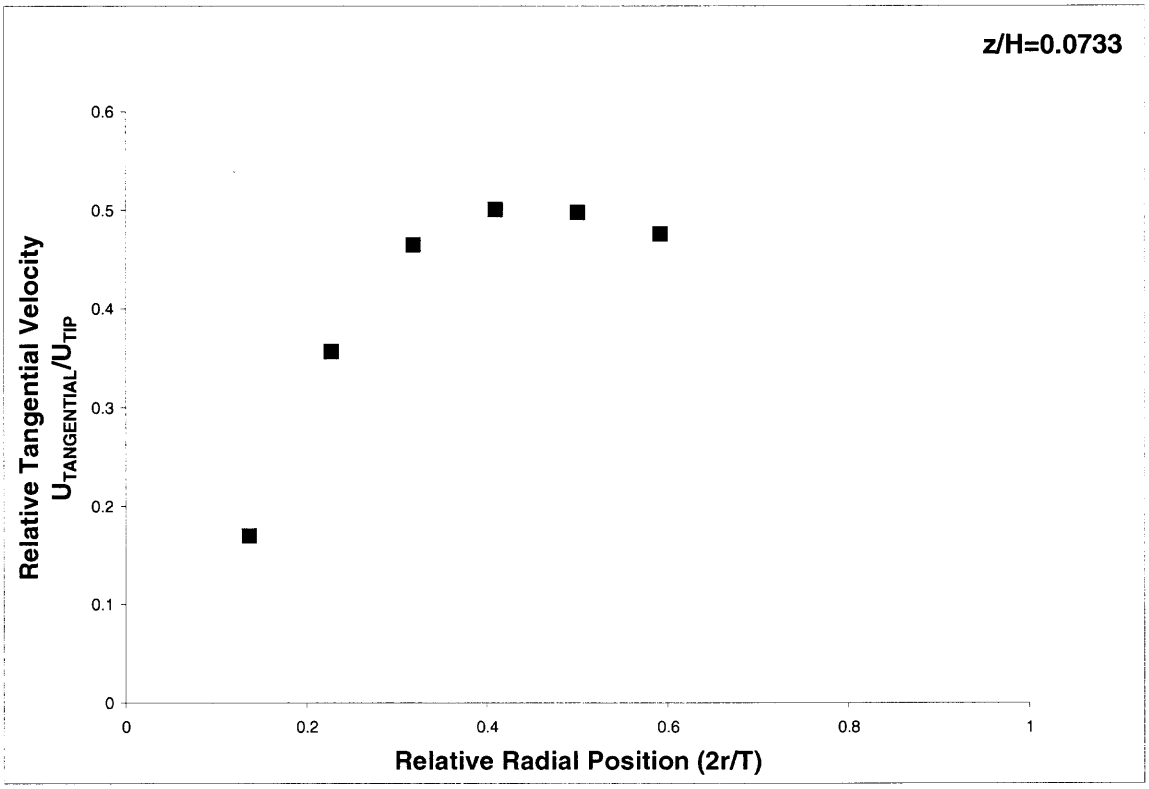
z/H=0.0733
Relative Tangential Velocity
$U_{TANGENTIAL}/U_{TIP}$
0.6
0.5
0.4
0.3
0.2
0.1
0
0
0.2
0.4
0.6
0.8
1
Relative Radial Position (2r/T)

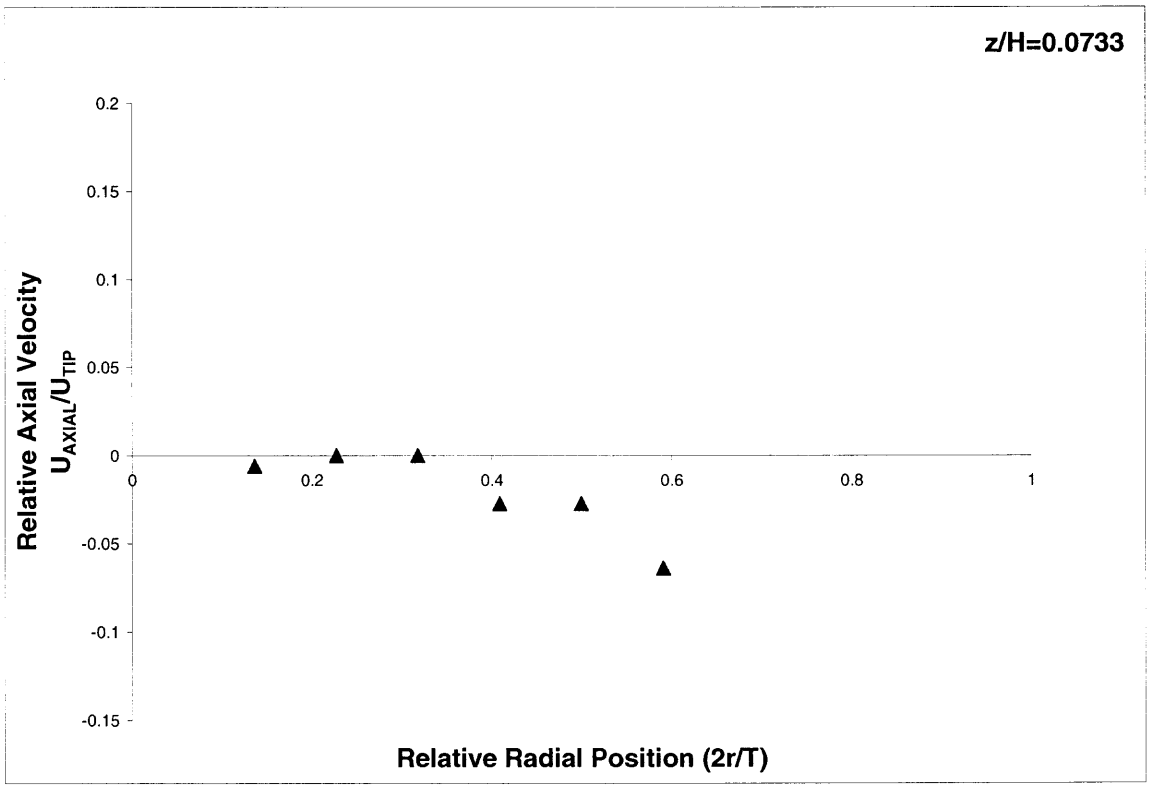
z/H=0.0733
Relative Axial Velocity
U_{AXIAL}/U_{TIP}
0.2
0.15
0.1
0.05
0
-0.05
-0.1
-0.15
0
0.2
0.4
0.6
0.8
1
Relative Radial Position (2r/T)

Figure 3.3.1 Experimental tangential and axial velocity data at iso plane z=22mm in the unbaffled cylindrical hemispherical-bottom tank.

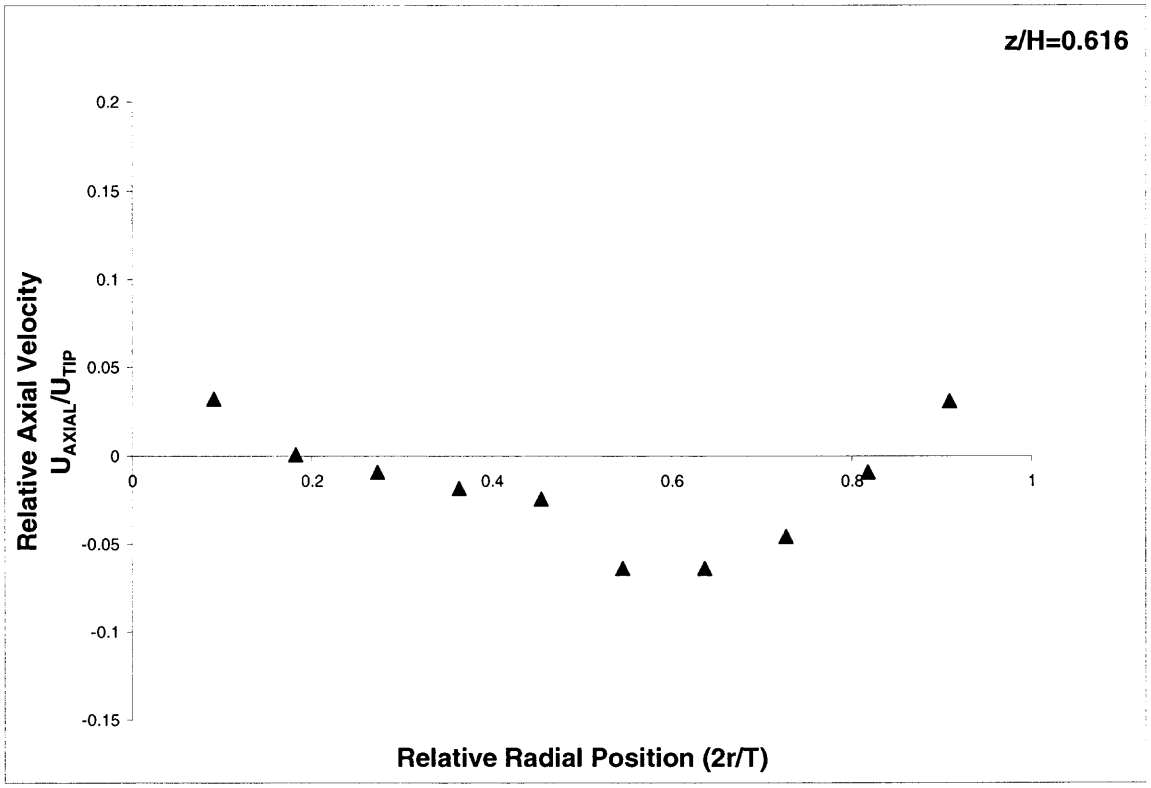

Figure 3.3.2 Experimental axial velocity data at iso plane z=185mm in the unbaffled cylindrical hemispherical-bottom tank.

3.4 Velocity Profile for the Baffled, Hemispherical-Bottom Tank

The velocity profiles for the case of the baffled, cylindrical, hemispherical-bottom tank are shown in Figures A.4.1.1-A.4.3.4, and examples are presented in Figure 3.4.1.

The velocity profiles obtained for the baffled, hemispherical-bottom tank has a lower tangential component of the velocity than the unbaffled case, as one can anticipate. The magnitude of the tangential velocity dropped significantly and was around 45% lower than that obtained in the unbaffled configuration. A comparison with the date obtained for the baffled, flat-bottom case; show that the velocity probates, both tangential and radial, in the upper portion of the tank are similar in both baffled cases. However, below the impeller, the presence of a different type of bottom results in different velocity profiles, especially in the axial direction. No radial data could be collected because of the problem generated by the curvature of the tank bottom.

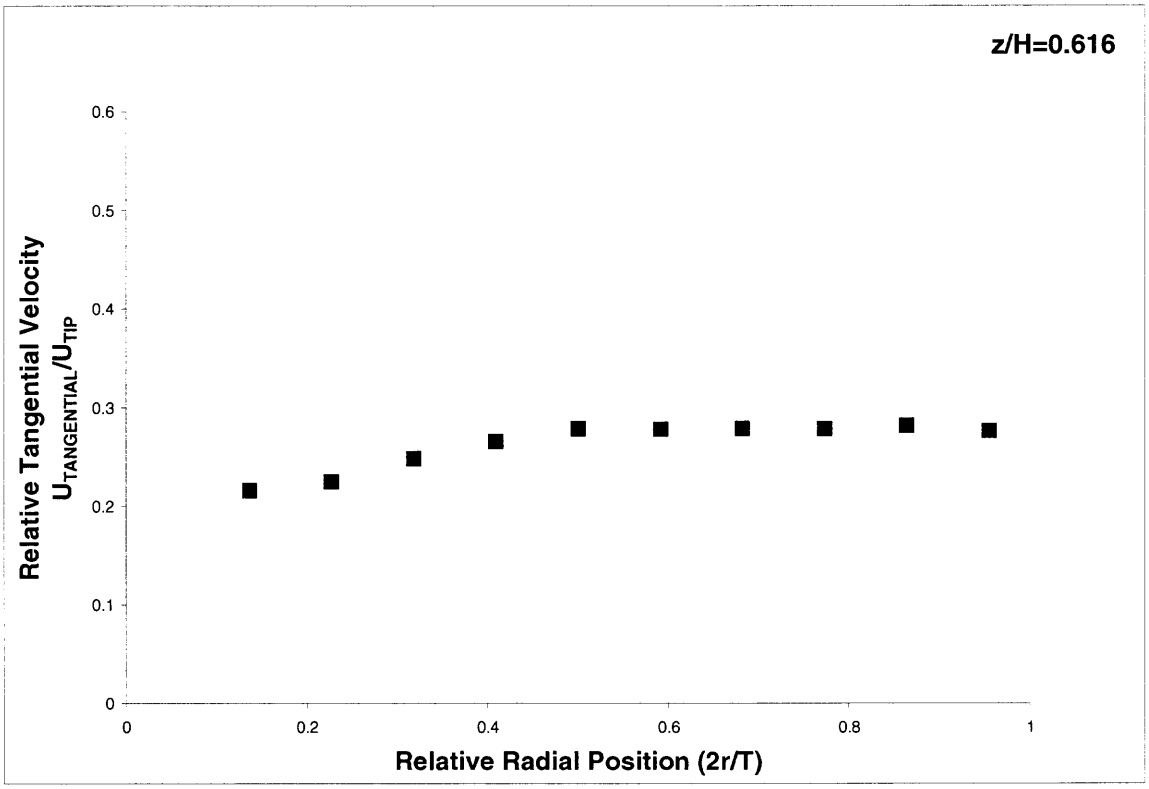

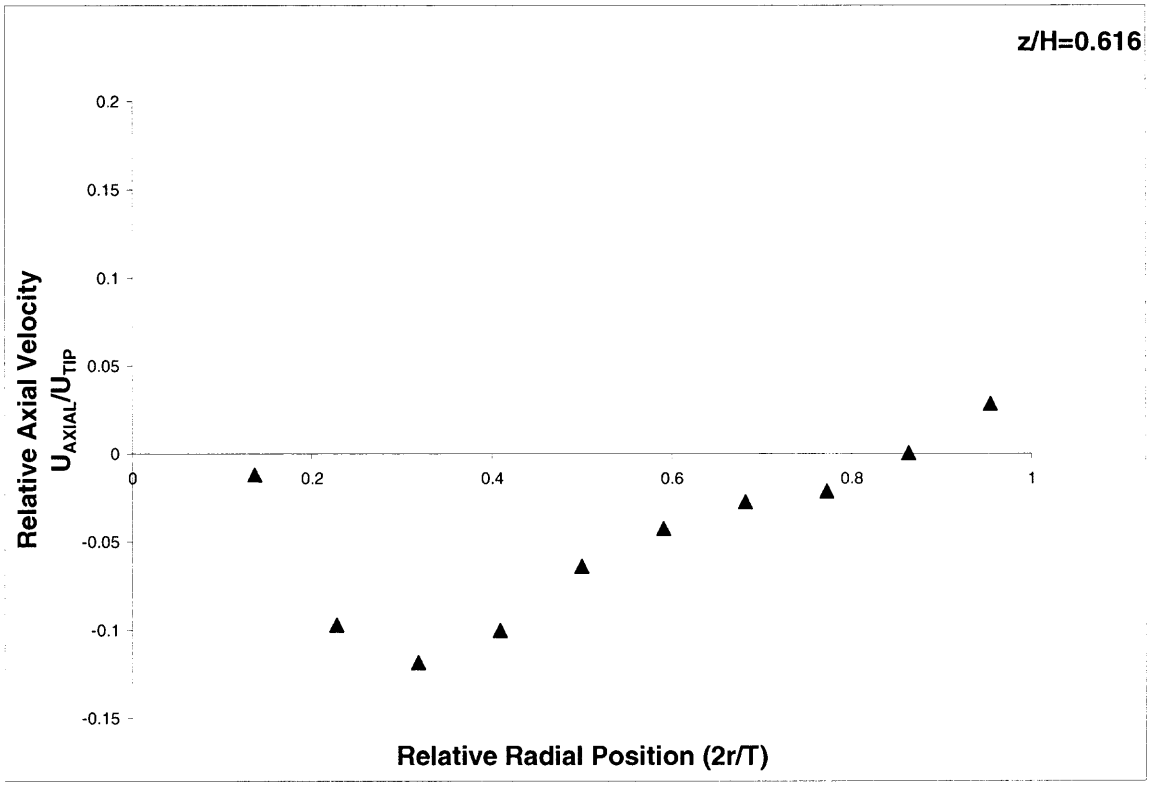

Figure 3.4.1 Experimental tangential and axial velocity data at iso plane z=185mm in the baffled cylindrical Hemispherical-bottom tank.

CHAPTER 4

DISCUSSION

The experimental data obtained in this work confirm that the flow in the unbaffled tank is dominated by the tangential velocity to a more significant extent than the baffled tank, irrespective of the shape of the tank bottom, which is what one would expect in such a case. In addition, the axial component of the velocity is larger in the baffled tank than in the unbaffled tank but only in the upper portion of the tank where the baffle is present. Below the impeller, where no baffling exists, the axial velocity profiles are rather weak with or without the baffle, indicating relatively little top to bottom recirculation in this critical region of the tank. The radial velocities are generally weak, with or without baffle, but the presence of the baffle changes the direction of the weak flow pattern depending on the location.

As already mentioned, little information is available in the literature on these systems. Even the few studies currently available (Campolo et. al., 2002, Dickey et al. 2004, Bakker et al., 2004, Li et al., 2004, Li et al., 2005, Ricard et al., 2005, Reilly et al., 2007) did not produce the same kind and volume of information produced here. For example, Reilly et al. (2007) investigated a small, conical-bottom tank with a relatively large and thick impeller that would not be scalable to a full-scale system. In addition, these authors, as well as nearly all other authors who looked at somewhat similar system, did not conduct any experimental determination of the velocity distribution in their systems, but almost exclusively carried out computational studies with no experimental, direct velocity verification. Furthermore, most of the few reports available in the literature did not examine systems similar to that investigated here, but instead examined impeller-tank

systems with relative dimensions that are quite different from a scaled down version of an industrial reactor, as it is the case here.

The experimental data obtained in this work can only be compared with the experimental results previously obtained by Giuseppe L. Di Benedetto (2007) in this laboratory using a slightly different LDV system with a different receiver operating in a forward scattering mode. The results can also be compared with his Computational Fluid Dynamics (CFD) simulation results. Such comparisons are shown in detail in Appendix B, and in Figures 4.1 and 4.2. The comparison between the experimental data of this work and Di Benedetto's experimental data show, in general, good agreement, especially as far as the dominating velocity is concerned, i.e., the tangential component of the velocity. Such as comparison validates the data collected here and the backscattering approach to LDV data collection used in the present work. When the data are compared with Di Benedetto's CFD predictions, the agreement is also rather favorable, especially for the tangential velocities in baffled systems, but less so for the unbaffled system.

In summary, this work presents an extensive and detailed set of experimental results for a system of significant industrial importance that has not been studied to any significant extent before. It is expected that this work can contribute to a better understanding of the way in which these reactors operate and help their users operate them more effectively.

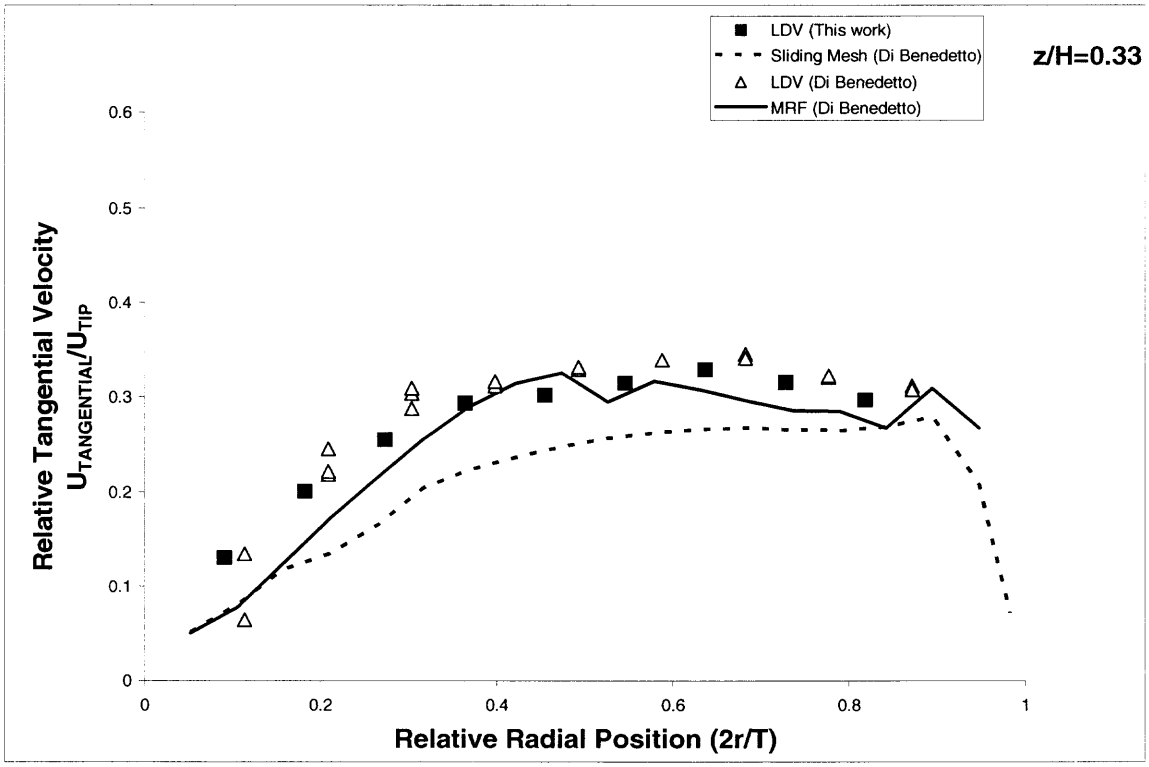

Figure 4.1 Comparison between LDV data and CFD prediction for tangential velocities at iso-surfaces z=96mm in the baffled flat-bottom tank.

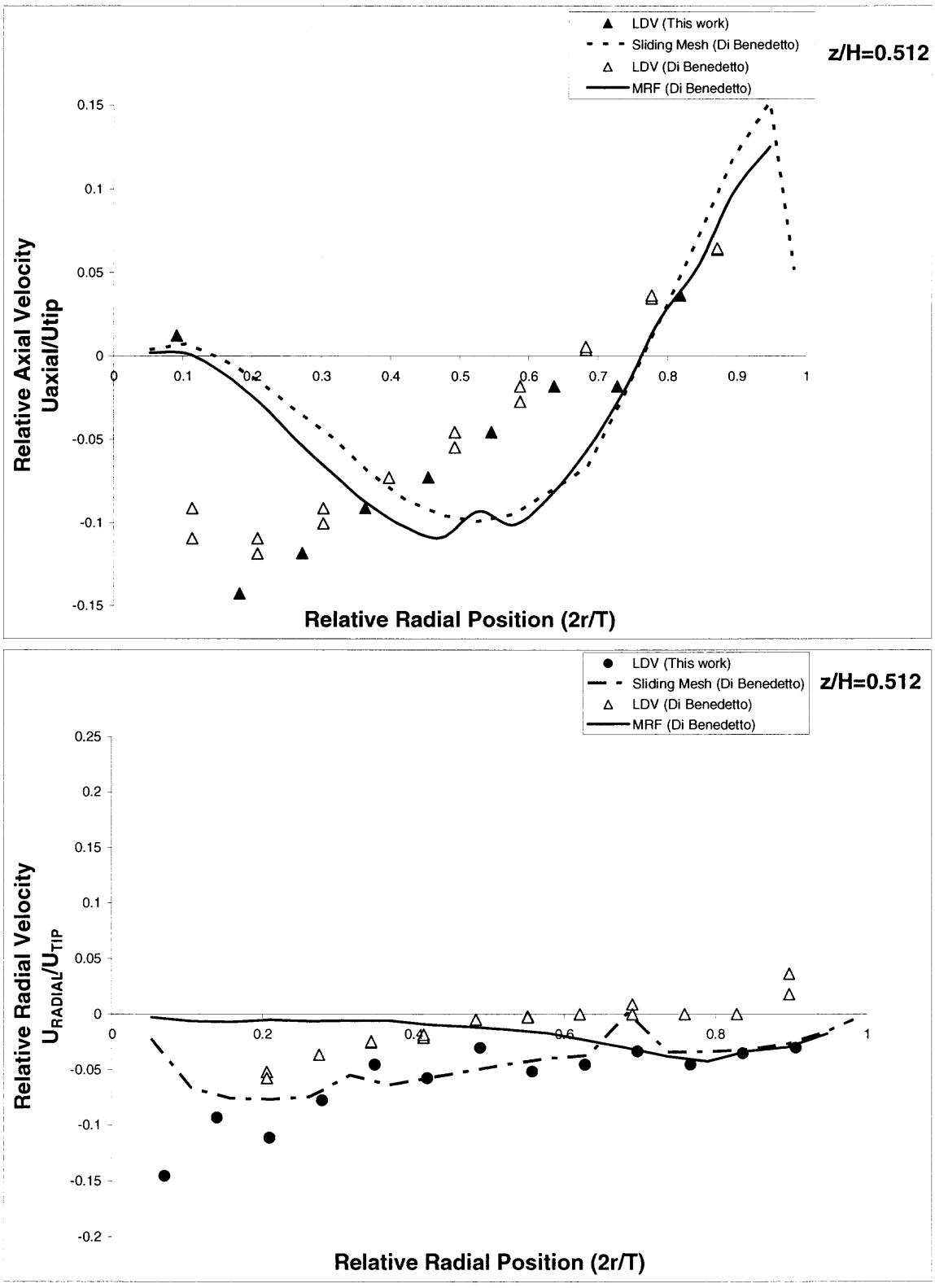

Figure 4.2 Comparison between LDV data and CFD prediction for radial and axial velocities at iso-surfaces z=147mm in the baffled flat-bottom tank.

CHAPTER 5

CONCLUSION

The following conclusions can be derived from this work:

- A significant amount of fluid velocity data was collected with an LDV system for unbaffled and partially baffled tank reactors provided with a retreat-blade impeller. In both cases, two systems were studied, i.e., one with a flat-bottom tank and another with a hemispherical-bottom tank.
- In all the systems investigated here, the tangential component of the velocity appears to dominate the flow over the axial and radial components. The highest tangential velocity is typically about 35% of the impeller tip speed for the baffled case and about 47% of the impeller tip speed for the unbaffled case, irrespective of the type of tank bottom.
- The axial component of the velocity was always significantly smaller than the tangential component, and was on the order of 5-15%, with the higher value obtained in the baffled configuration.
- The radial component of the velocity was found to be the smallest of the three, with velocity magnitudes ranging from 0-10%.
- The presence of a hemispherical bottom instead of a flat bottom did not significantly alter the velocity profiles above the impeller, when similarly baffled systems were compared. However, this was not entirely the case below the impeller, where the presence of the hemispherical bottom resulted in a slightly larger down-flow next to the wall.

- The dominance of the tangential velocity and the small value of the radial and especially axial velocity in all the system investigated here indicate a poor vertical recirculation of the fluid inside the tank and therefore a reduced mixing efficiency for this type of reactors.
- The experimental results obtained in this work compare favorably with the experimental results and the computational predictions obtained previously in this laboratory.
- Together with recent data obtained in this laboratory, the data presented here constitute the first detailed mapping of the flow distribution inside a system of significant industrial importance that has not been studied to any significant extent before. It is expected that this work can contribute to a better understanding of the way in which these reactors operate and help their users operate them more effectively.

APPENDIX A

EXPERIMENTAL RESULTS

Experimental LDV results are presented in this Appendix as follows:

A.1 Experimental data in case of unbaffled, cylindrical, flat-bottom tank

A.1.1 Experimental tangential velocities obtained in the unbaffled, cylindrical, flat-bottom tank:

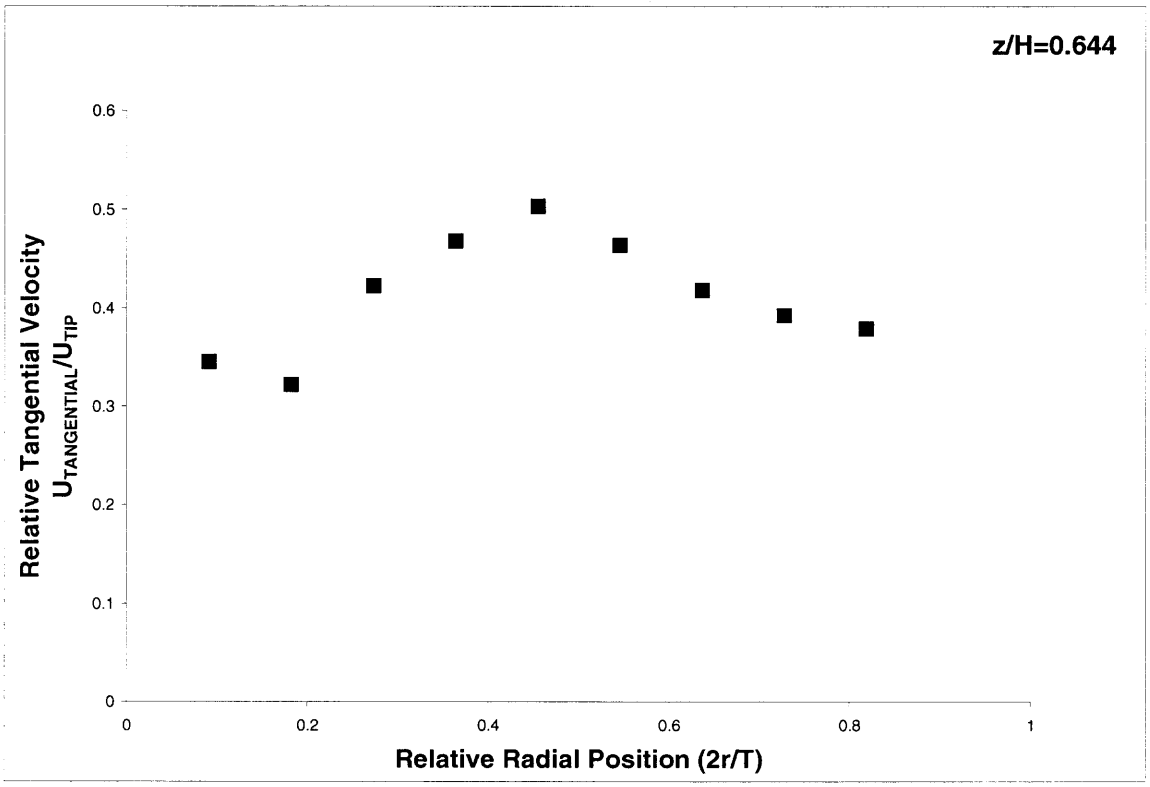

Figure A.1.1.1 Experimental tangential velocity data at iso plane z=185mm in the unbaffled, cylindrical, flat-bottom tank.

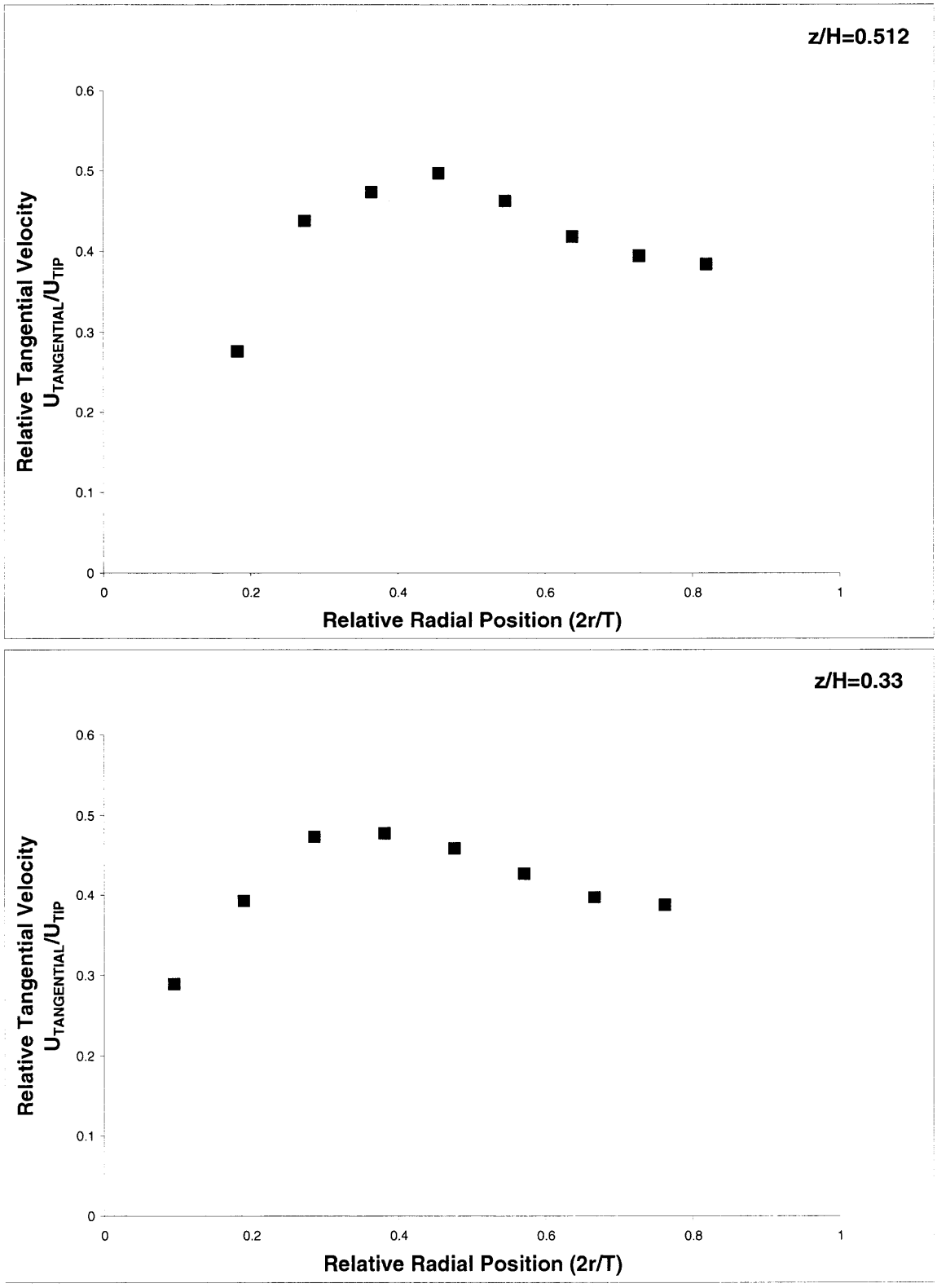

Figure A.1.1.2 Experimental tangential velocity data at iso plane z=147mm and z=96mm in the unbaffled, cylindrical, flat-bottom tank.

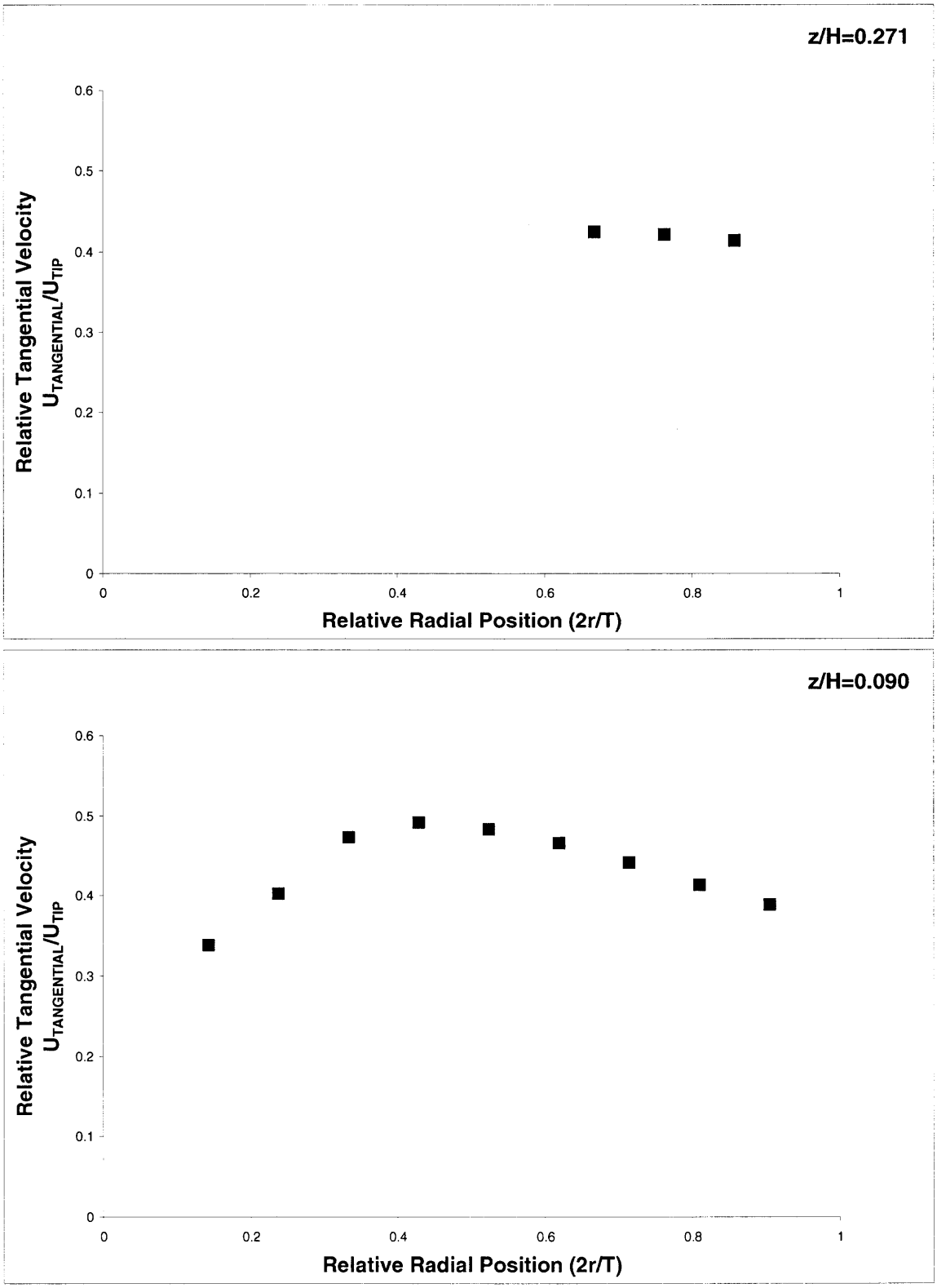

Figure A.1.1.3 Experimental tangential velocity data at iso plane z=78mm and z=26mm in the unbaffled, cylindrical, flat-bottom tank.

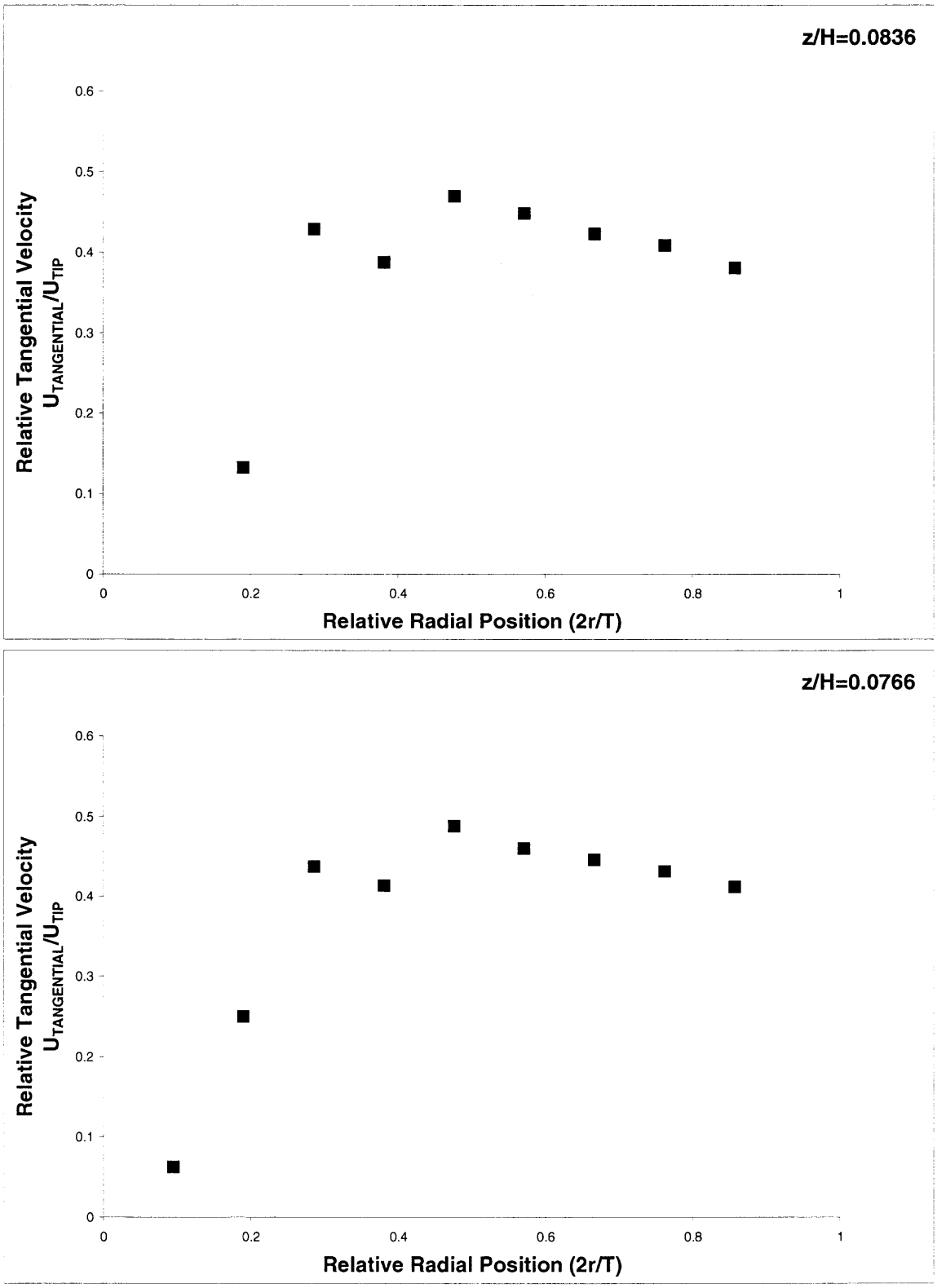

Figure A.1.1.4 Experimental tangential velocity data at iso plane z=24mm and z=22mm in the unbaffled, cylindrical, flat-bottom tank.

A.1.2 Experimental axial velocities in the unbaffled, cylindrical, flat-bottom tank:

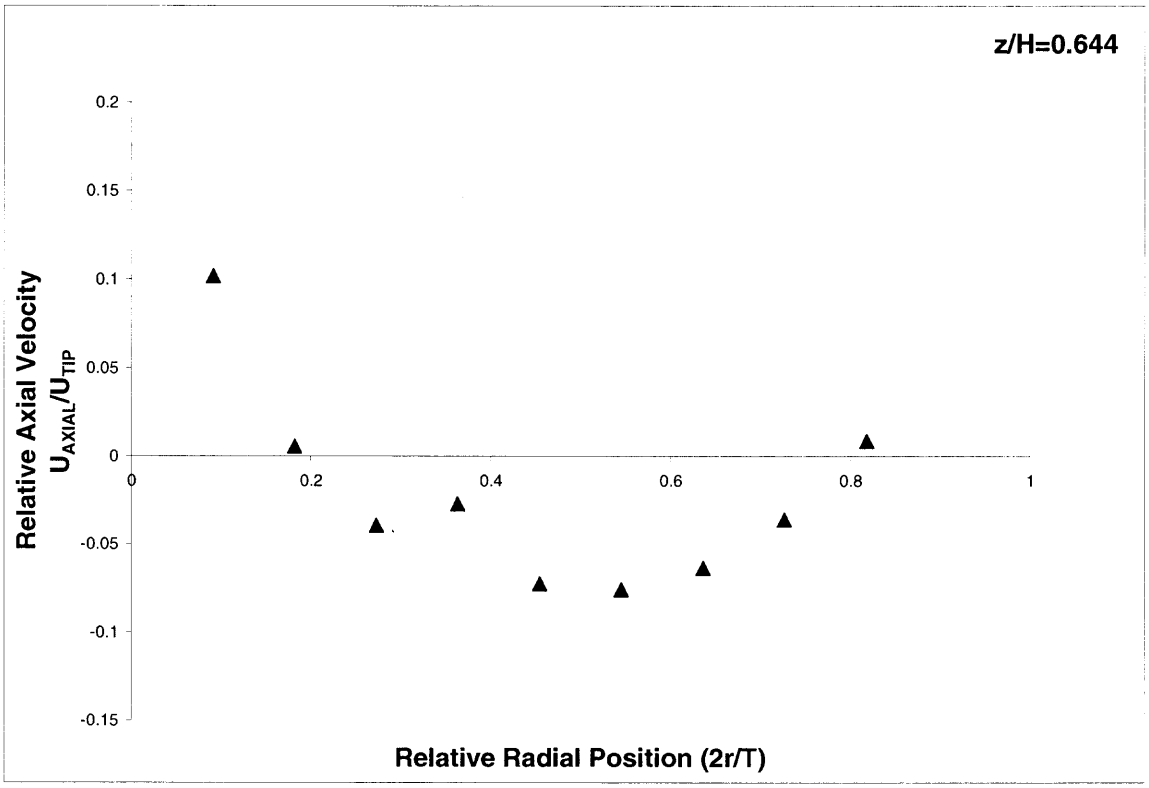

Figure A.1.2.1 Experimental axial velocity data at iso plane z=185mm in the unbaffled, cylindrical, flat-bottom tank.

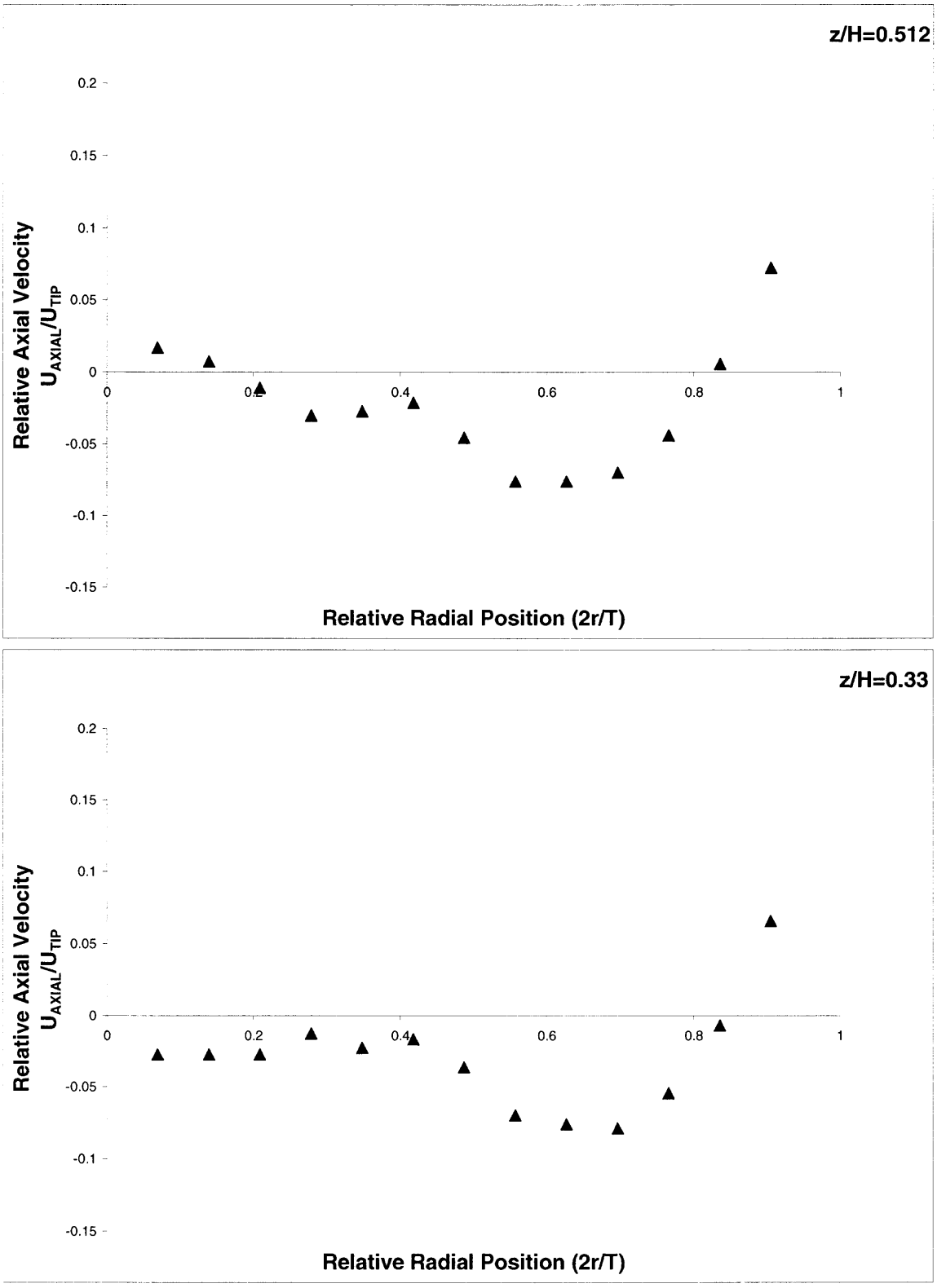

Figure A.1.2.2 Experimental axial velocity data at iso plane z=96mm and z=78mm in the unbaffled, cylindrical, flat-bottom tank.

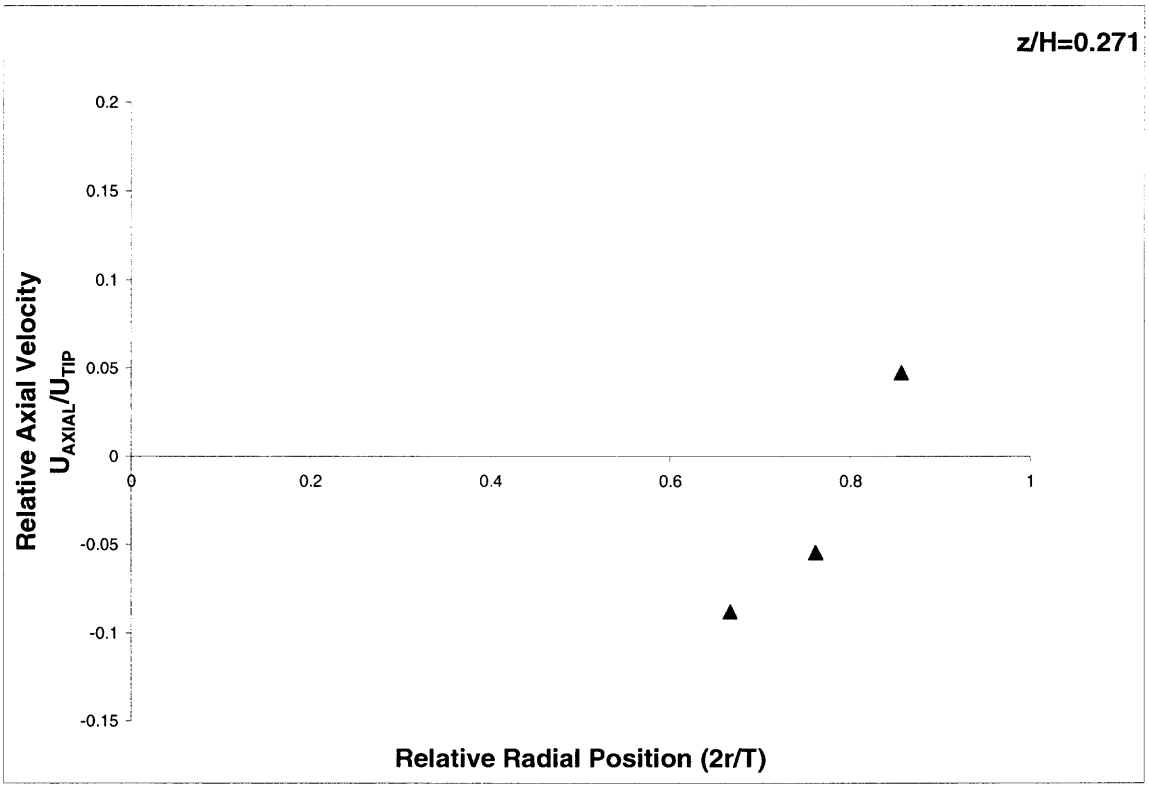

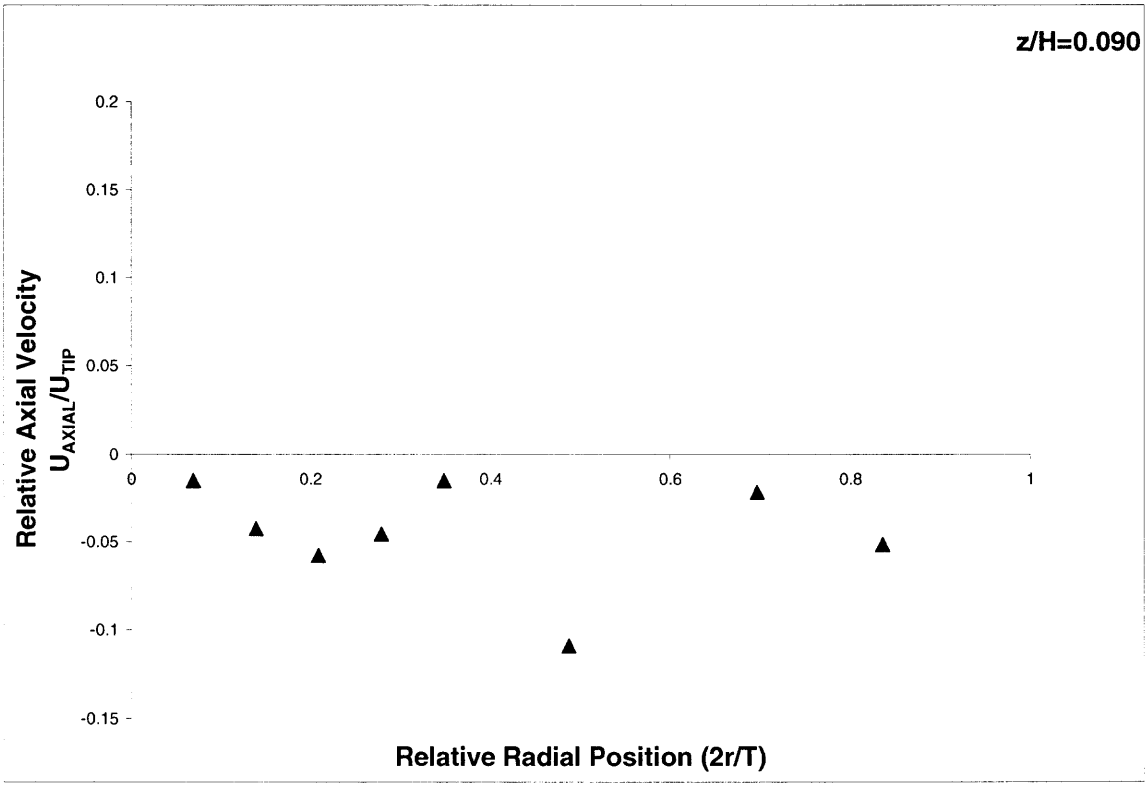

Figure A.1.2.3 Experimental axial velocity data at iso plane z=26mm and z=24mm in the unbaffled, cylindrical, flat-bottom tank

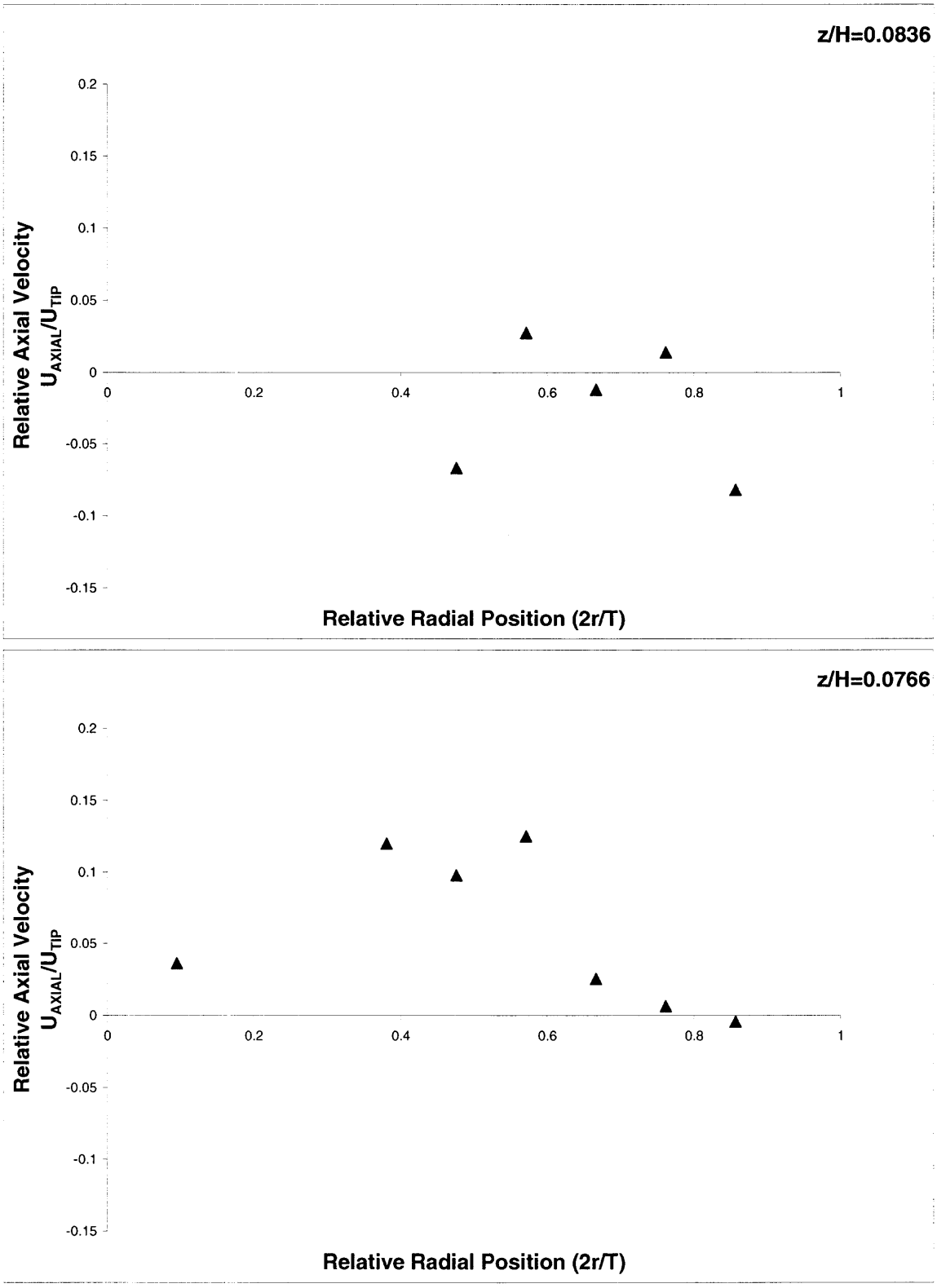

Figure A.1.2.4 Experimental axial velocity data at iso plane z=24mm and z=22mm in the unbaffled, cylindrical, flat-bottom tank.

A.1.3 Experimental radial velocities in the unbaffled, cylindrical, flat-bottom tank:

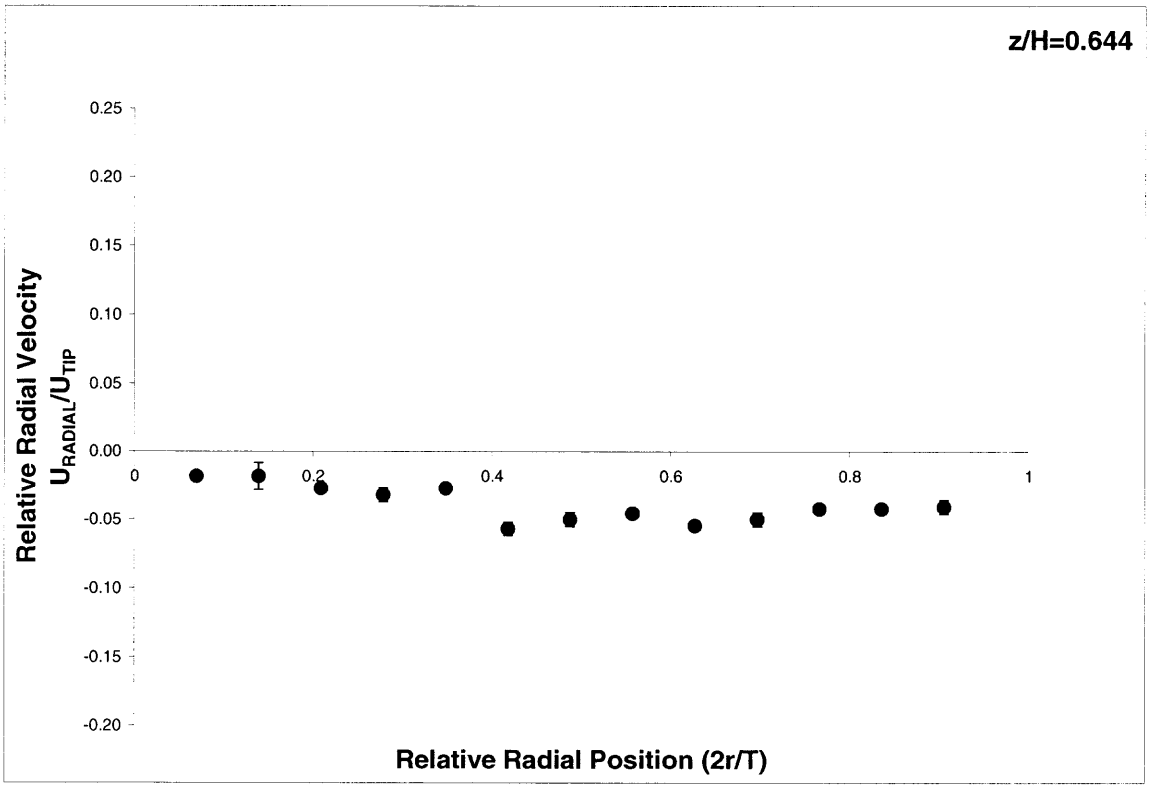

Figure A.1.3.1 Experimental radial velocity data at iso plane z=185mm in the unbaffled, cylindrical, flat-bottom tank with the standard error.

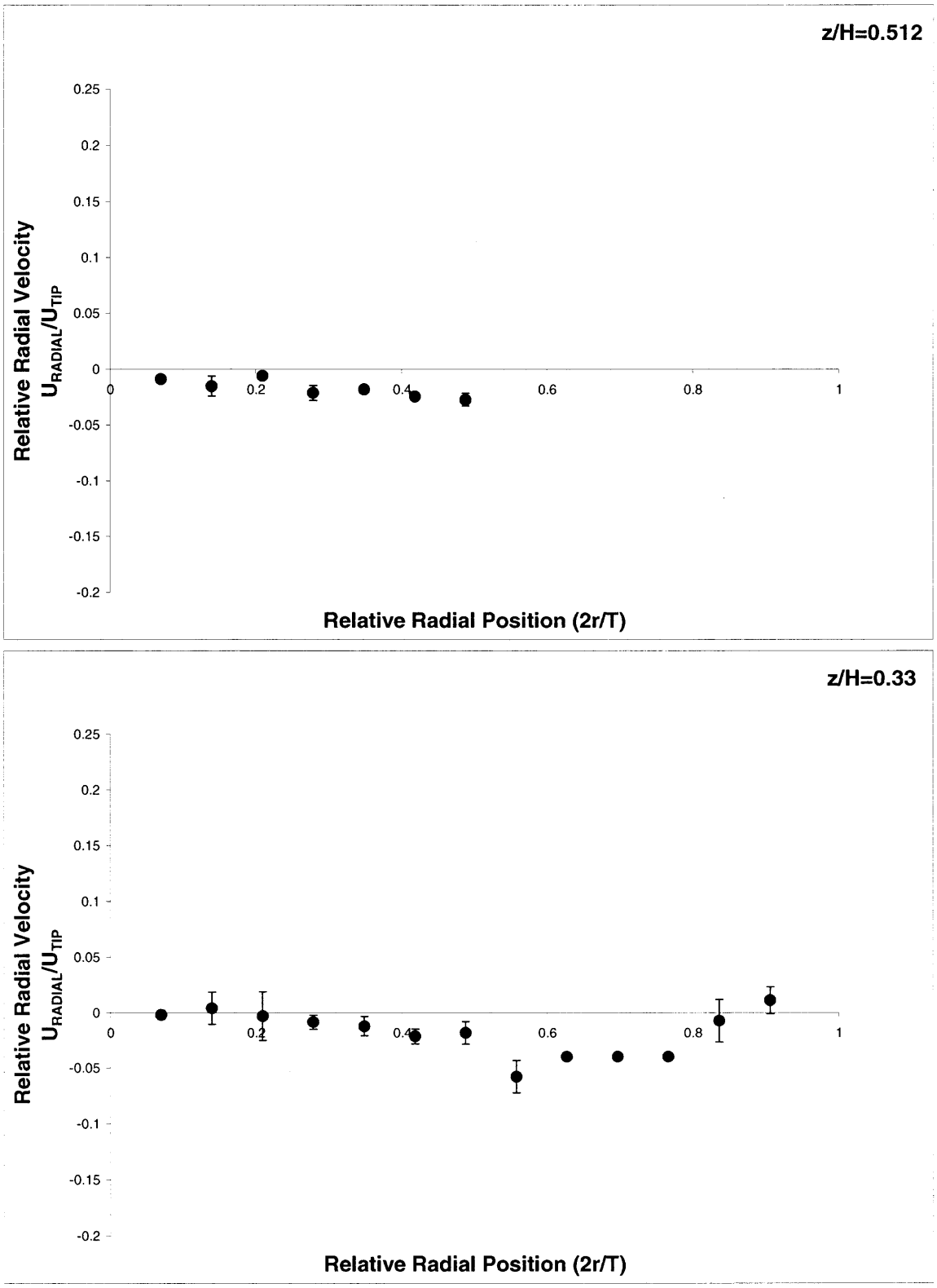

Figure A.1.3.2 Experimental radial velocity data at iso plane z=147mm and z=96mm in the unbaffled, cylindrical, flat-bottom tank with the standard error.

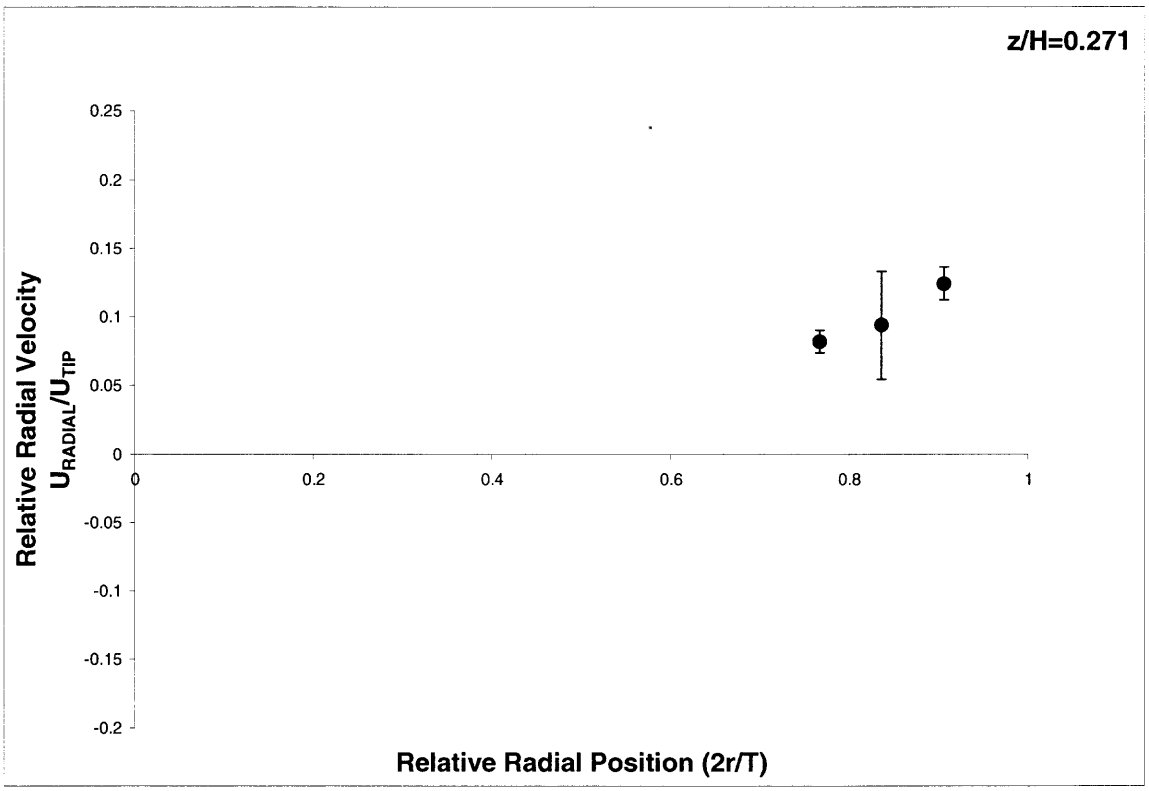

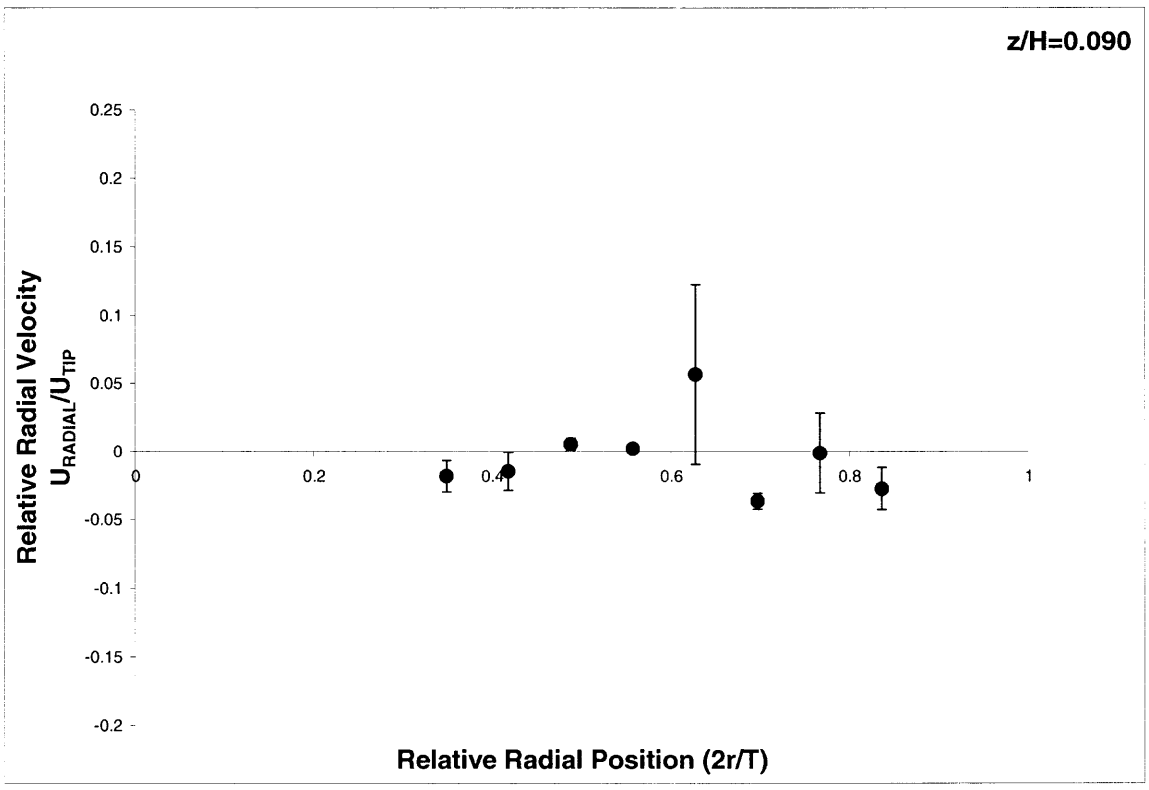

Figure A.1.3.3 Experimental radial velocity data at iso plane z=78mm and z=26mm in the unbaffled, cylindrical, flat-bottom tank with the standard error.

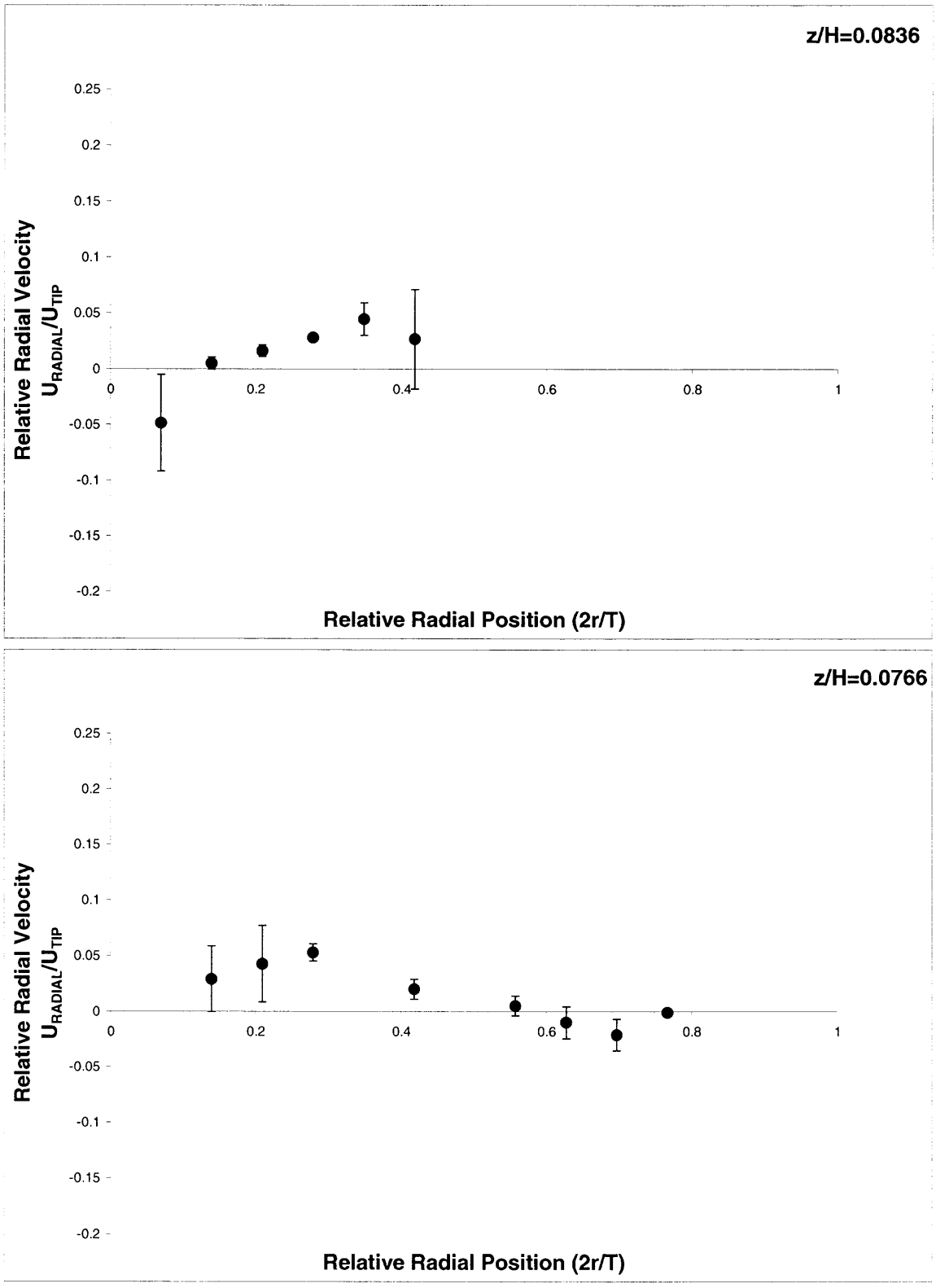

Figure A.1.3.4 Experimental radial velocity data at iso plane z=24mm and z=22mm in the unbaffled, cylindrical, flat-bottom tank with the standard error.

A.2 Experimental data in case of baffled, cylindrical, flat-bottom tank

A.2.1 Experimental tangential velocities obtained in the baffled, cylindrical, flat-bottom tank:

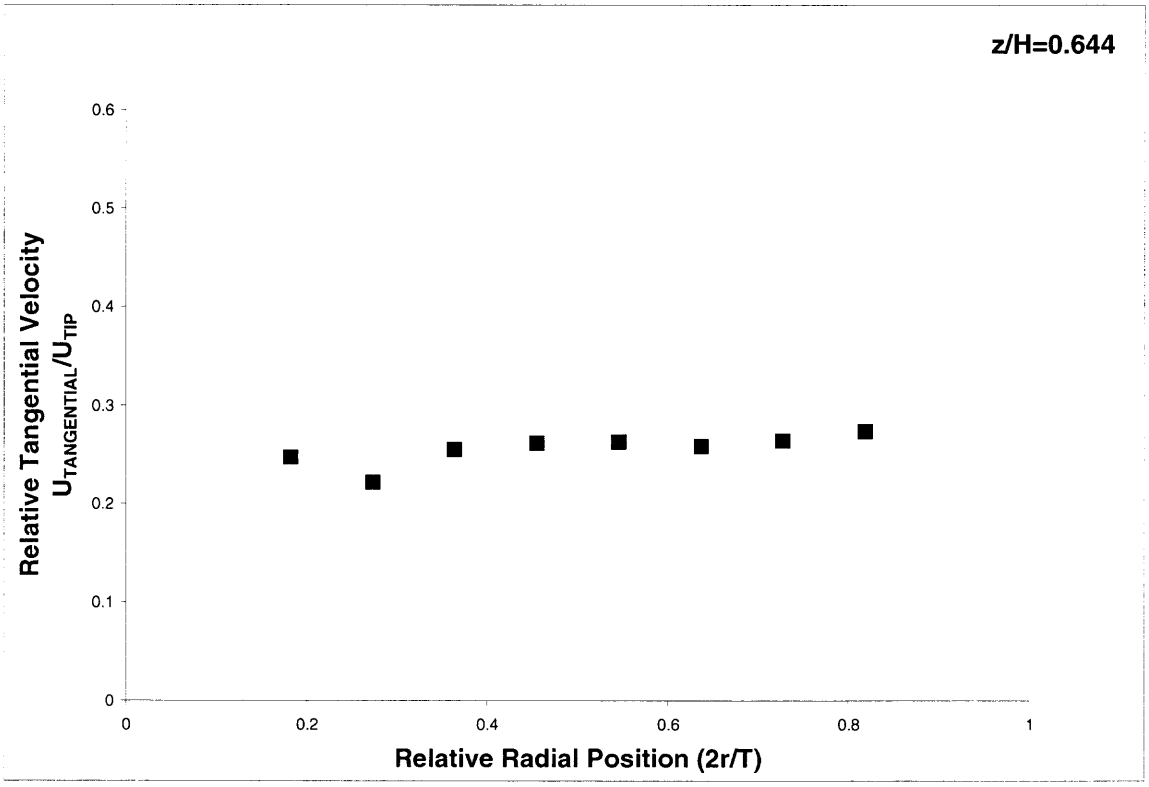

Figure A.2.1.1 Experimental tangential velocity data at iso plane z=185mm in the baffled, cylindrical, flat-bottom tank

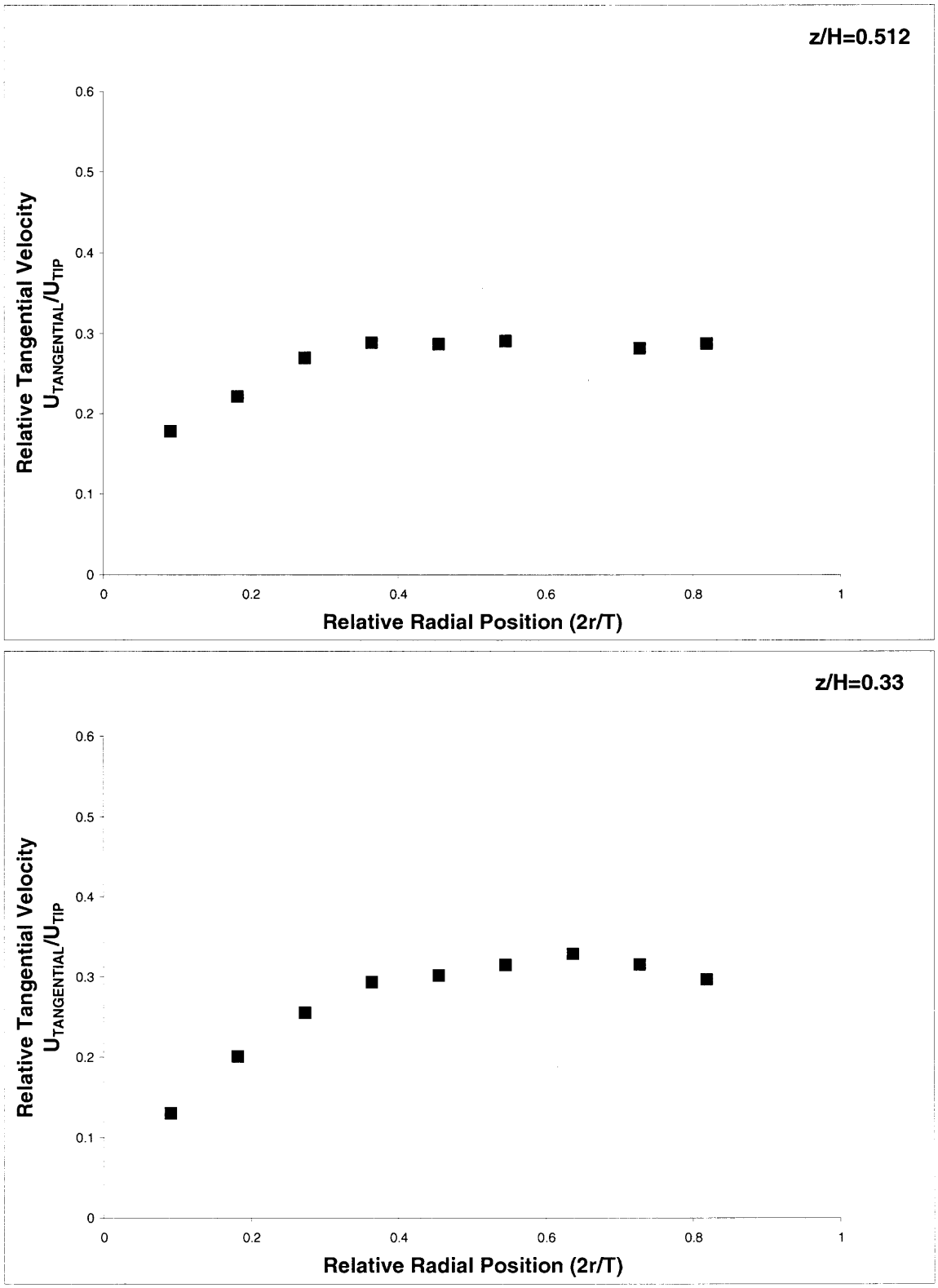

Figure A.2.1.2 Experimental tangential velocity data at iso plane z=147mm and z=96mm in the baffled, cylindrical, flat-bottom tank.

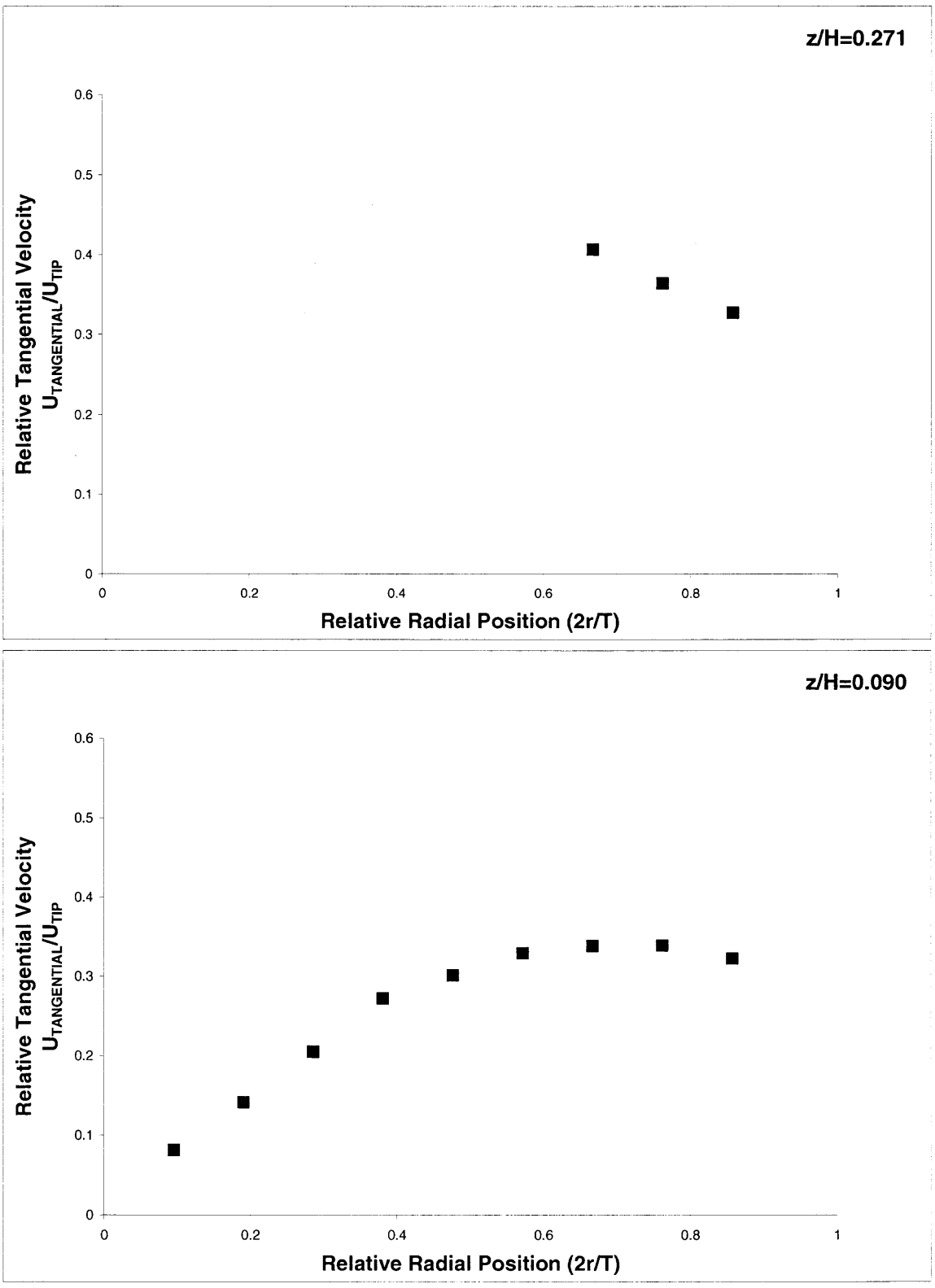

Figure A.2.1.3 Experimental tangential velocity data at iso plane z=78mm and z=26mm in the baffled, cylindrical, flat-bottom tank.

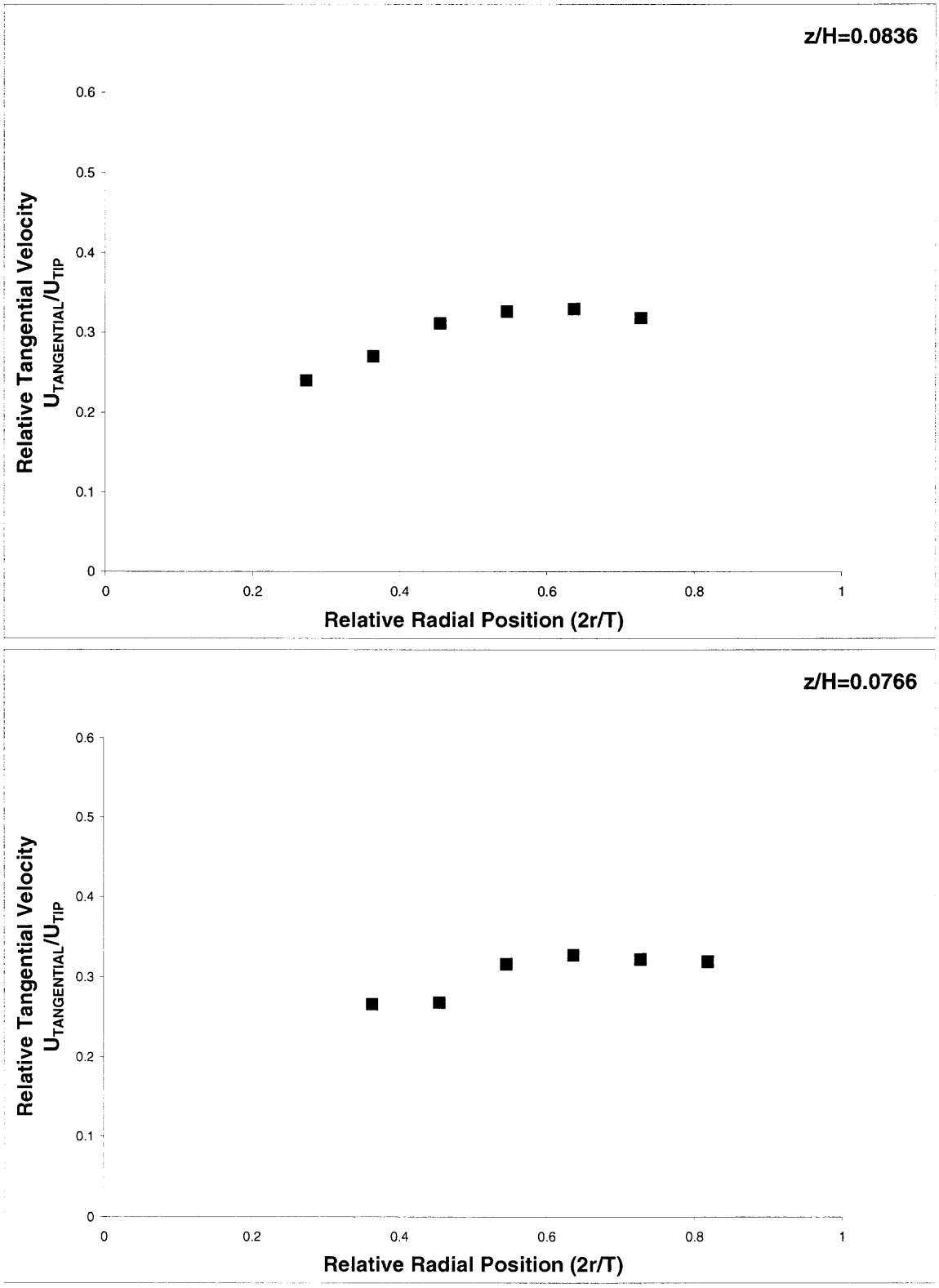

Figure A.2.1.4 Experimental tangential velocity data at iso plane z=24mm and z=22mm in the baffled, cylindrical, flat-bottom tank.

A.2.2 Experimental axial velocities obtained in the baffled, cylindrical, flat-bottom tank.

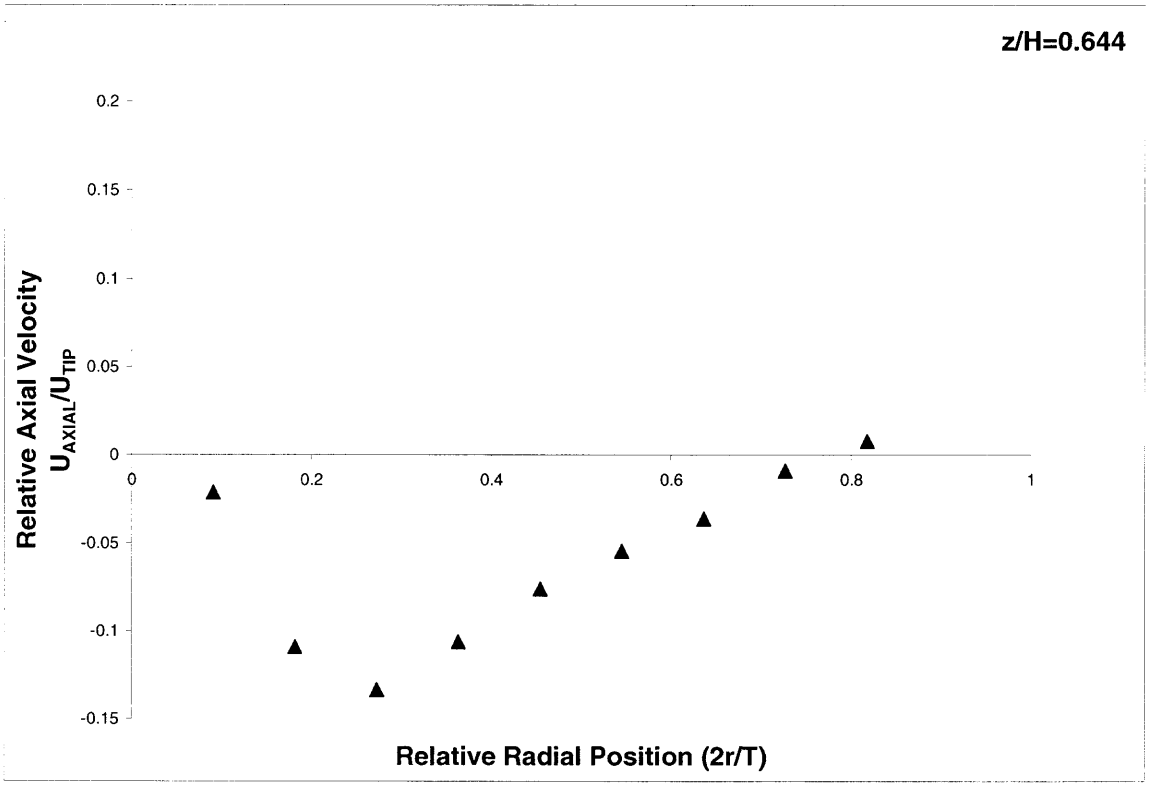

Figure A.2.2.1 Experimental axial velocity data at iso plane z=185mm and z=147mm in the baffled, cylindrical, flat-bottom tank

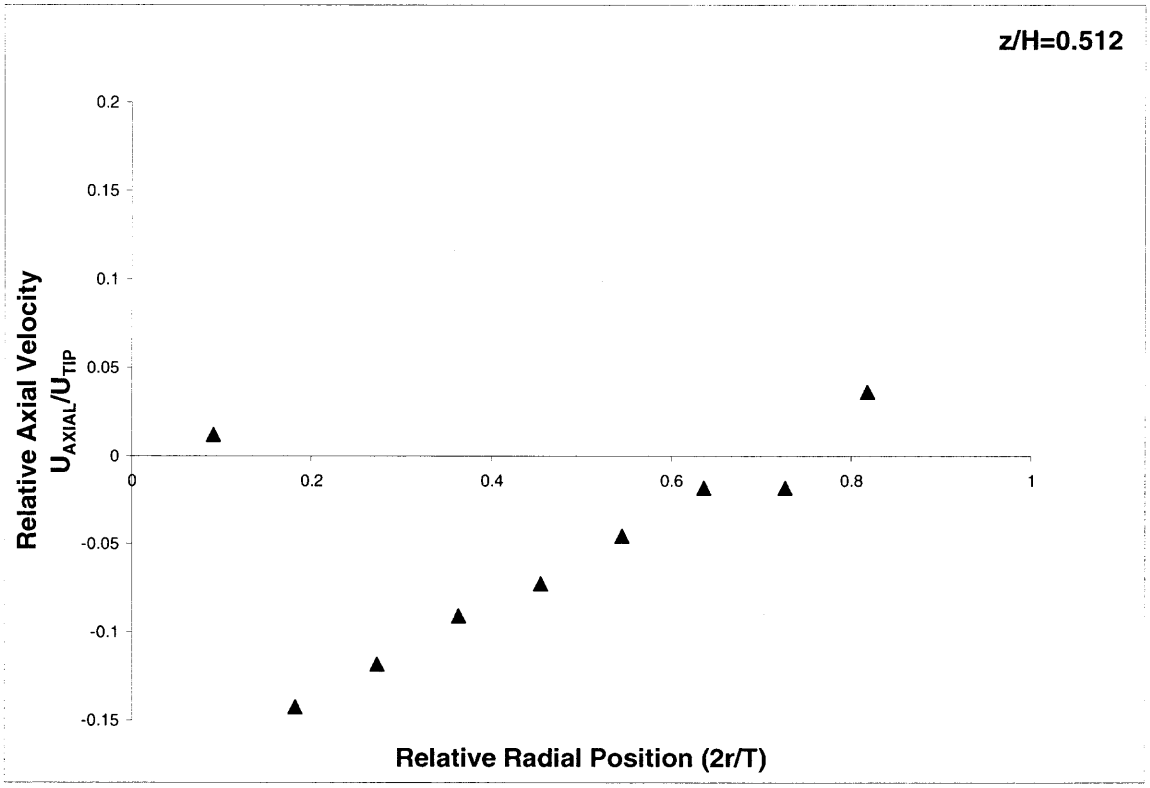

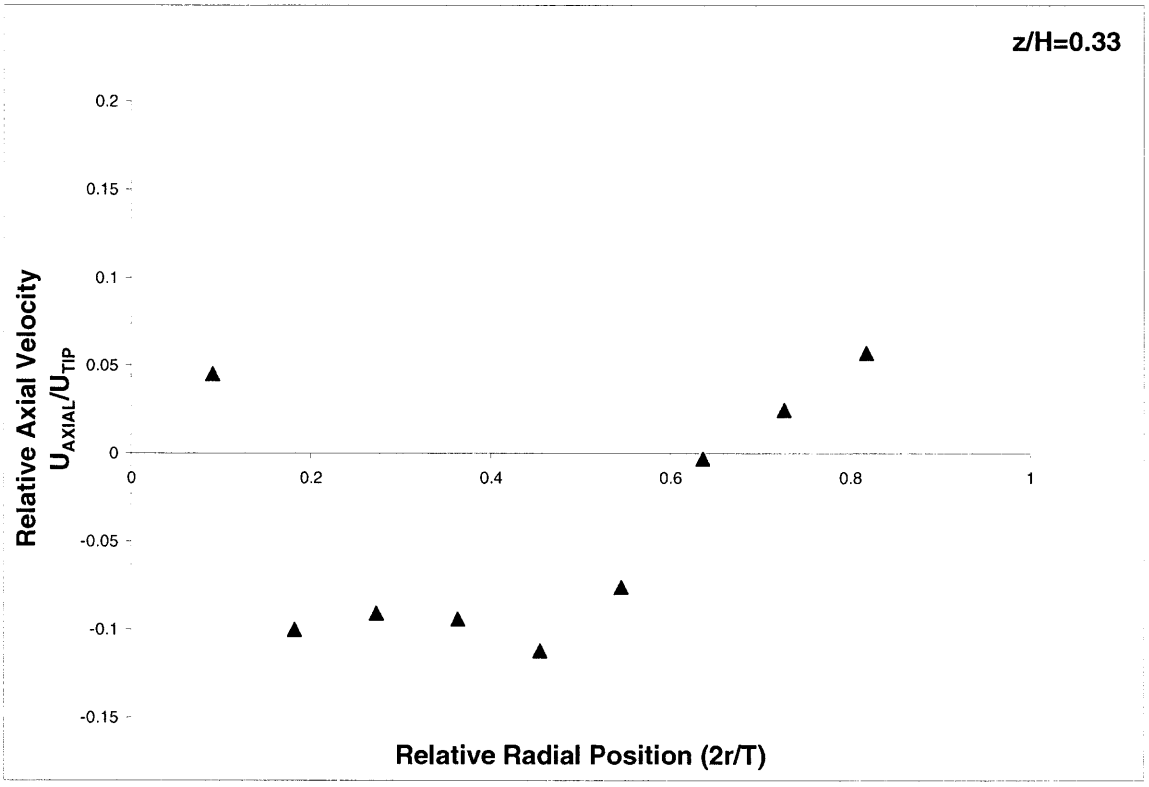

Figure A.2.2.2 Experimental axial velocity data at iso plane z=147mm and z=96mm in the baffled, cylindrical, flat-bottom tank.

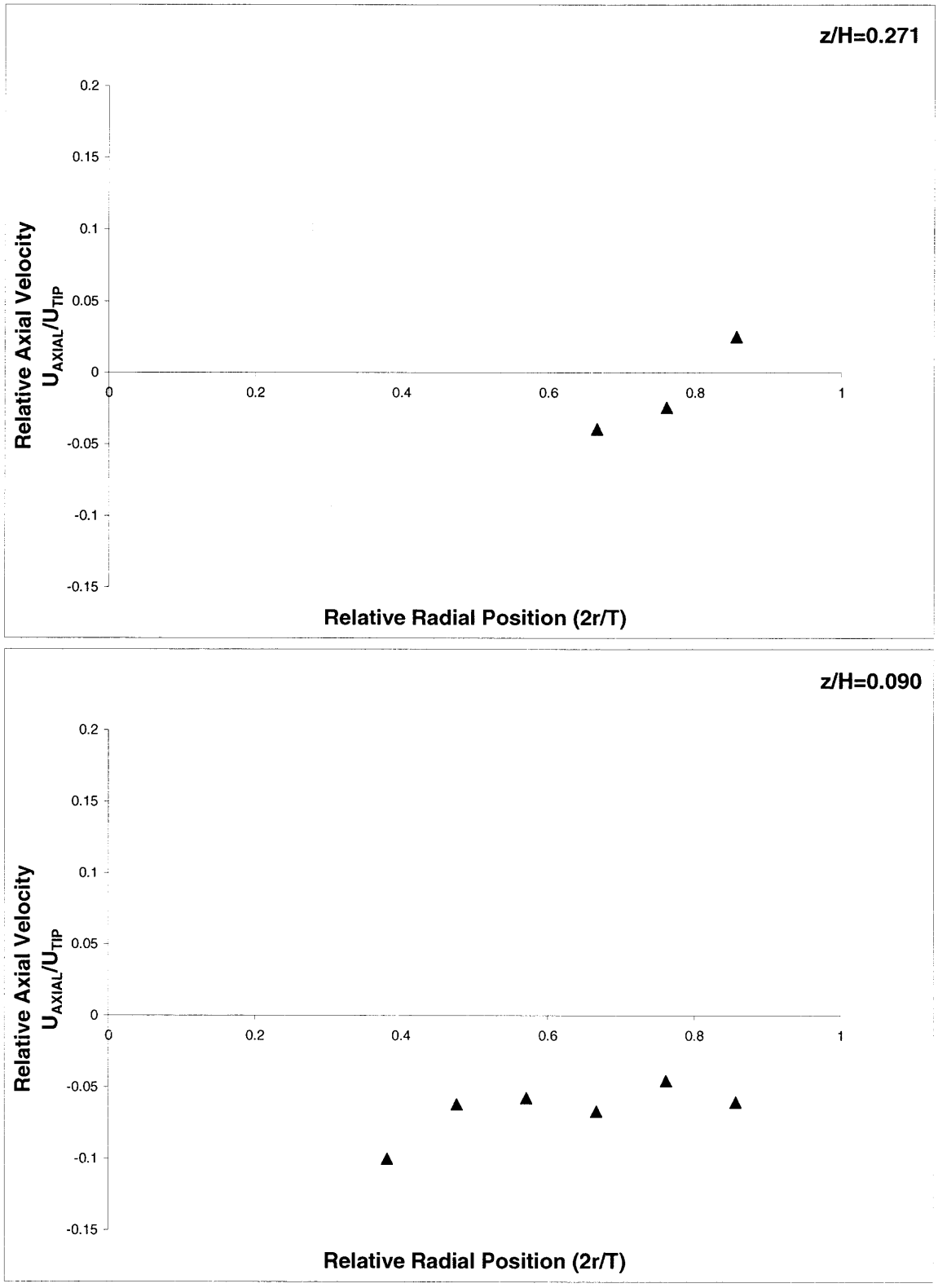

Figure A.2.2.3 Experimental axial velocity data at iso plane z=78mm and z=26mm in the baffled, cylindrical, flat-bottom tank.

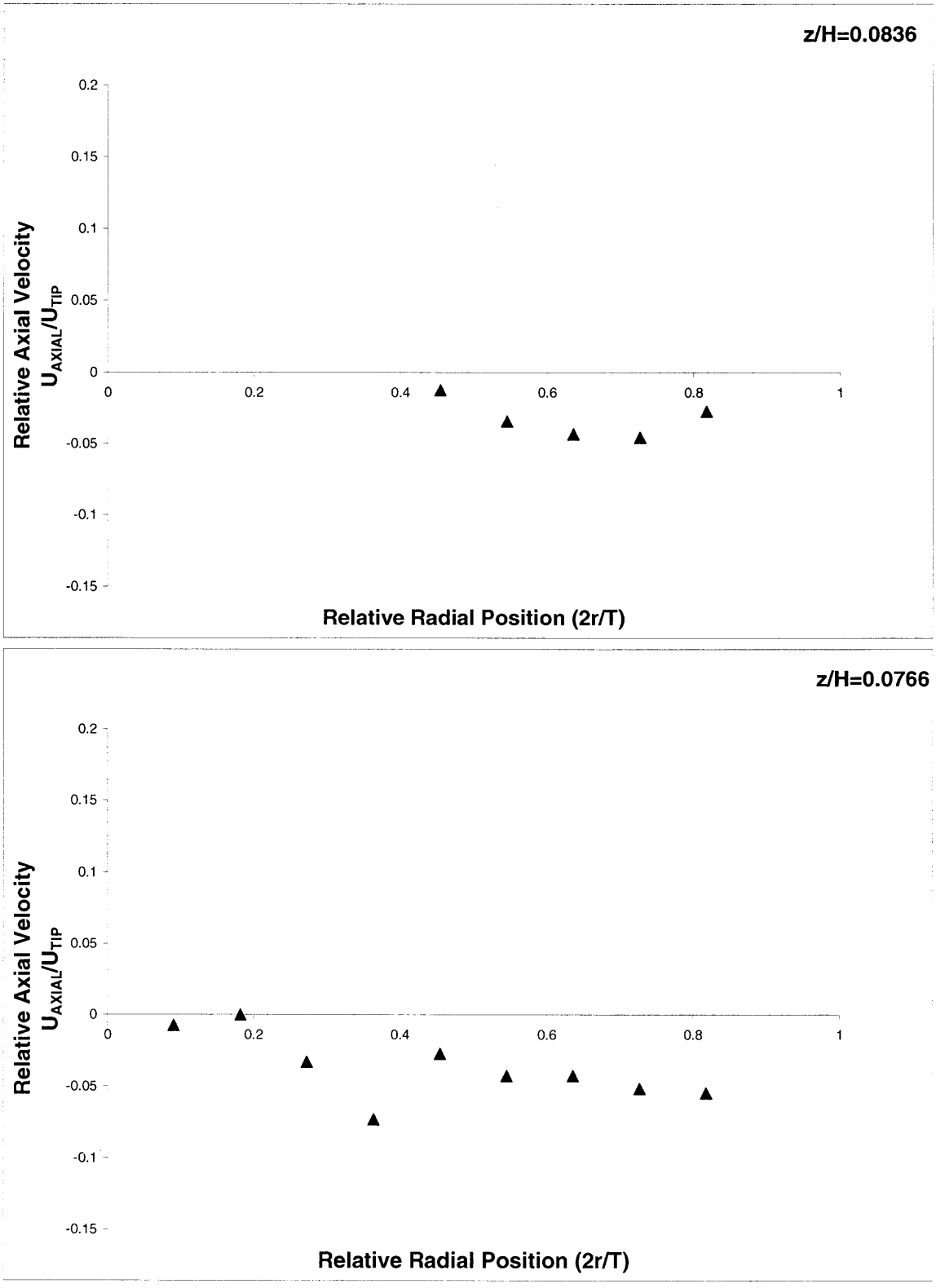

Figure A.2.2.4 Experimental radial velocity data at iso plane z=24mm and z=22mm in the baffled, cylindrical, flat-bottom tank.

A.2.3 Experimental radial velocities obtained in the baffled, cylindrical, flat-bottom:

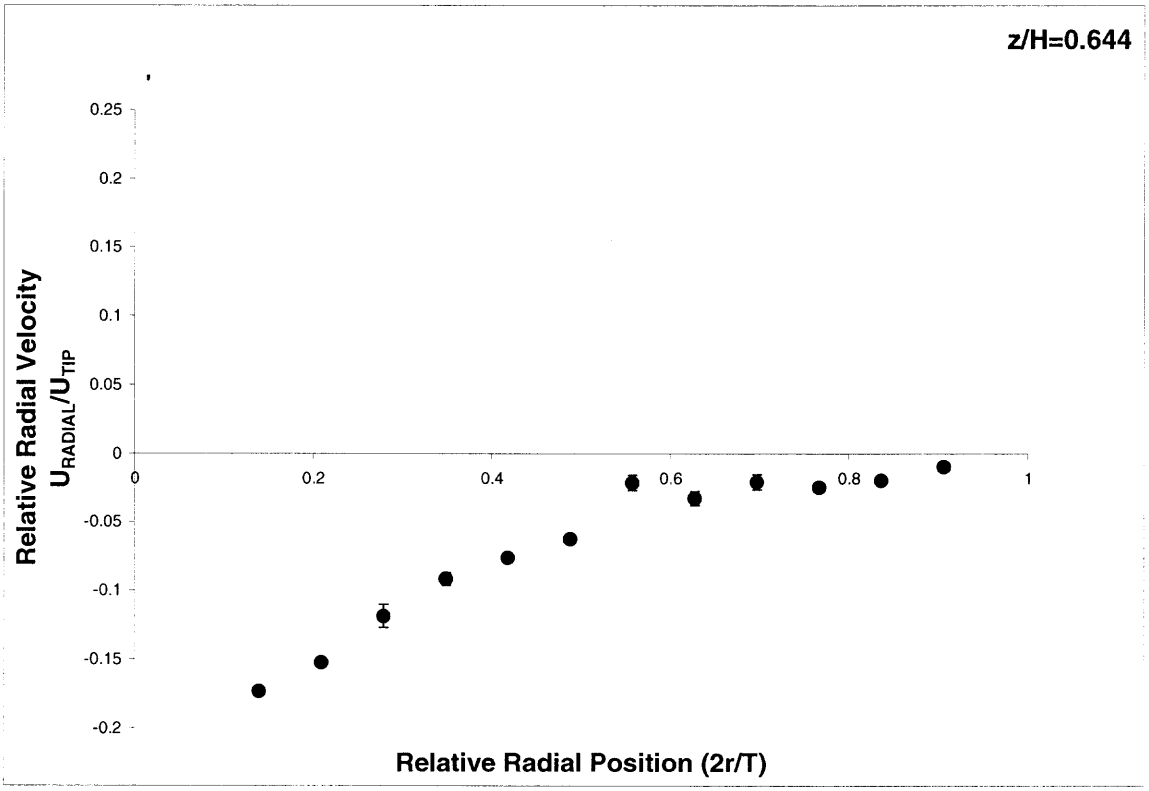

Figure A.2.3.1 Experimental radial velocity data at iso plane z=185mm in the baffled, cylindrical, flat-bottom tank with the standard error.

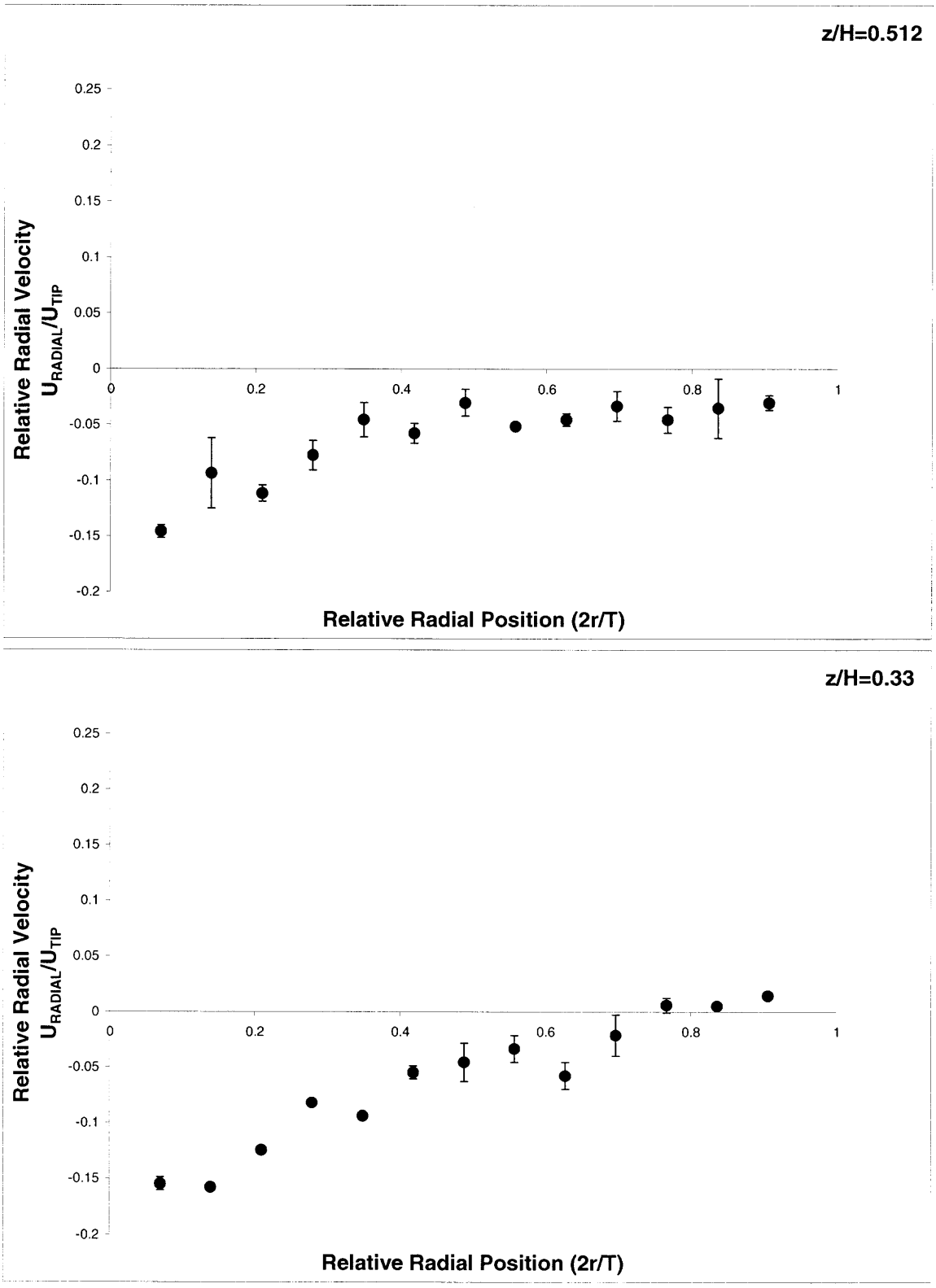

Figure A.2.3.2 Experimental radial velocity data at iso plane z=147mm and z=96mm in the baffled, cylindrical, flat-bottom tank with the standard error.

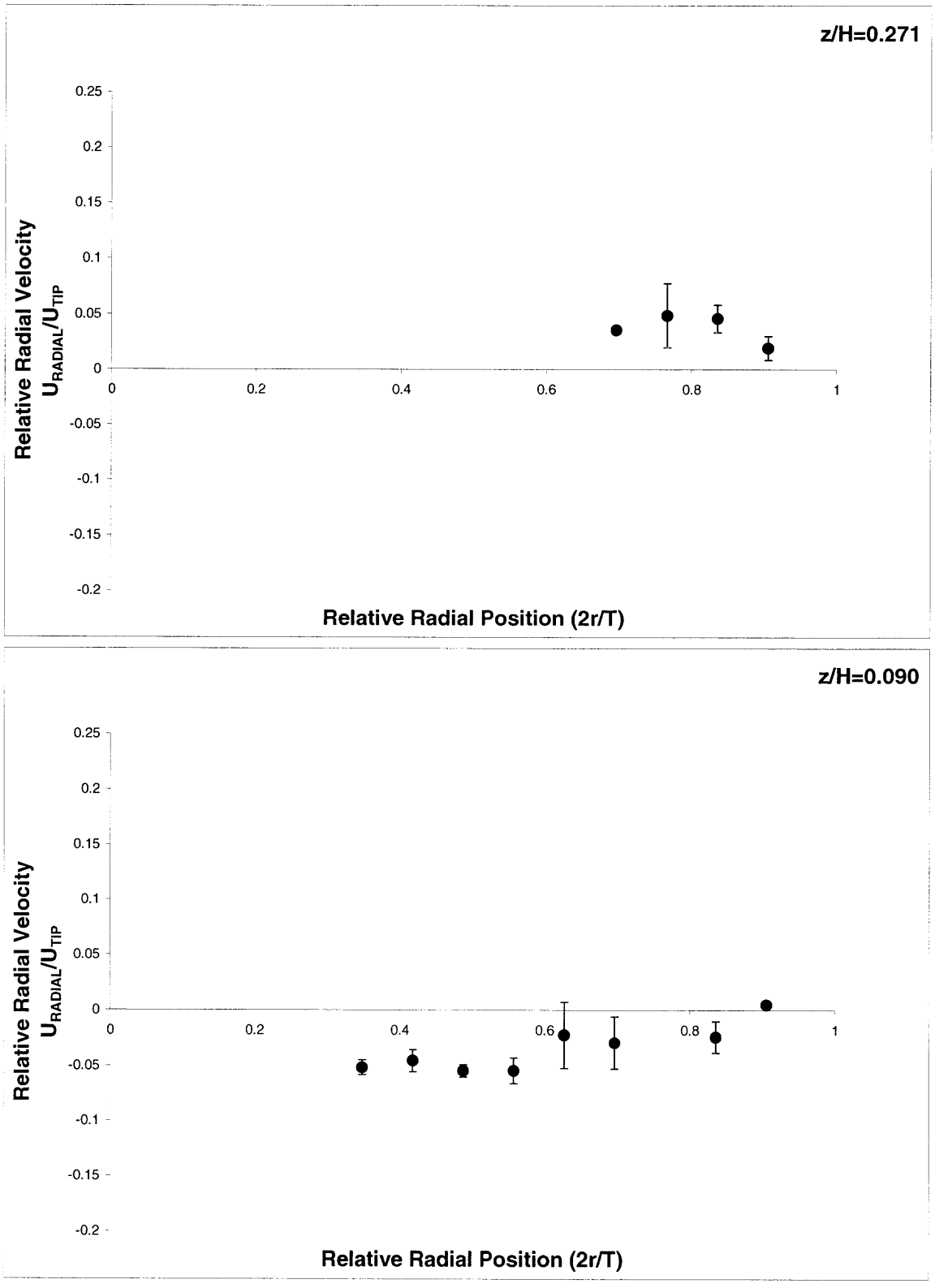

Figure A.2.3.3 Experimental radial velocity data at iso plane z=78mm and z=26mm in the baffled, cylindrical, flat-bottom tank with the standard error.

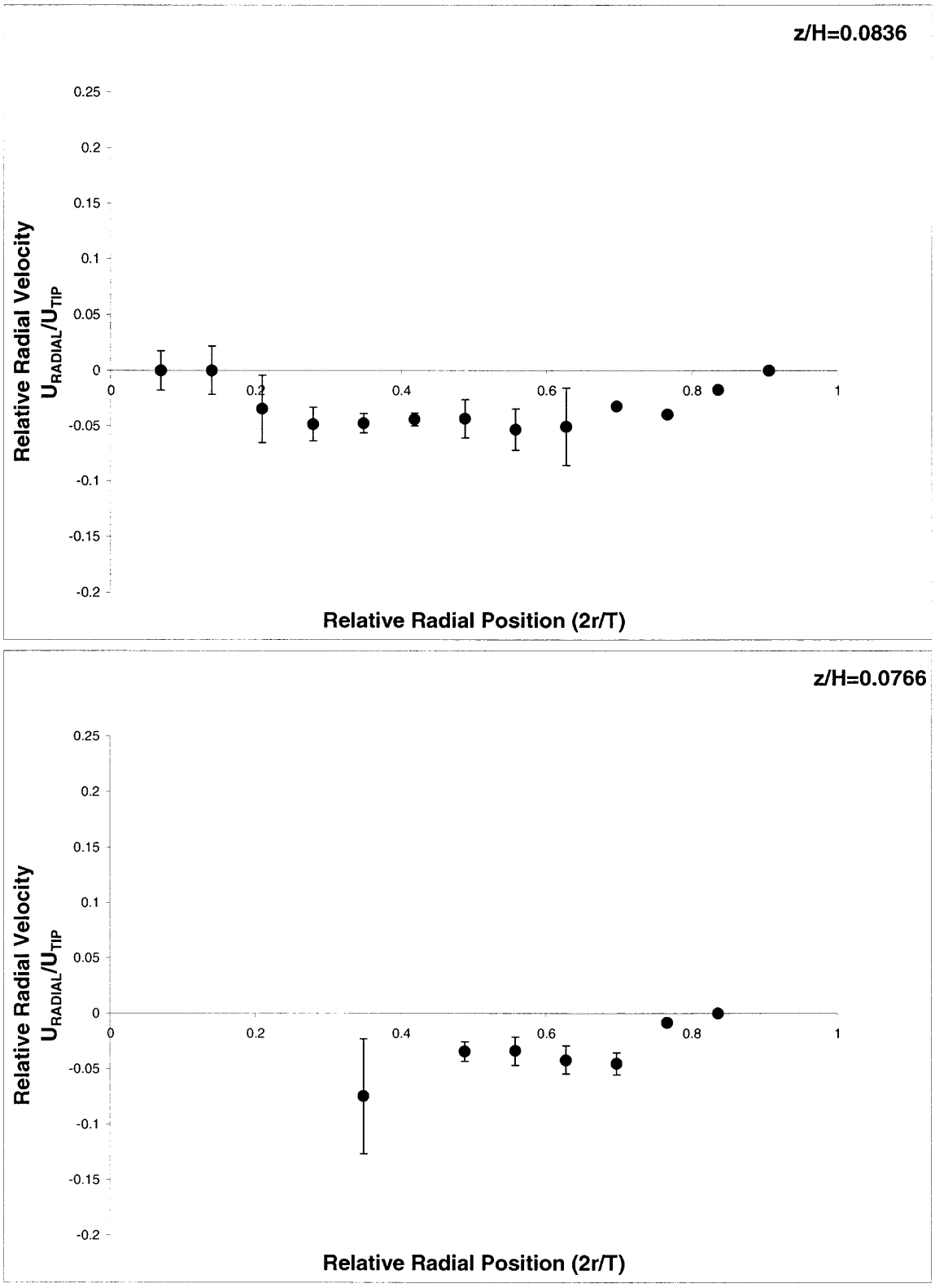

Figure A.2.3.4 Experimental radial velocity data at iso plane z=24mm and z=22mm in the baffled, cylindrical, flat-bottom tank with the standard error.

A.3 Experimental data in case of unbaffled, cylindrical, Hemispherical-bottom tank

A.3.1 Experimental tangential velocities obtained in the unbaffled, cylindrical, Hemispherical-bottom tank:

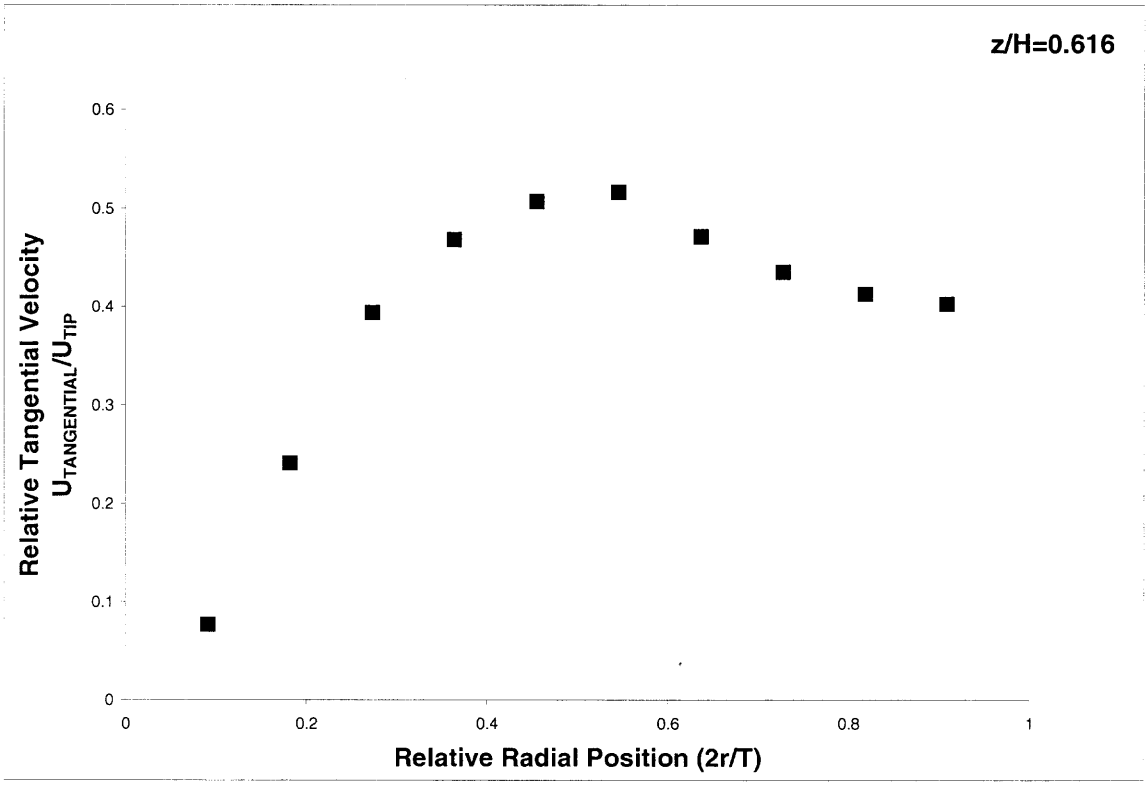

Figure A.3.1.1 Experimental tangential velocity data at iso plane z=185mm in the unbaffled, cylindrical, hemispherical-bottom tank.

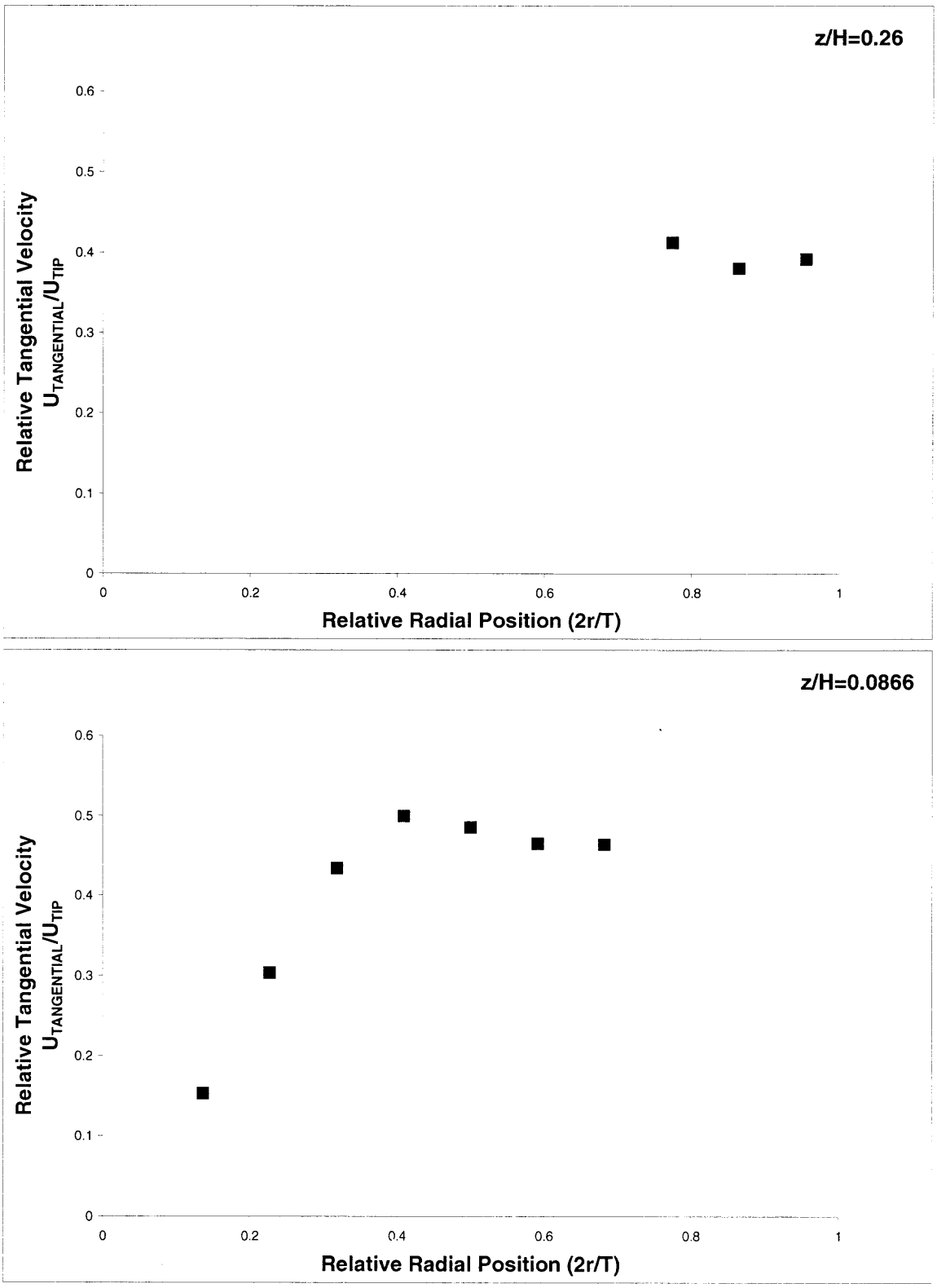

Figure A.3.1.2 Experimental tangential velocity data at iso plane z=78mm and z=26mm in the unbaffled, cylindrical, hemispherical-bottom tank.

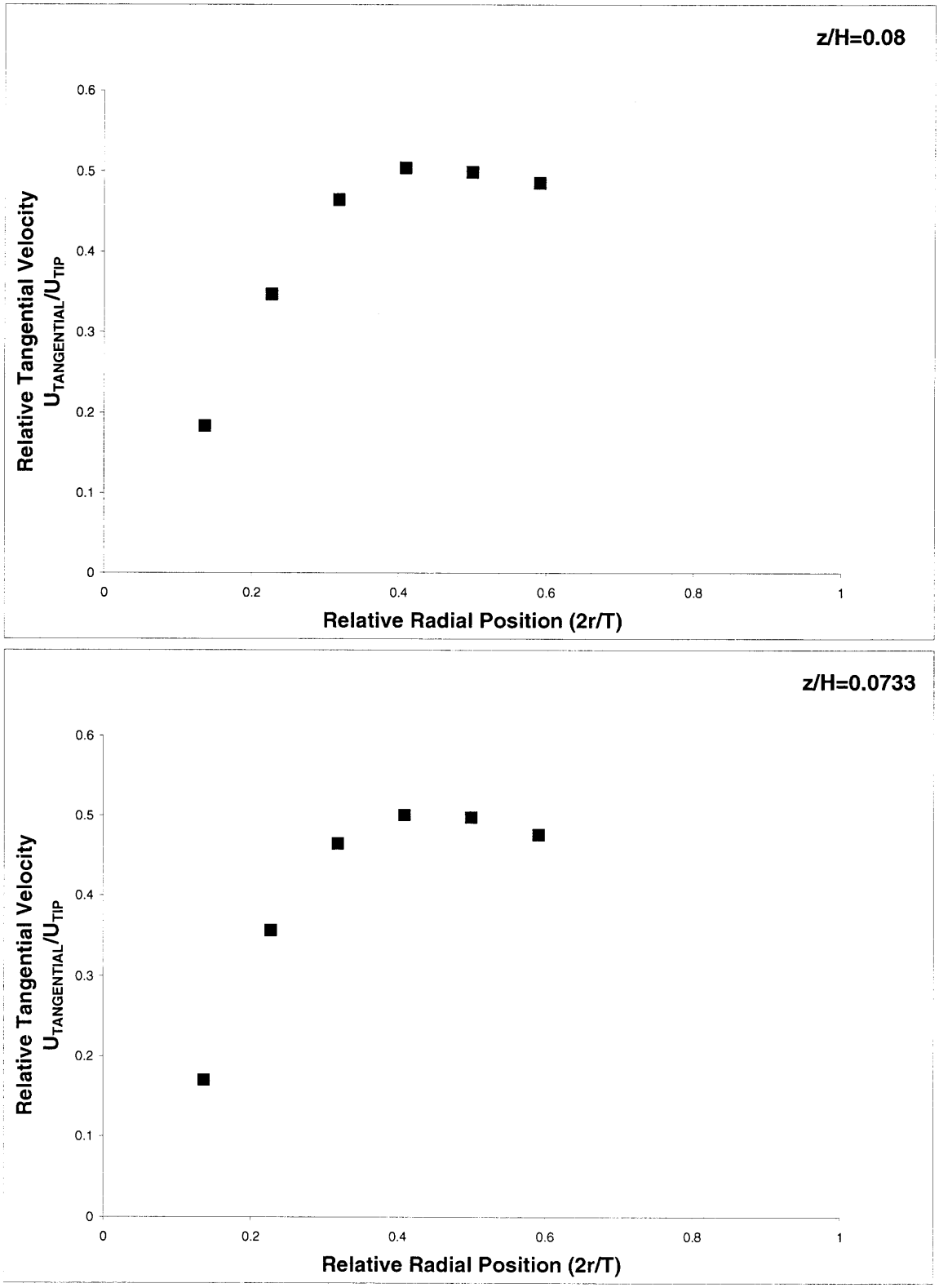

Figure A.3.1.3 Experimental tangential velocity data at iso plane z=24mm and z=24mm in the unbaffled, cylindrical, hemispherical-bottom tank.

A.3.2 Experimental axial velocities obtained in the unbaffled, cylindrical, Hemispherical-bottom tank:

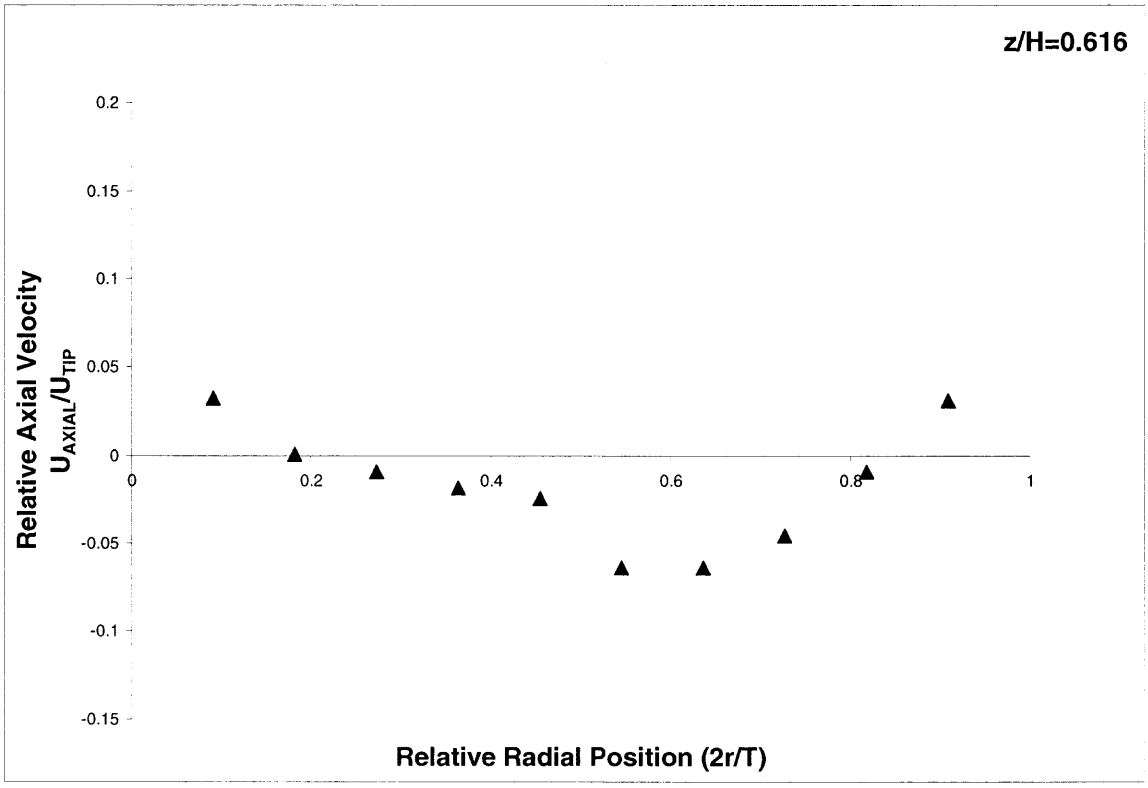

Figure A.3.2.1 Experimental axial velocity data at iso plane z=185mm in the unbaffled, cylindrical, hemispherical-bottom tank.

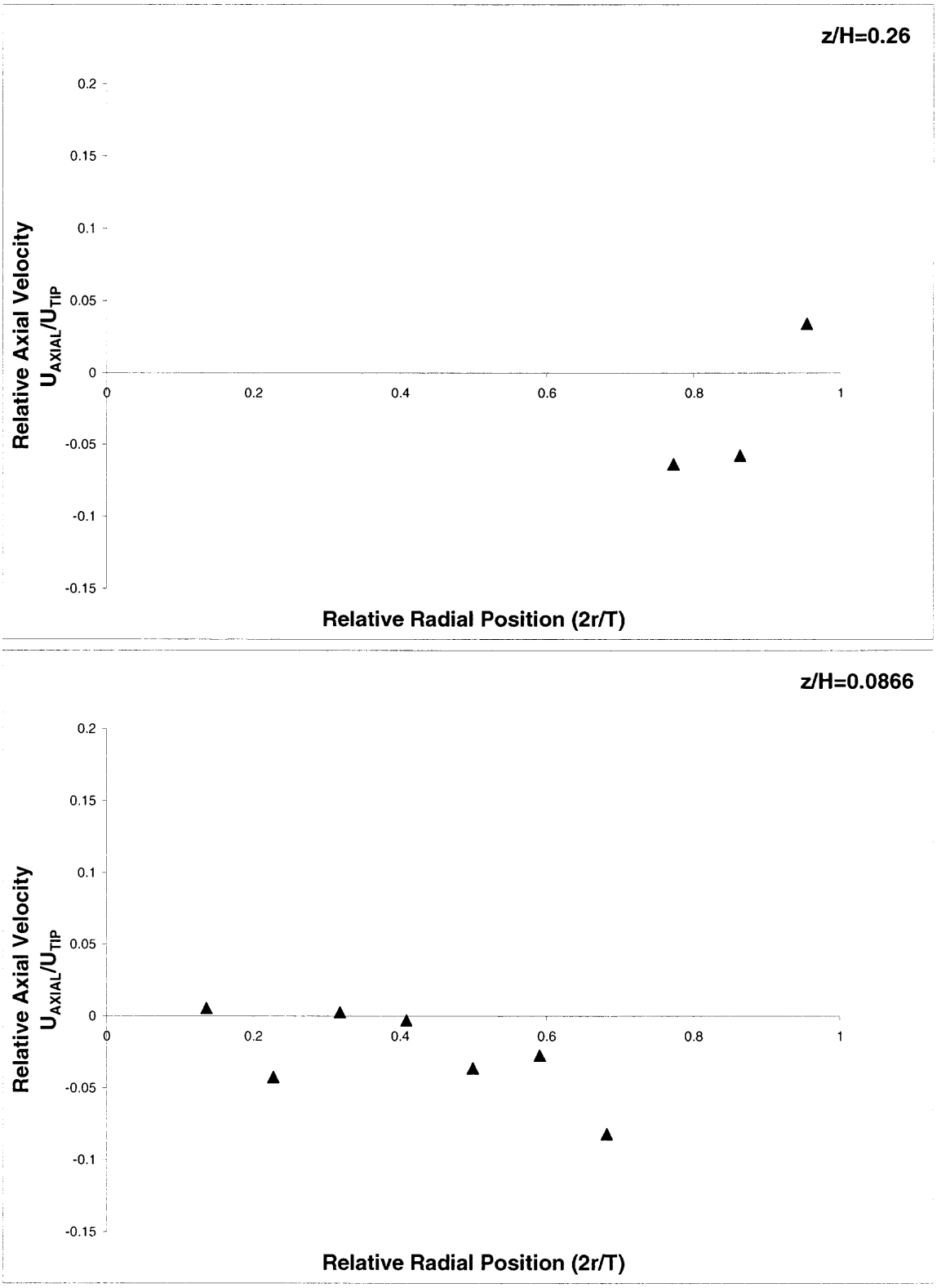

Figure A.3.2.2 Experimental axial velocity data at iso plane z=78mm and z=26mm in the unbaffled, cylindrical, hemispherical-bottom tank.

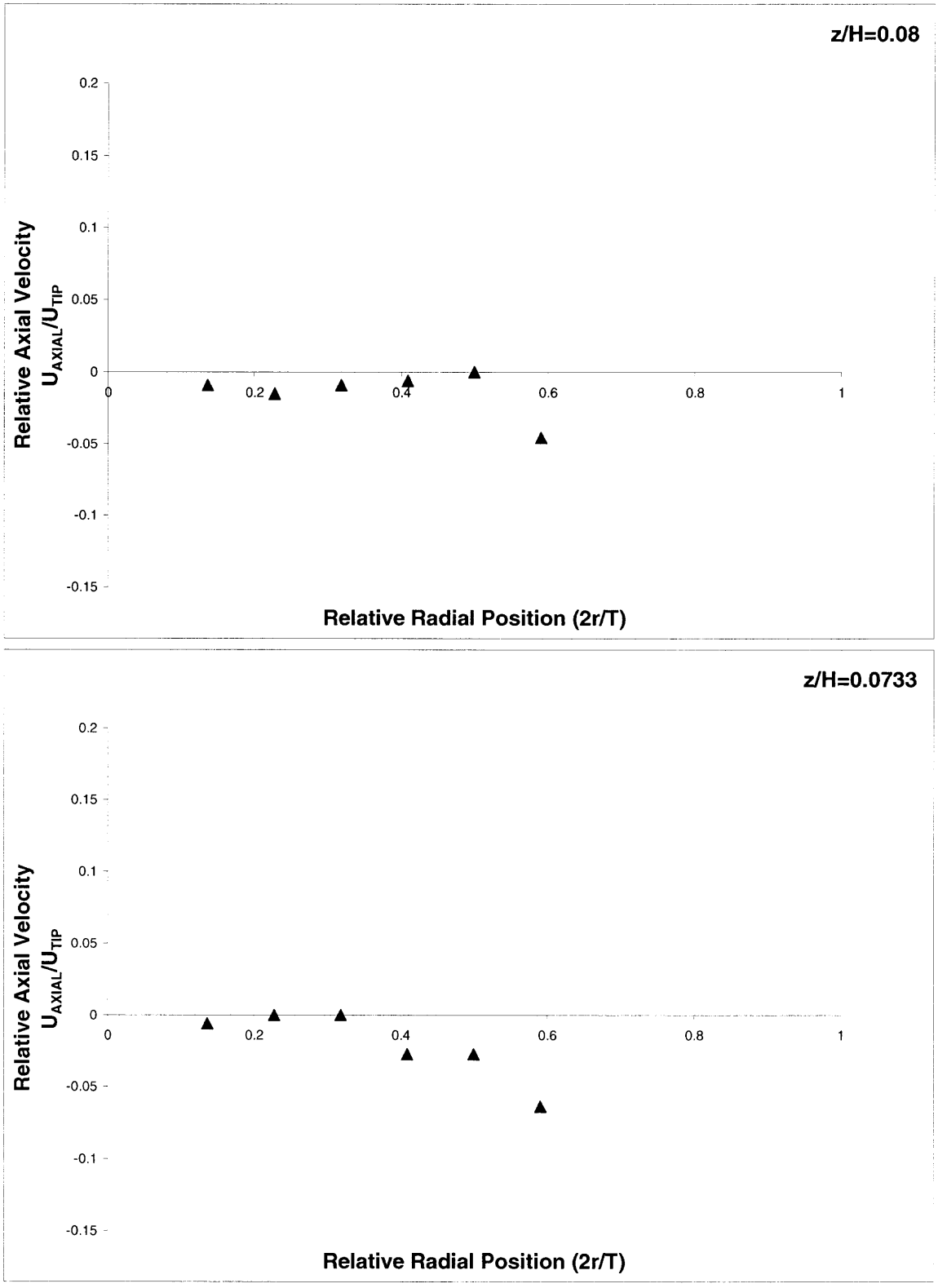

Figure A.3.2.3 Experimental axial velocity data at iso plane z=22mm in the unbaffled, cylindrical, hemispherical-bottom tank.

A.4 Experimental data in case of baffled, cylindrical, Hemispherical-bottom tank

A.4.1 Experimental tangential velocities obtained in the unbaffled, cylindrical, Hemispherical-bottom tank:

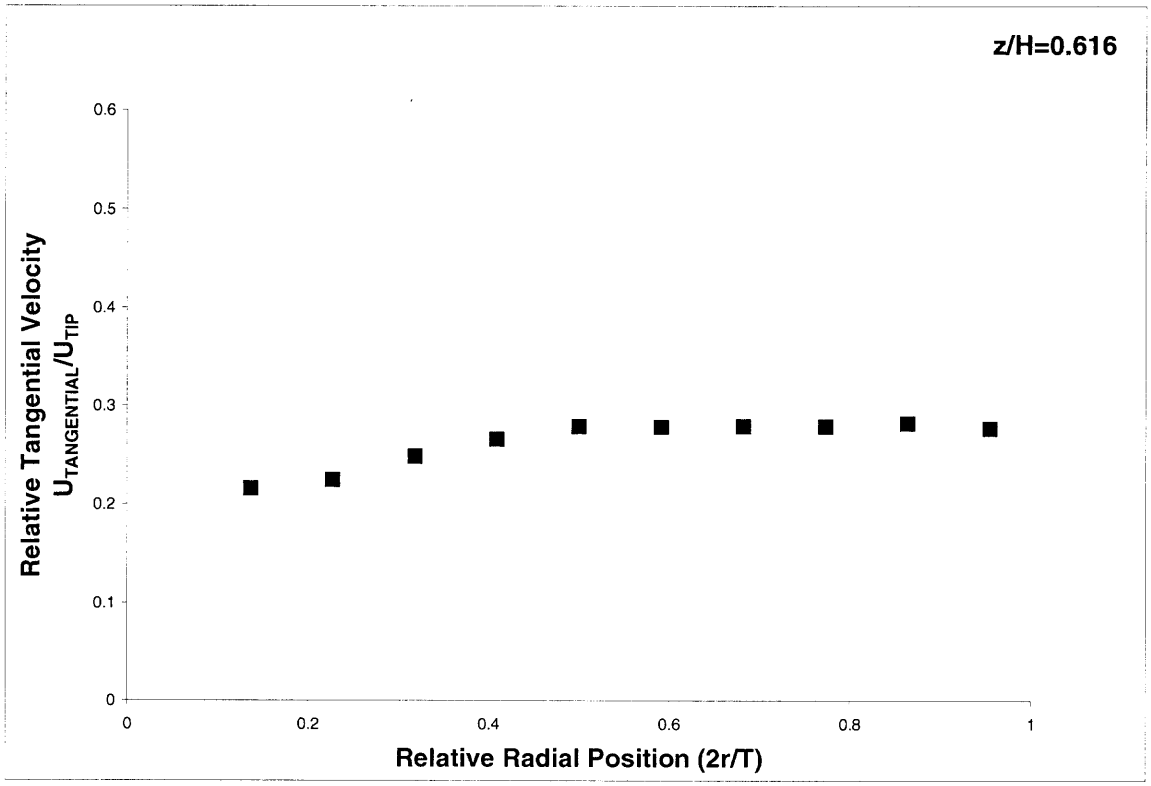

Figure A.4.1.1 Experimental tangential velocity data at iso plane z=185mm in the baffled, cylindrical, hemispherical-bottom tank.

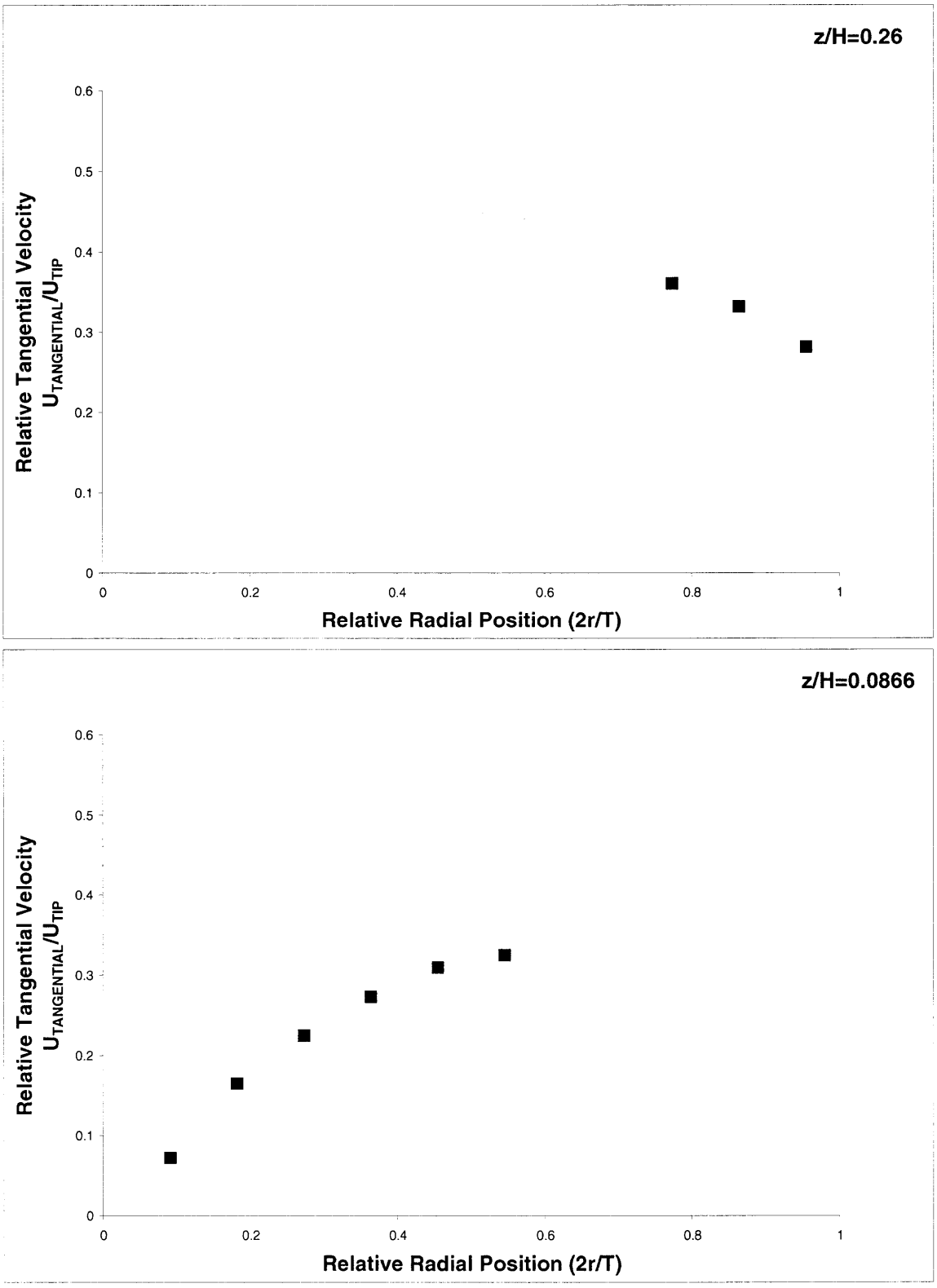

Figure A.4.1.2 Experimental tangential velocity data at iso plane z=78mm and z=26mm in the baffled, cylindrical, hemispherical-bottom tank.

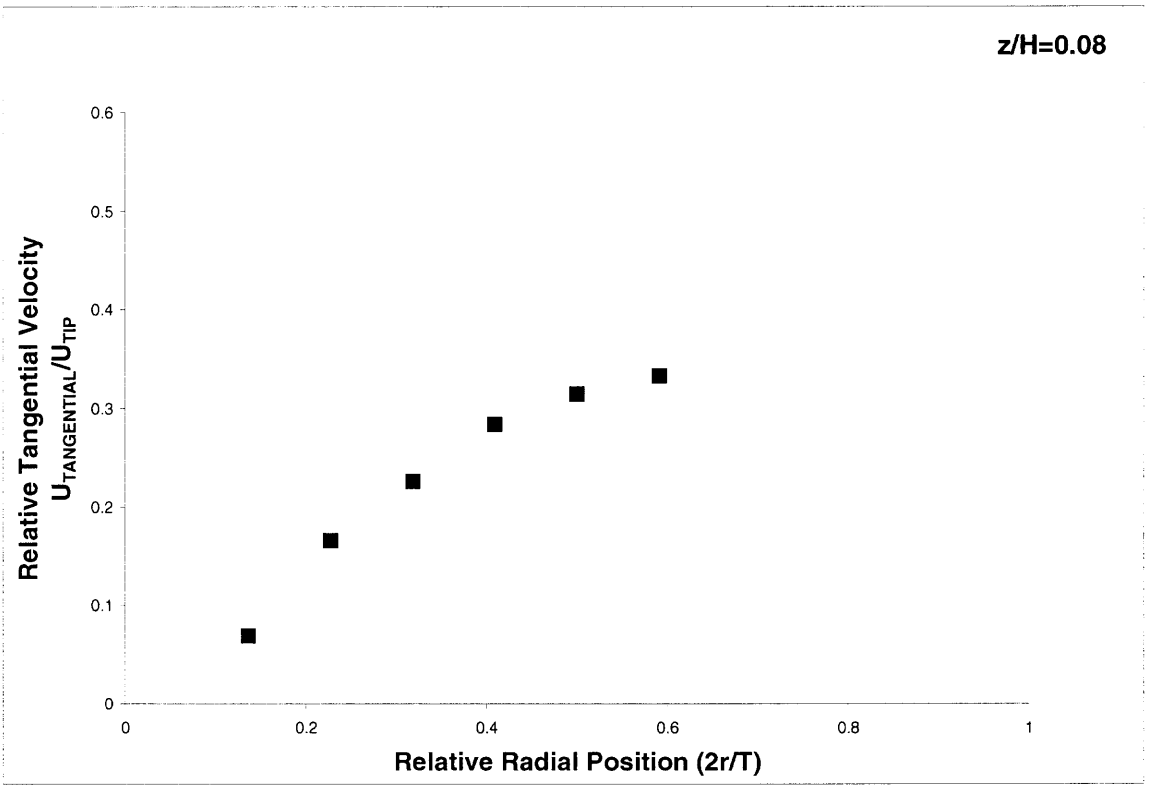

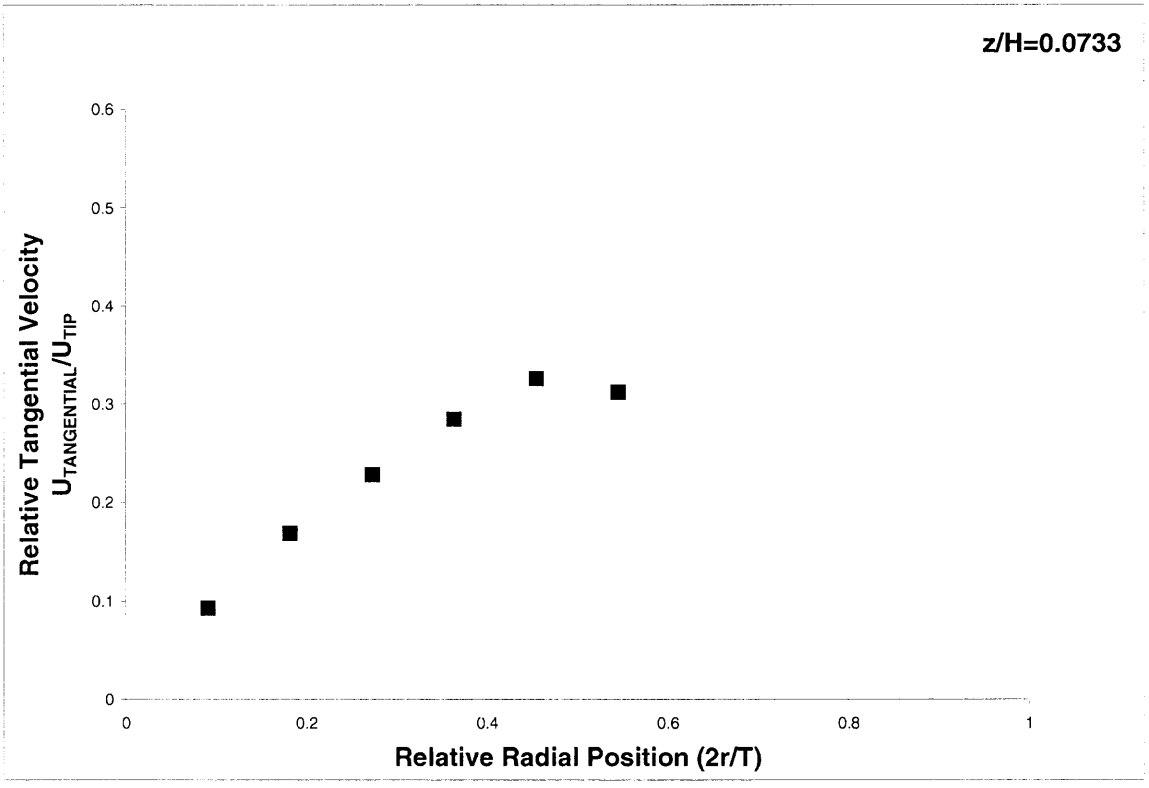

Figure A.4.1.3 Experimental tangential velocity data at iso plane z=24mm and z=22mm in the baffled, cylindrical, hemispherical-bottom tank.

A.4.2 Experimental axial velocities obtained in the unbaffled, cylindrical, Hemispherical-bottom tank:

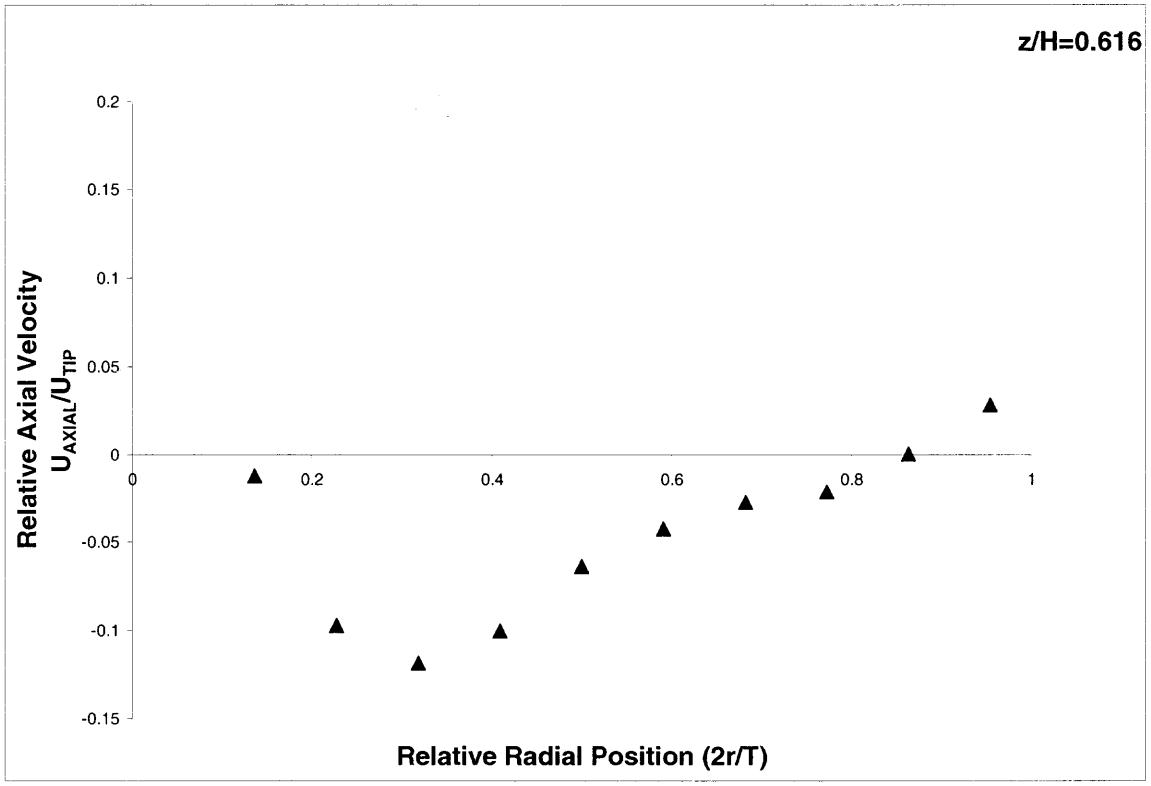

Figure A.4.2.1 Experimental axial velocity data at iso plane z=185mm in the baffled, cylindrical, hemispherical-bottom tank.

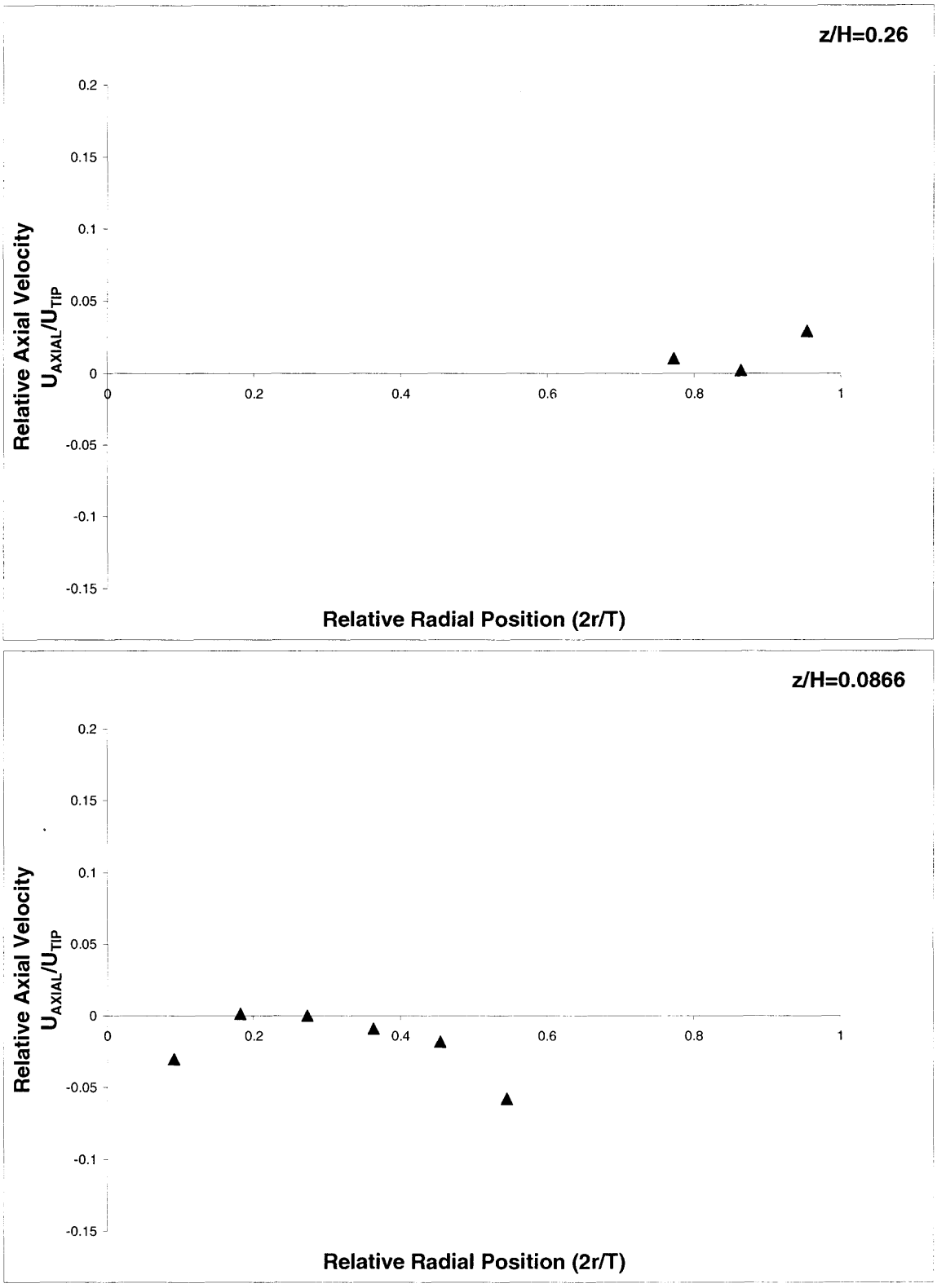

Figure A.4.2.2 Experimental axial velocity data at iso plane z=78mm and z=26mm in the baffled, cylindrical, hemispherical-bottom tank

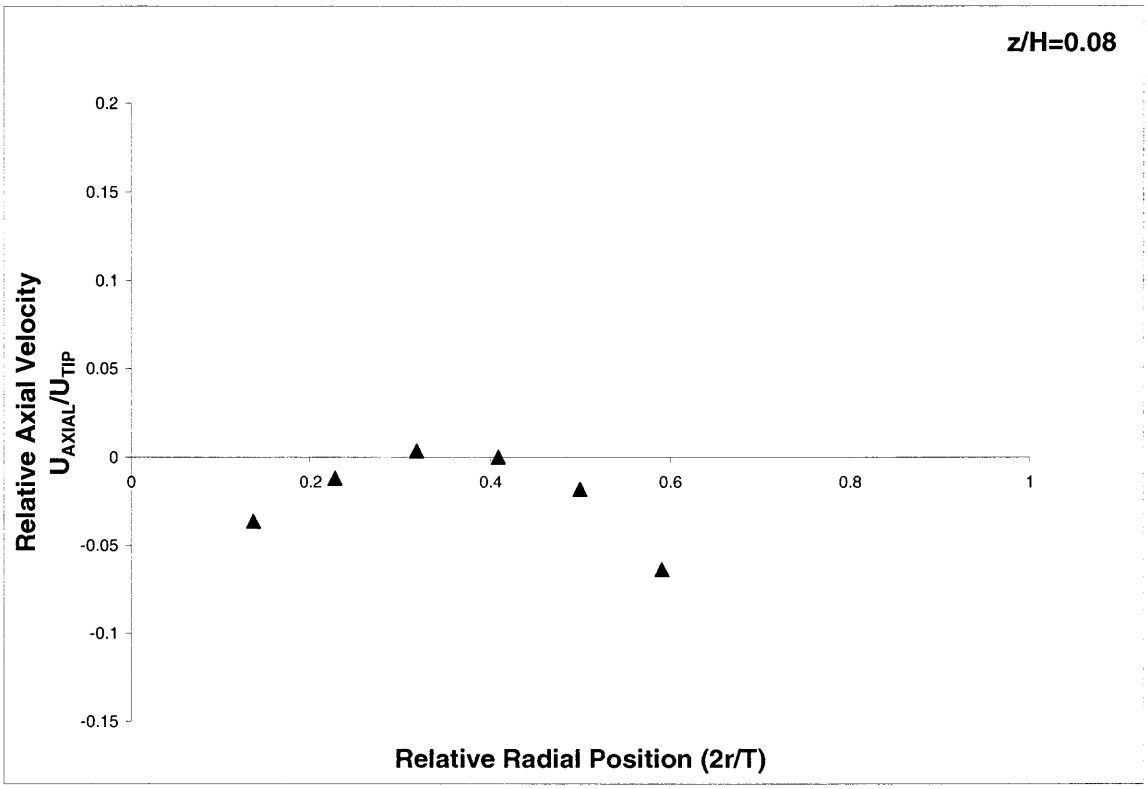

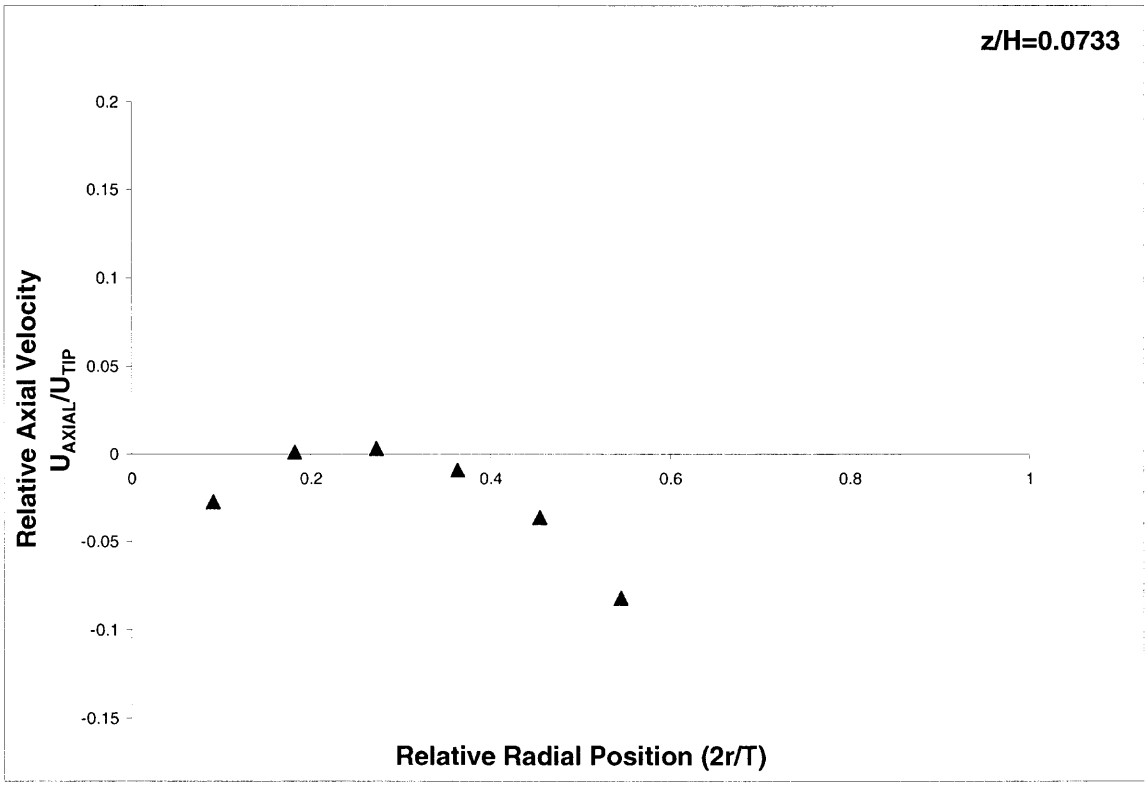

Figure A.4.2.3 Experimental axial velocity data at iso plane z=24mm and z=22mm in the unbaffled, cylindrical, hemispherical-bottom tank.

APPENDIX B

COMPARISON BETWEEN LDV EXPERIMENTAL RESULTS AND CFD PREDICTIONS

Experimental LDV results are presented in this Appendix as follows:

APPENDIX B

COMPARISON BETWEEN LDV DATA AND CFD PREDICTIONS

B.1 Comparison between LDV data and the CFD prediction in unbaffled, flat-bottom tank.

B.1.1 Comparison between LDV data and CFD prediction for tangential velocities:

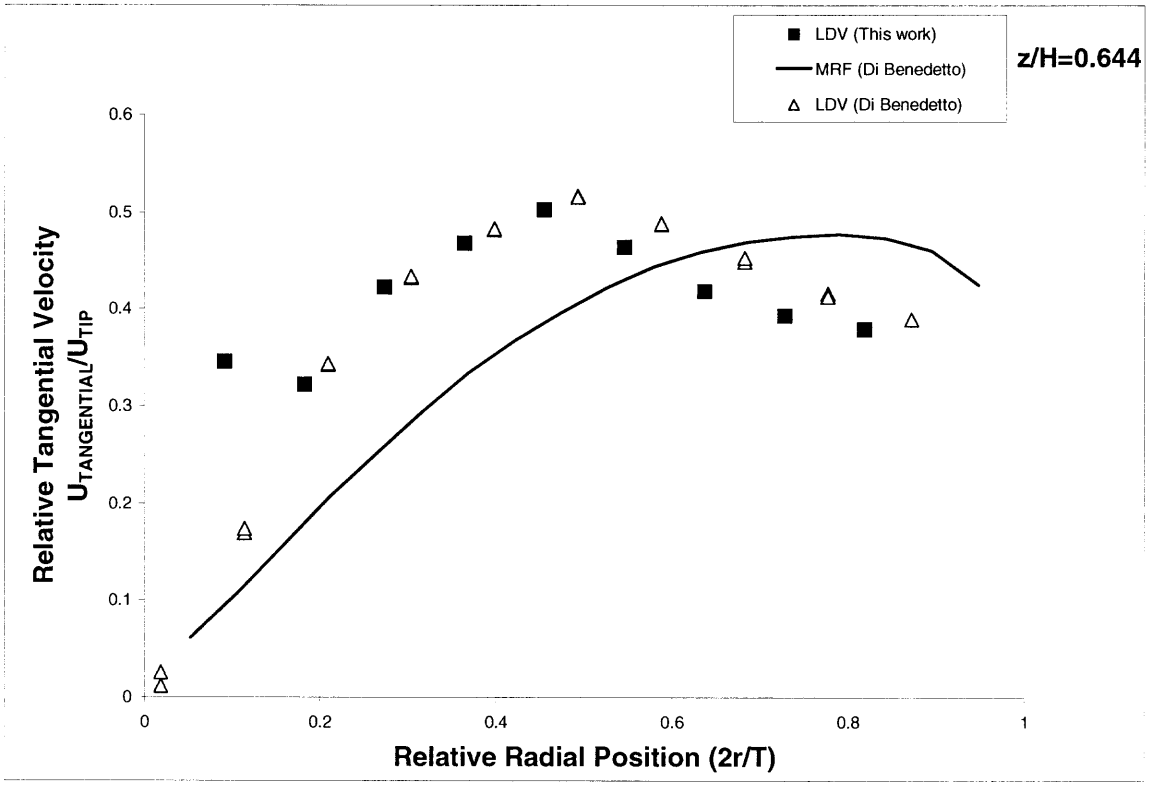

Figure B.1.1.1 Comparison between LDV data and CFD prediction for tangential velocities at iso-surfaces z=185mm in the unbaffled, flat-bottom tank.

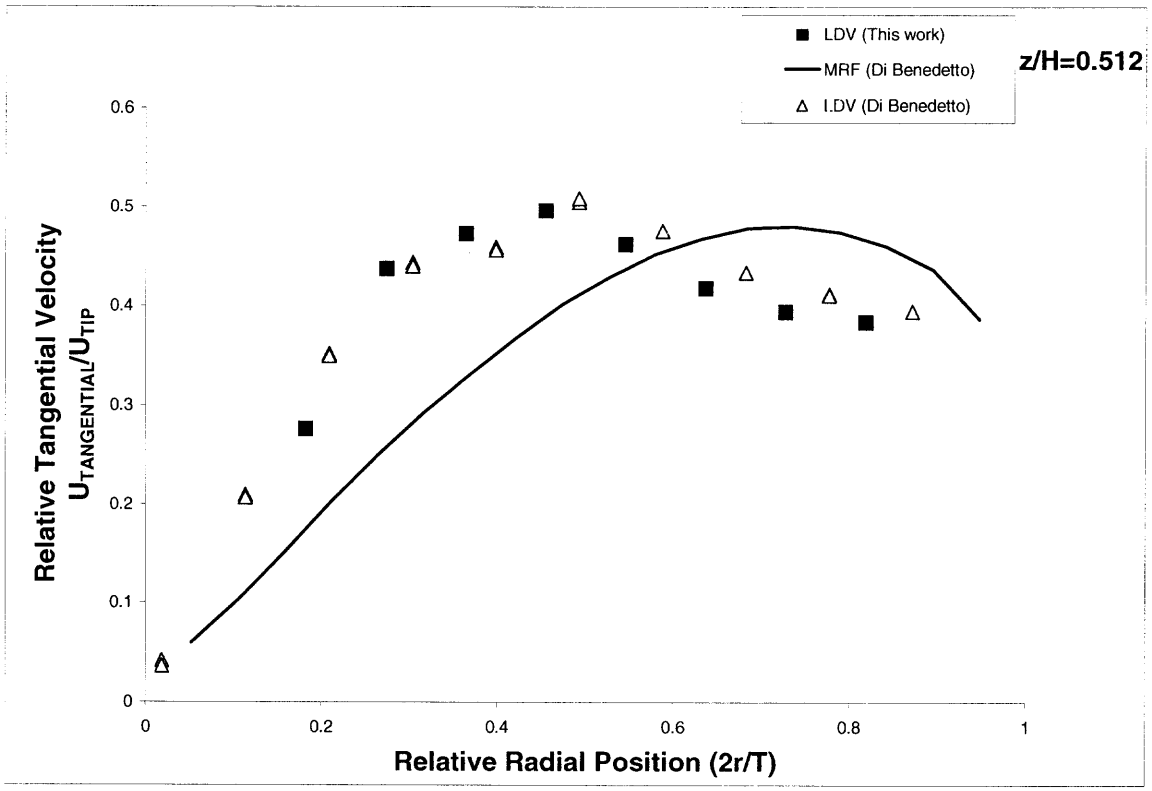

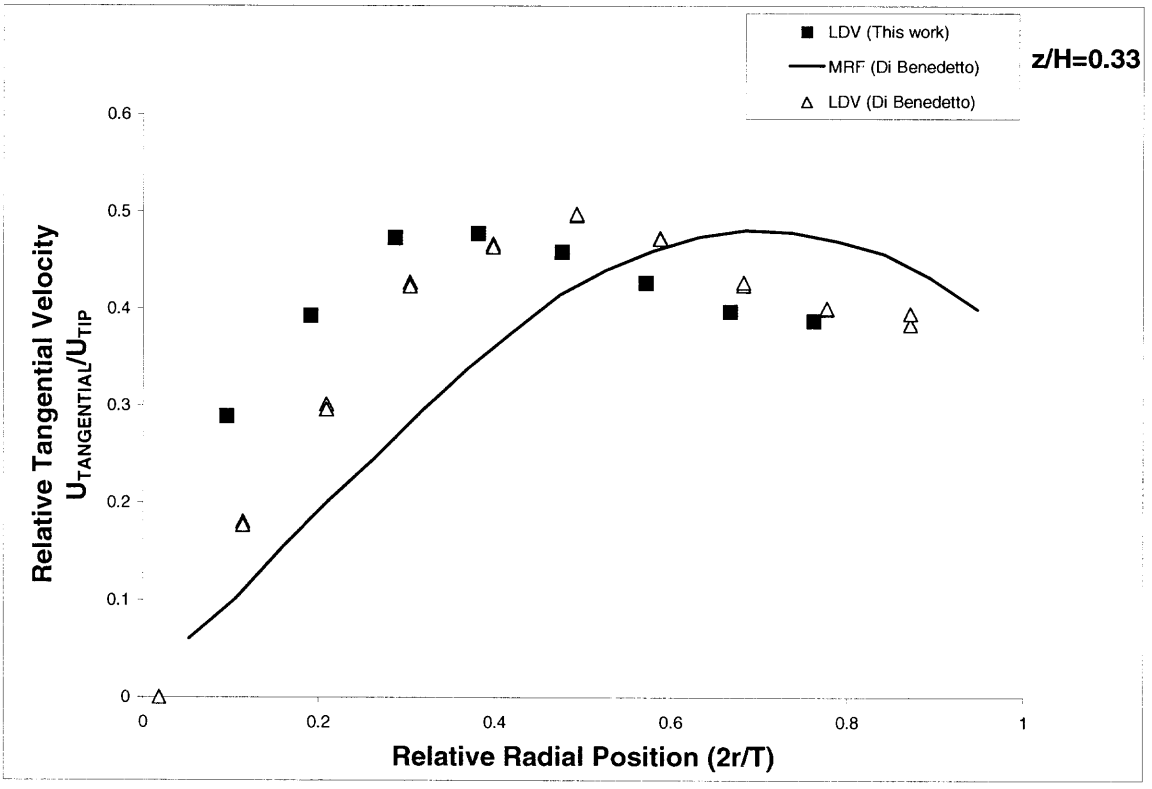

Figure B.1.1.2 Comparison between LDV data and CFD prediction for tangential velocities at iso-surfaces z=147mm and z=96mm in the unbaffled, flat-bottom tank.

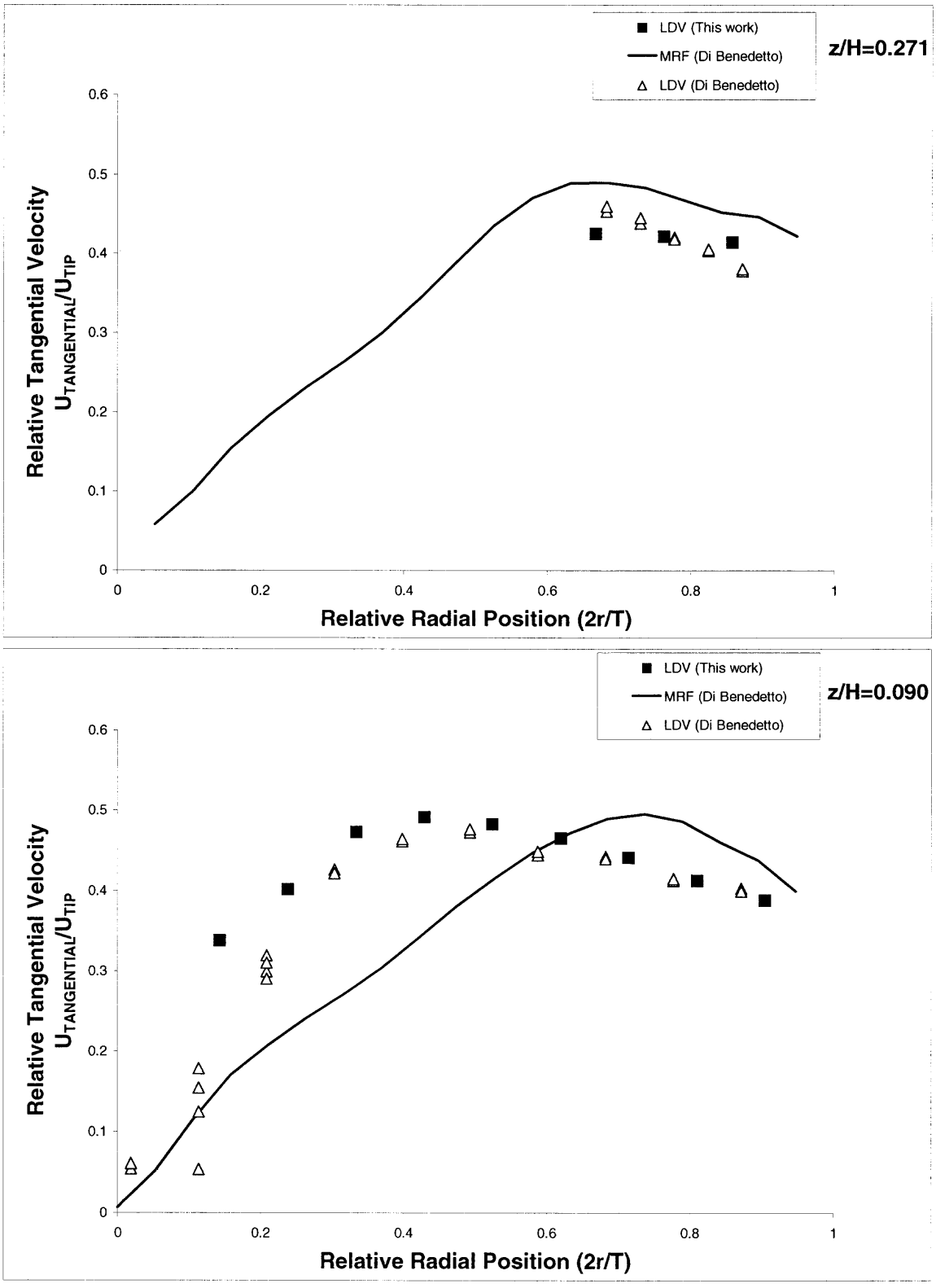

Figure B.1.1.3 Comparison between LDV data and CFD prediction for tangential velocities at iso-surfaces z=78mm and z=26mm in the unbaffled, flat-bottom tank.

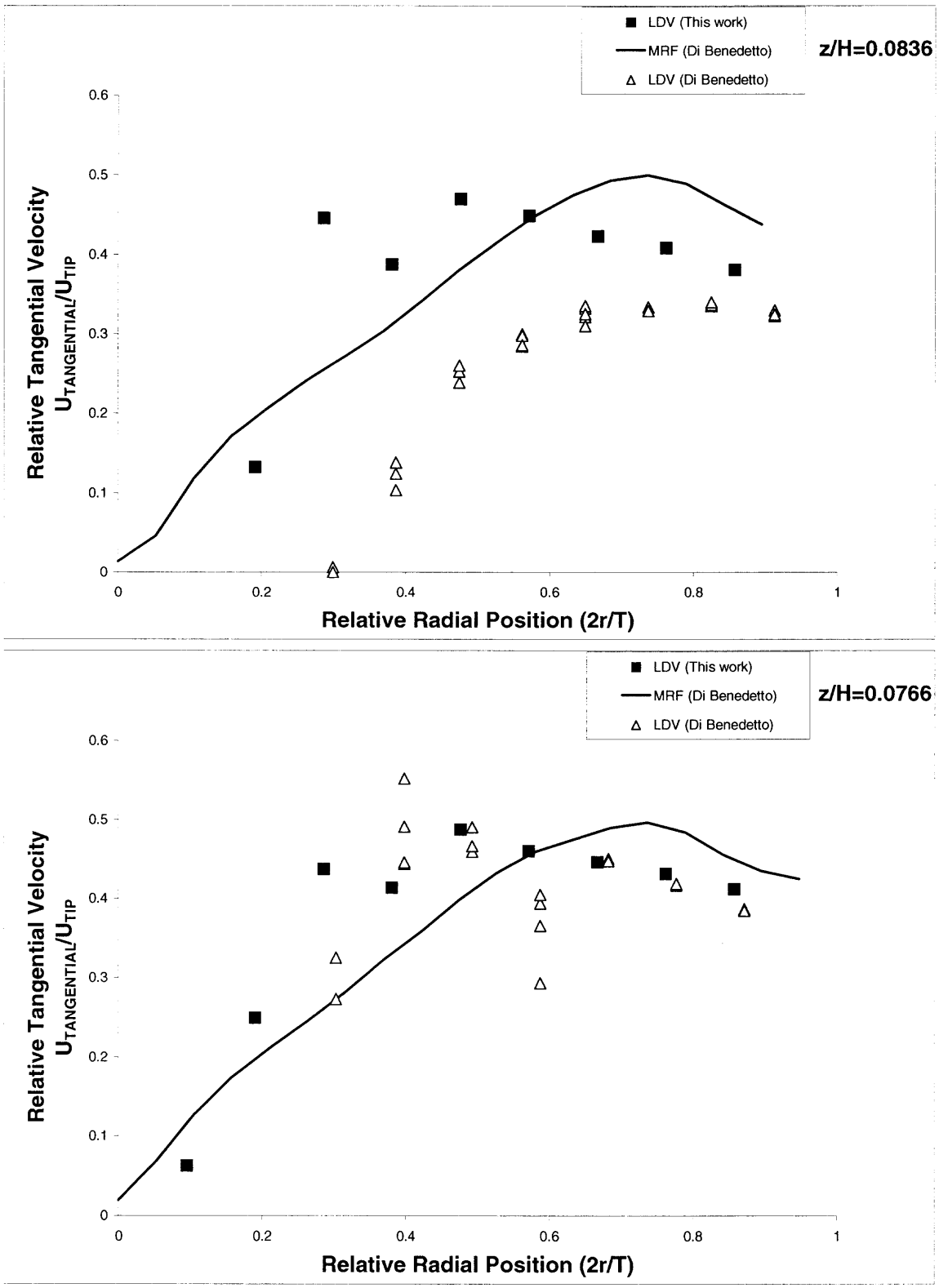

Figure B.1.1.4 Comparison between LDV data and CFD prediction for tangential velocities at iso-surfaces z=24mm and z=22mm in the unbaffled, flat-bottom tank.

B.1.2 Comparison between LDV data and CFD prediction for axial velocities:

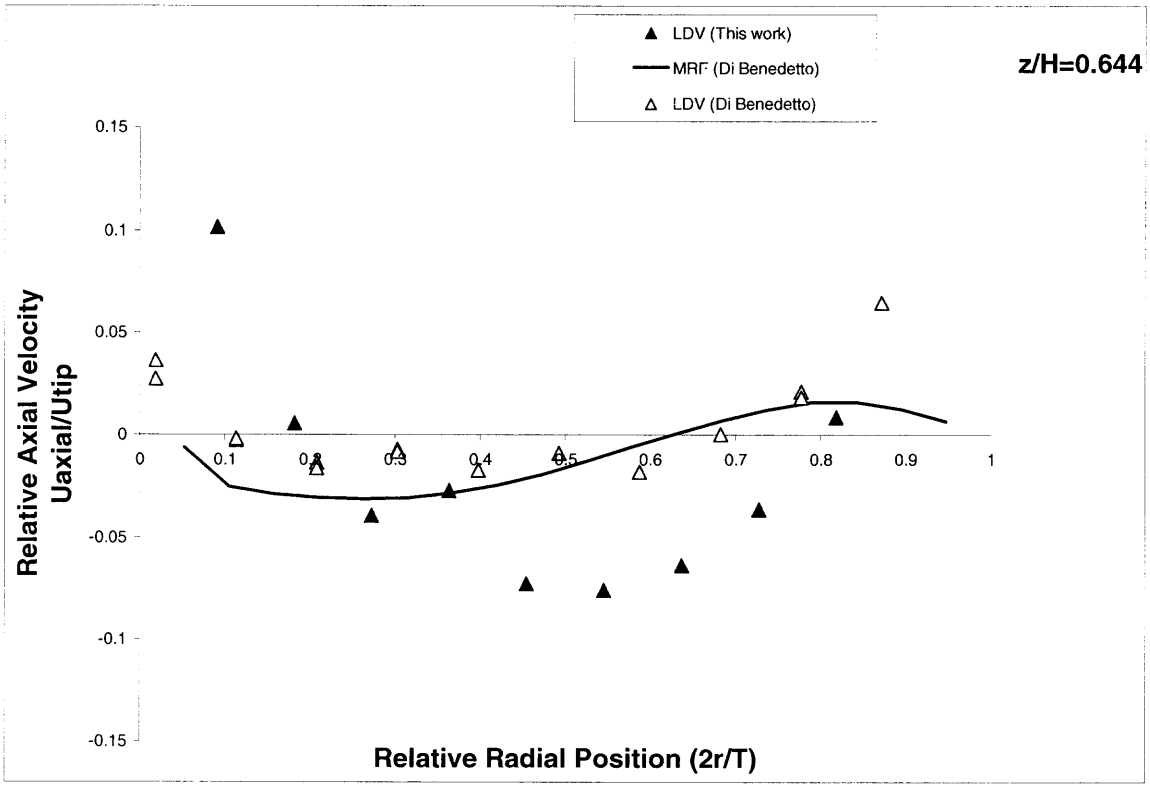

Figure B.1.2.1 Comparison between LDV data and CFD prediction for axial velocities at iso-surfaces z=185mm in the unbaffled, flat-bottom tank.

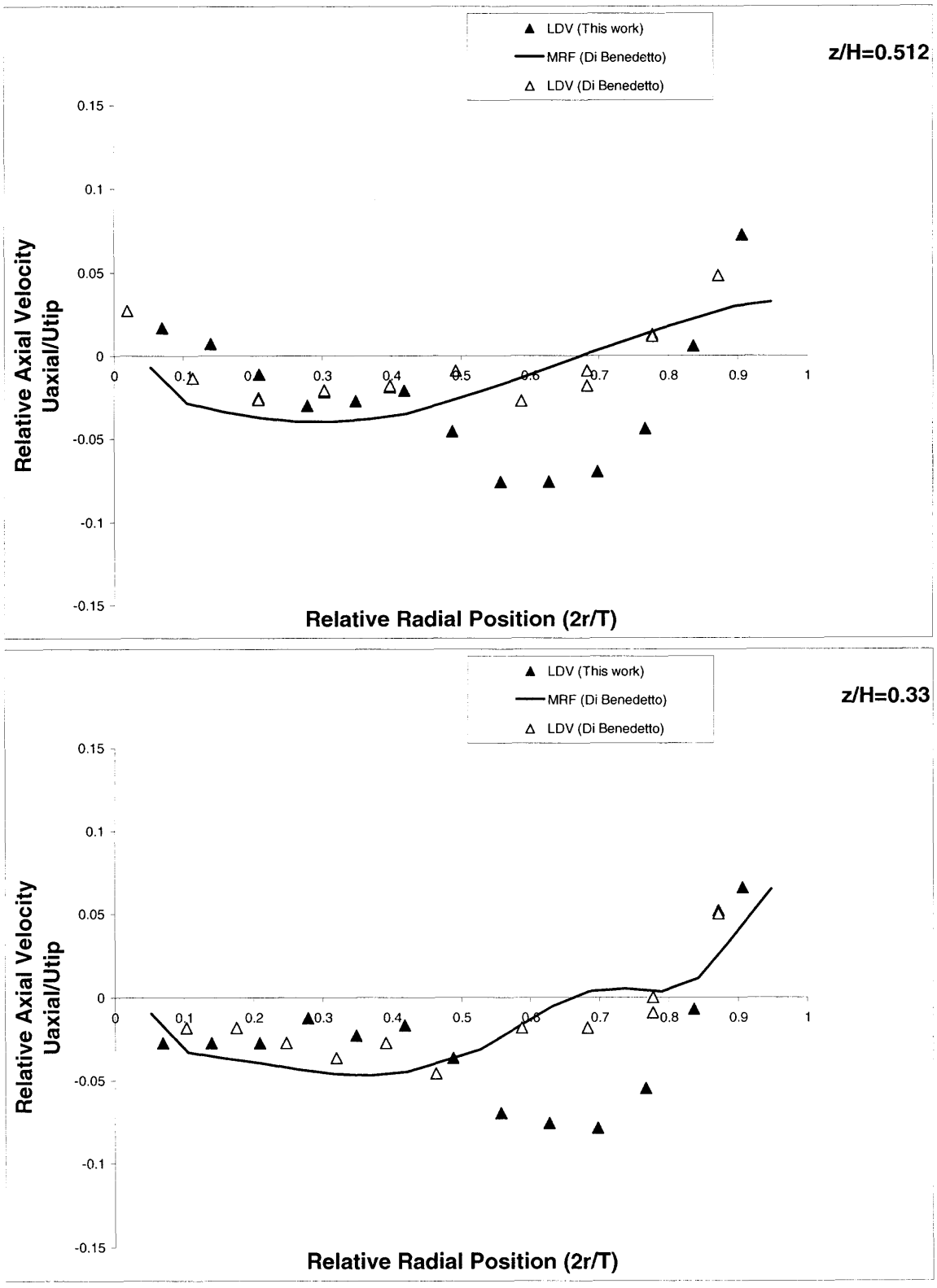

Figure B.1.2.2 Comparison between LDV data and CFD prediction for axial velocities at iso-surfaces z=147mm and z=96mm in the unbaffled, flat-bottom tank

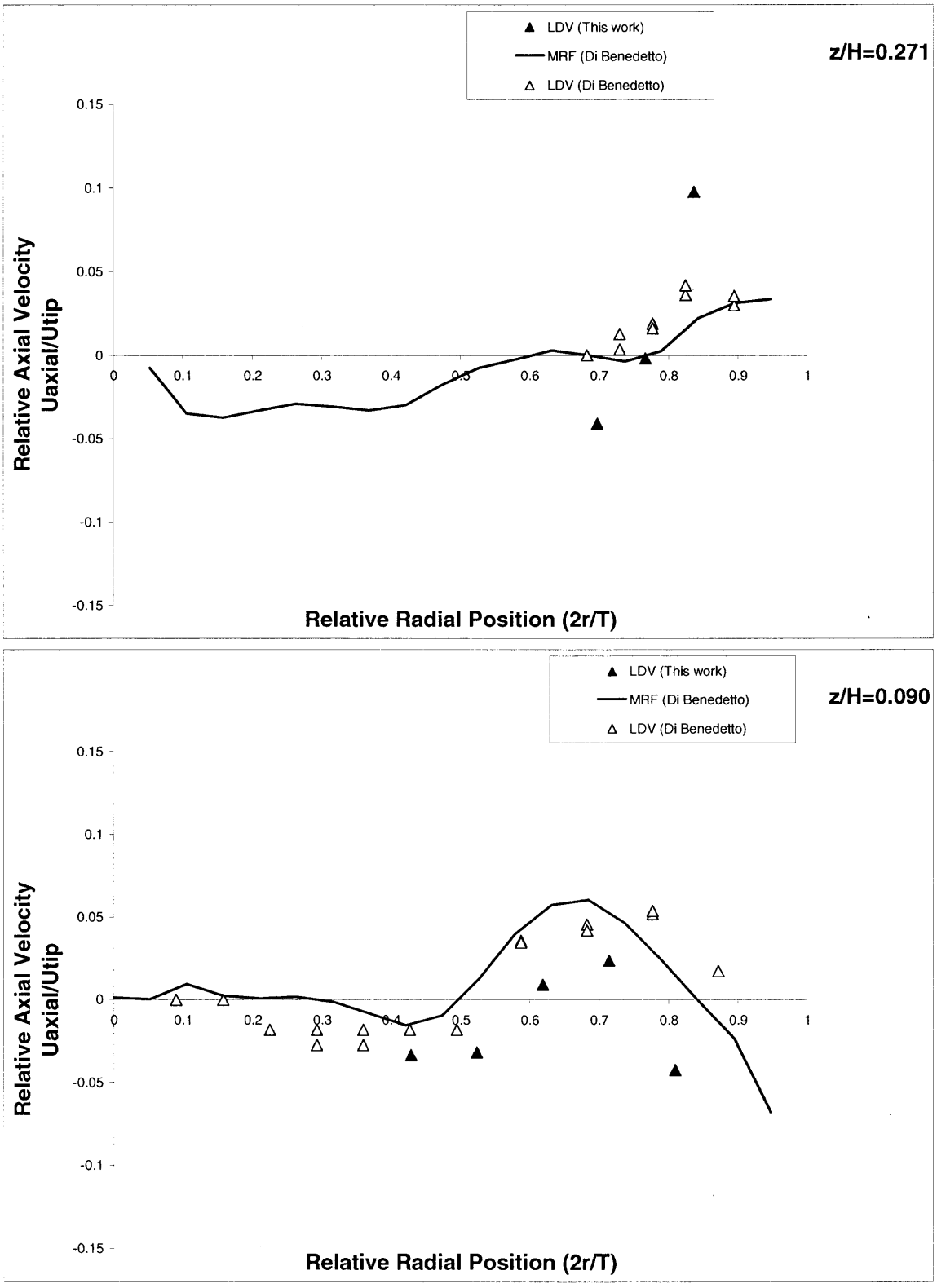

Figure B.1.2.3 Comparison between LDV data and CFD prediction for axial velocities at iso-surfaces z=78mm and z=26mm in the unbaffled, flat-bottom tank.

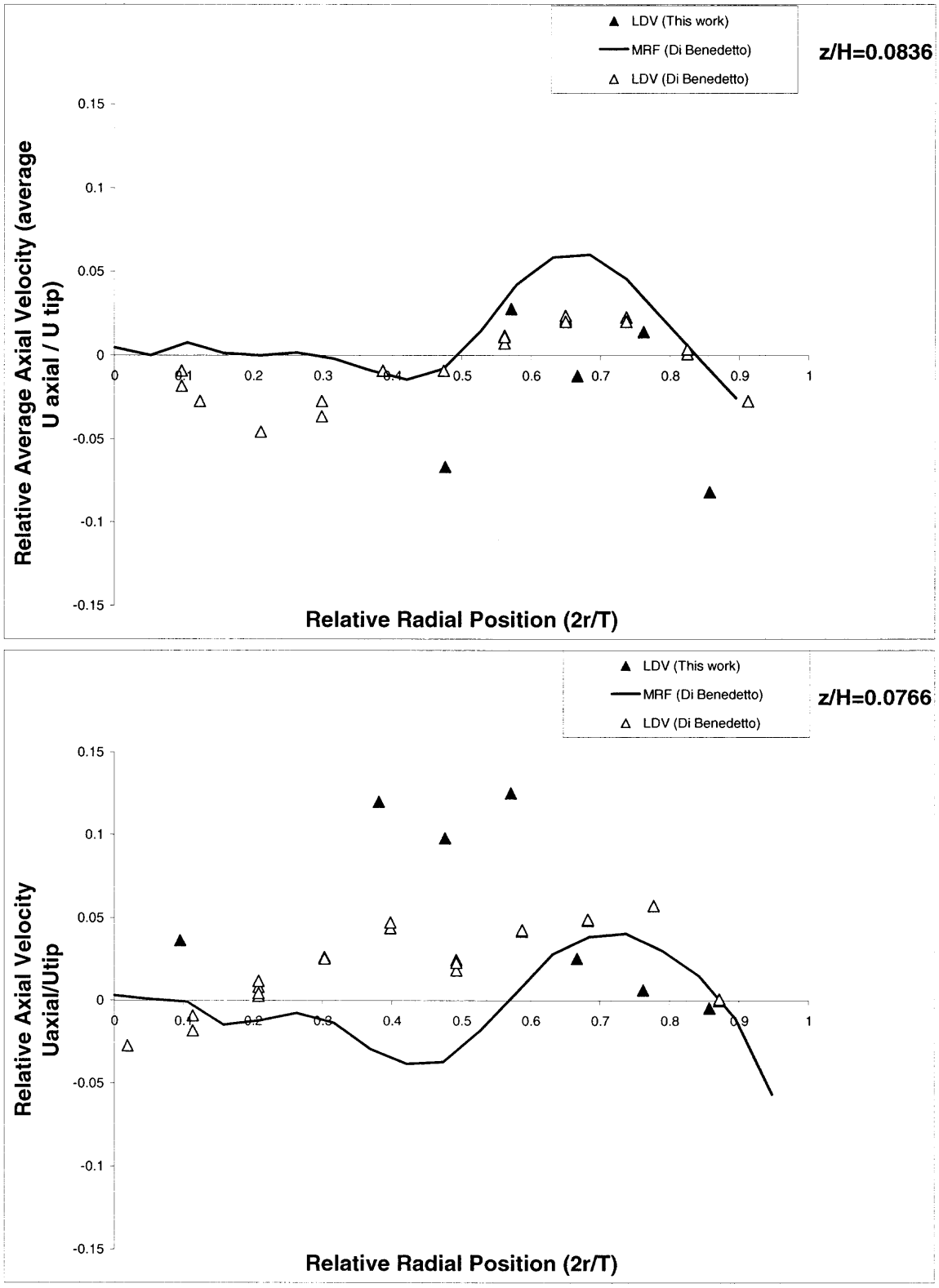

Figure B.1.2.4 Comparison between LDV data and CFD prediction for axial velocities at iso-surfaces z=24mm and z=22mm in the unbaffled, flat-bottom tank.

B.1.3 Comparison between LDV data and CFD prediction for radial velocities:

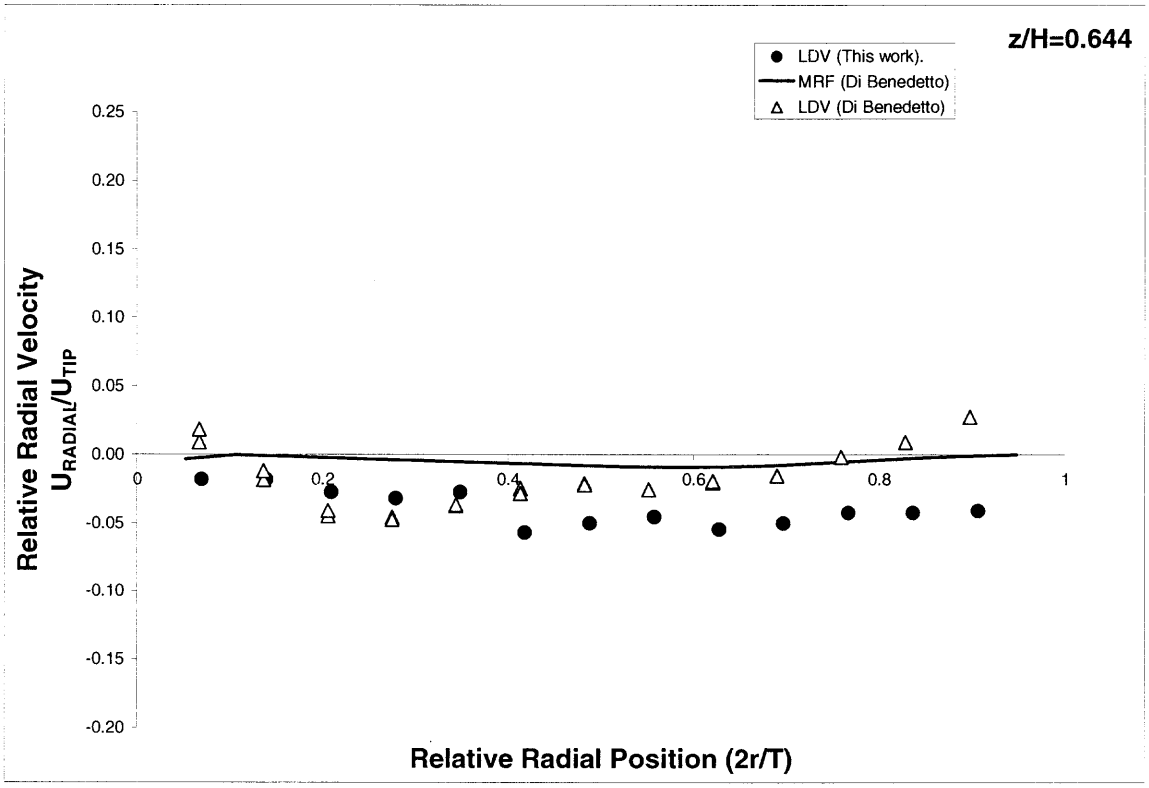

Figure B.1.3.1 Comparison between LDV data and CFD prediction for radial velocities at iso-surfaces z=185mm in the unbaffled, flat-bottom tank

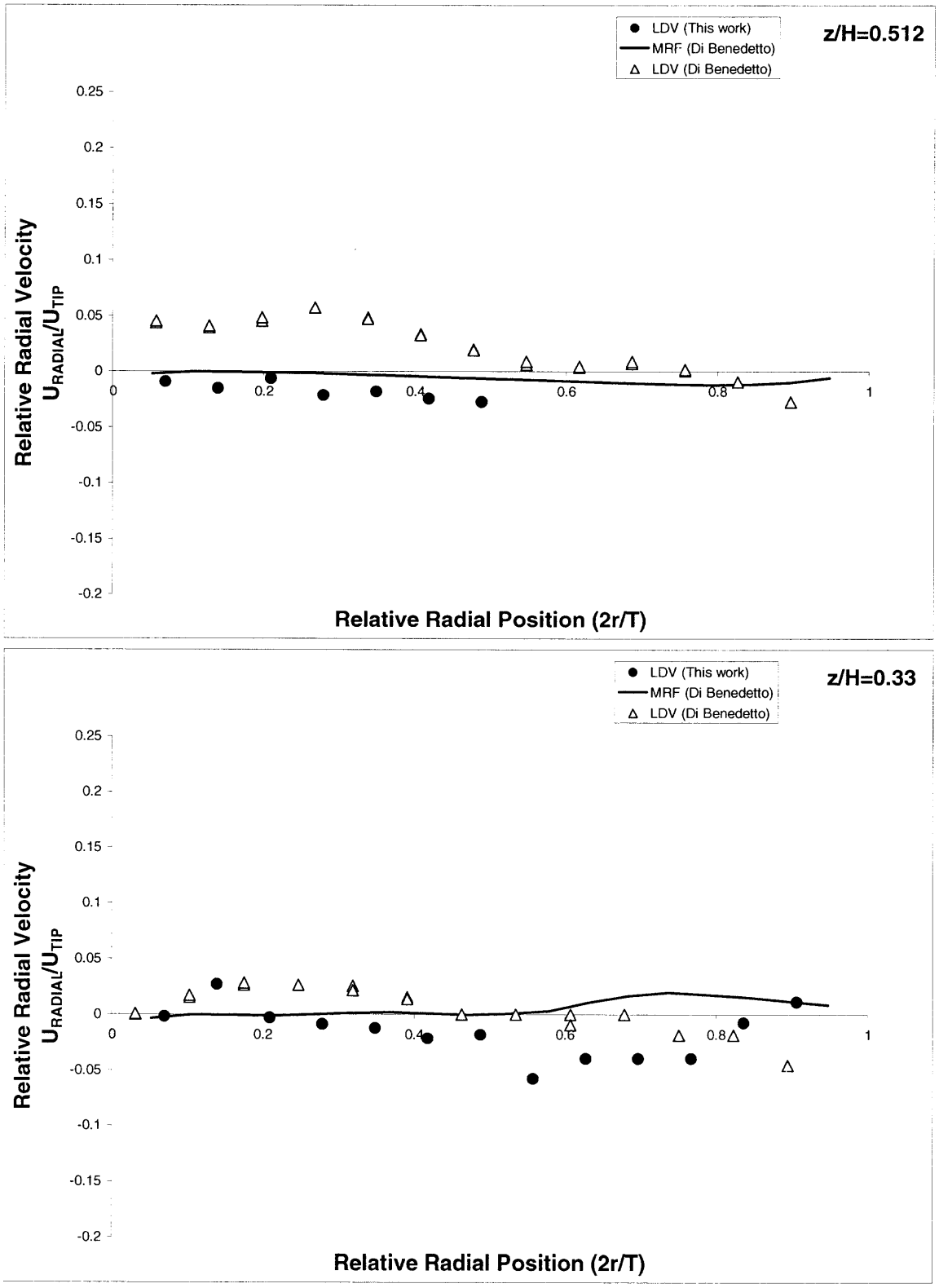

Figure B.1.3.2 Comparison between LDV data and CFD prediction for radial velocities at iso-surfaces z=147mm and z=96mm in the unbaffled, flat-bottom tank.

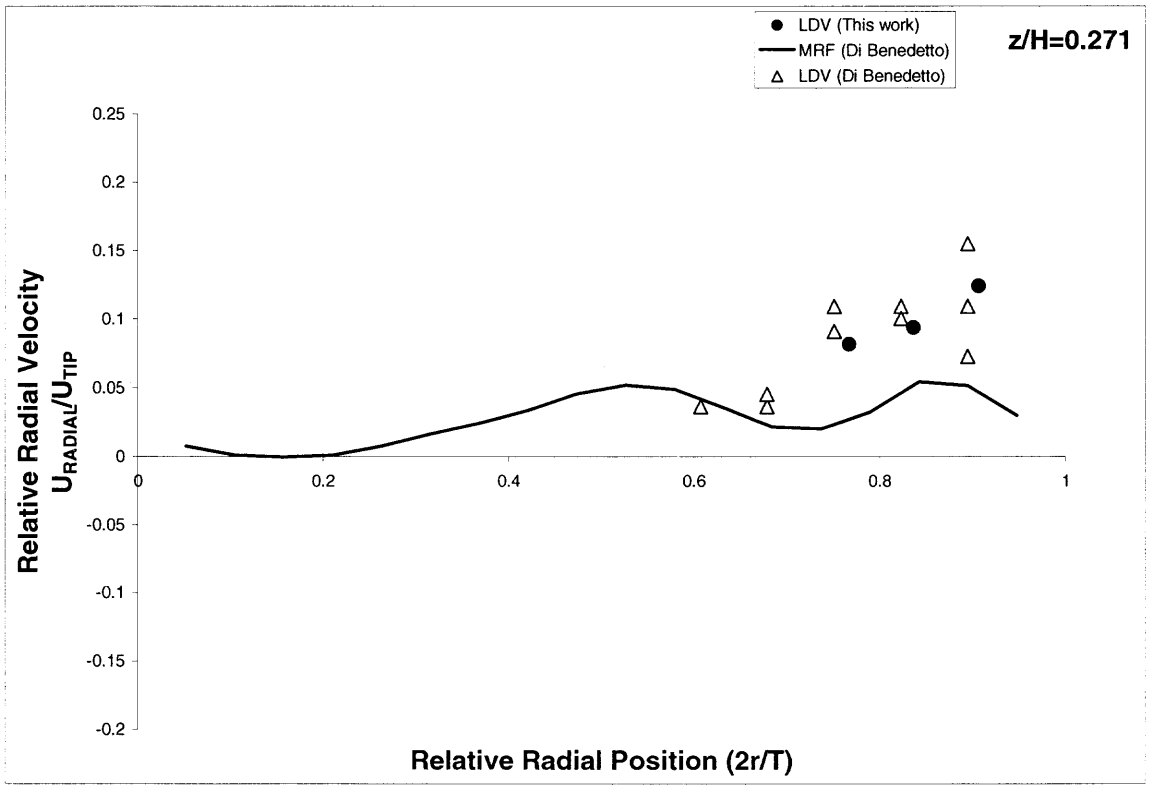

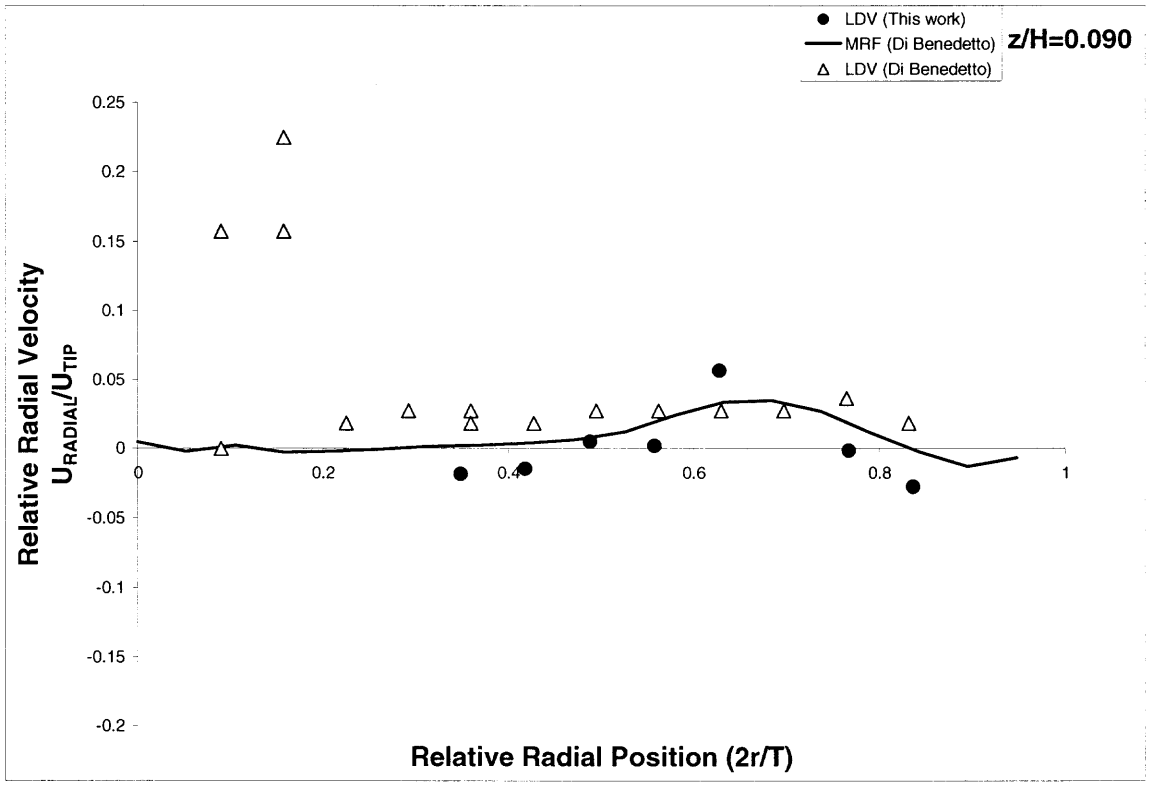

Figure B.1.3.3 Comparison between LDV data and CFD prediction for radial velocities at iso-surfaces z=78mm and z=26mm in the unbaffled,flat-bottom tank

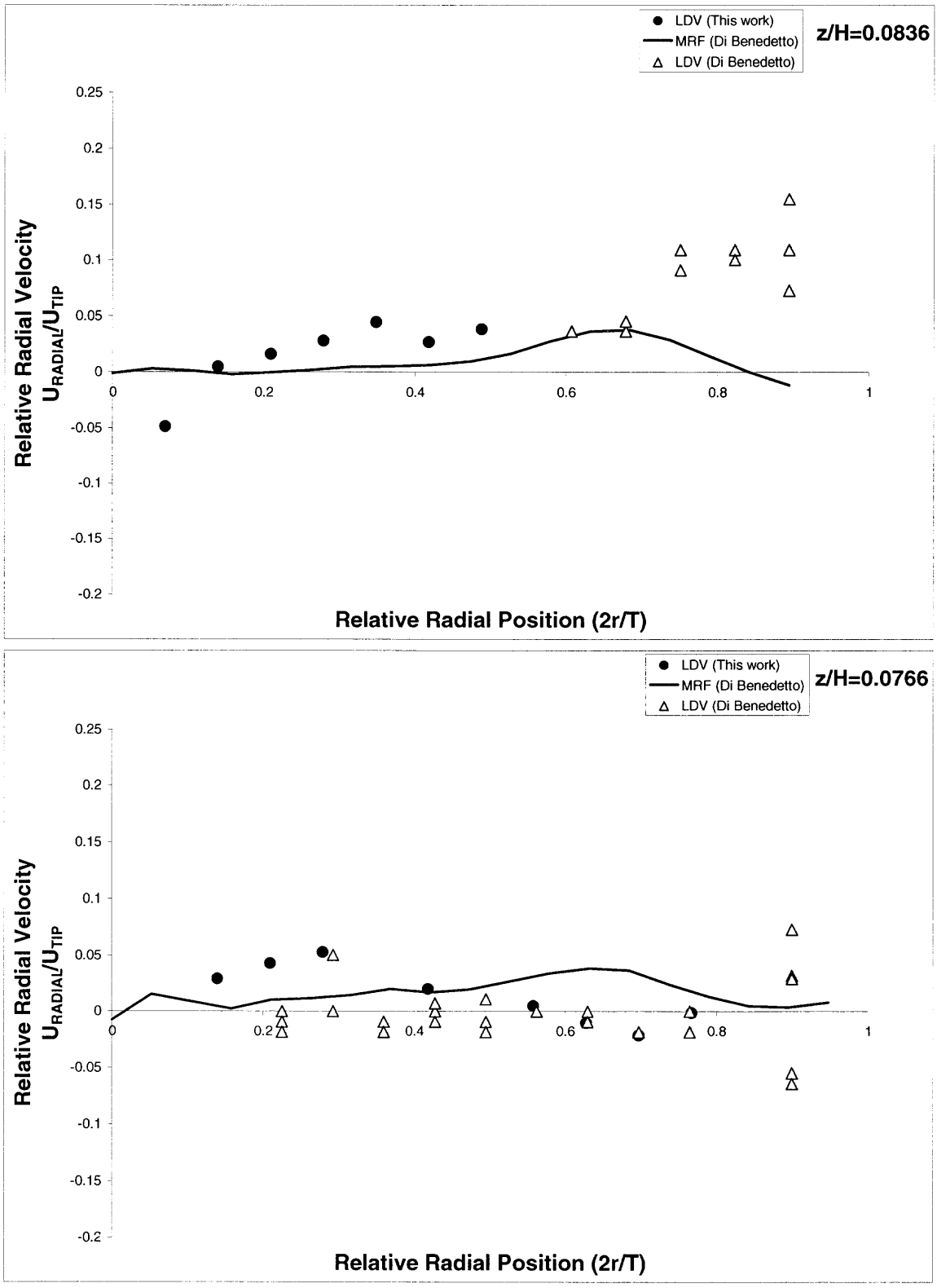

Figure B.1.3.4 Comparison between LDV data and CFD prediction for radial velocities at iso-surfaces z=24mm and z=22mm in the unbaffled, flat-bottom tank.

B.2 Comparison between LDV data and the CFD prediction in baffled, flat-bottom tank.

B.2.1 Comparison between LDV data and CFD prediction for tangential velocities:

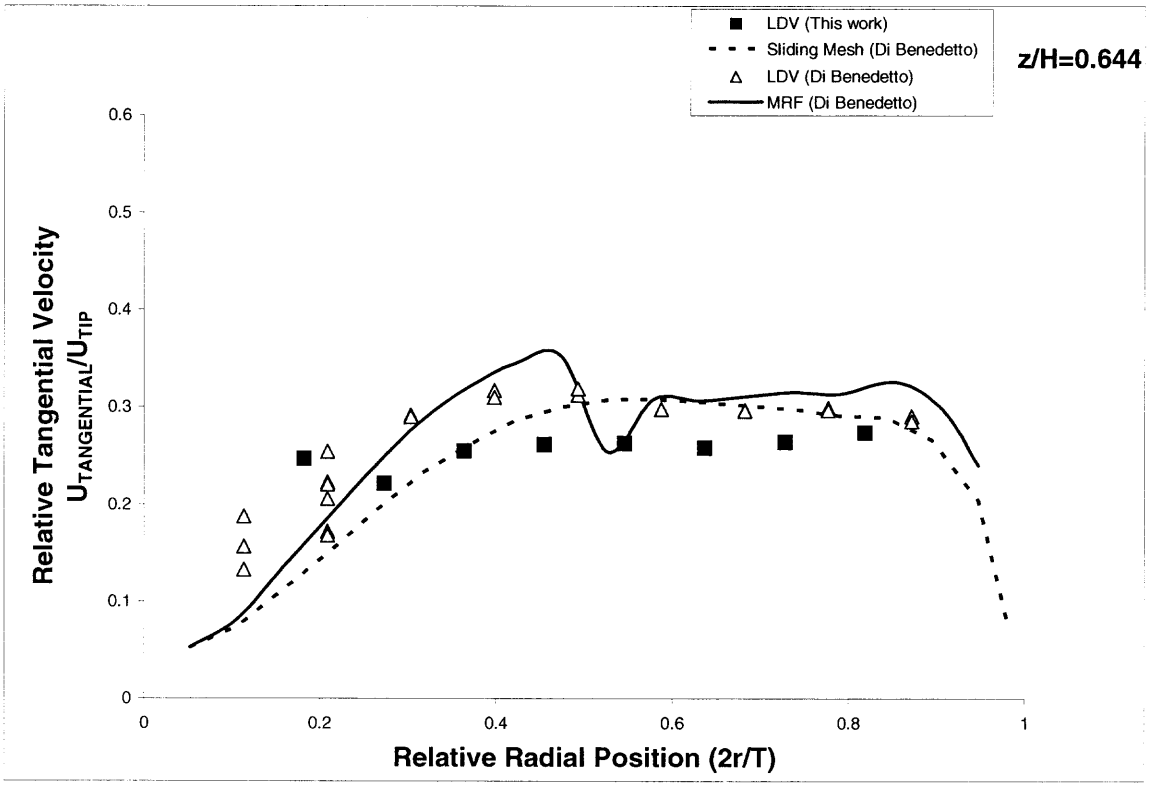

Figure B.2.1.1 Comparison between LDV data and CFD prediction for tangential velocities at iso-surfaces z=185mm in the baffled, flat-bottom tank

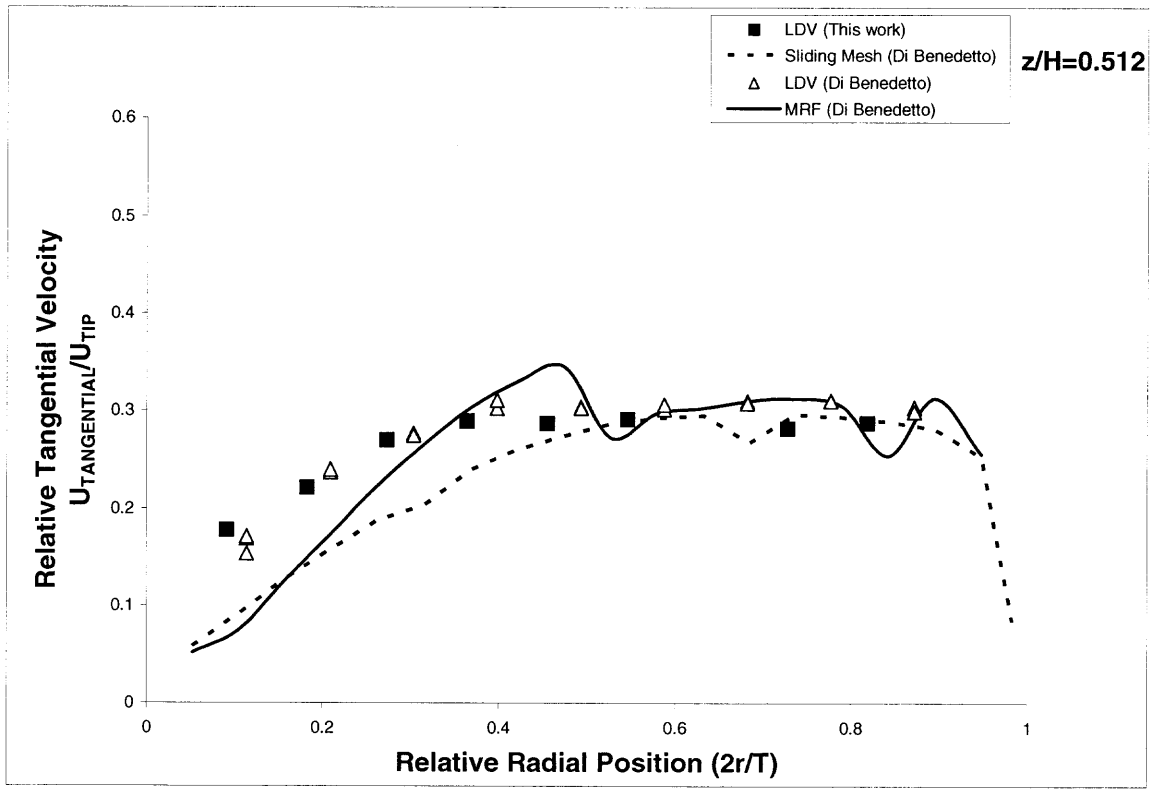

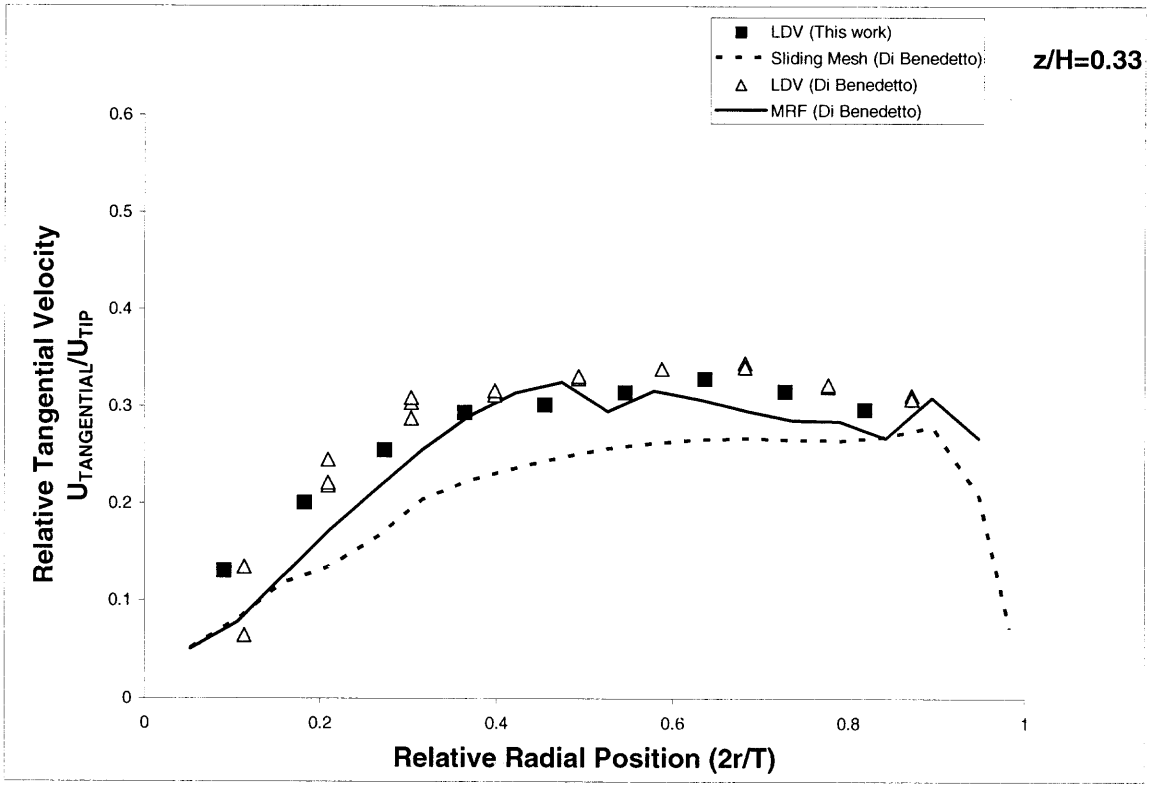

Figure B.2.1.2 Comparison between LDV data and CFD prediction for tangential velocities at iso-surfaces z=147mm and z=96mm in the baffled, flat-bottom tank

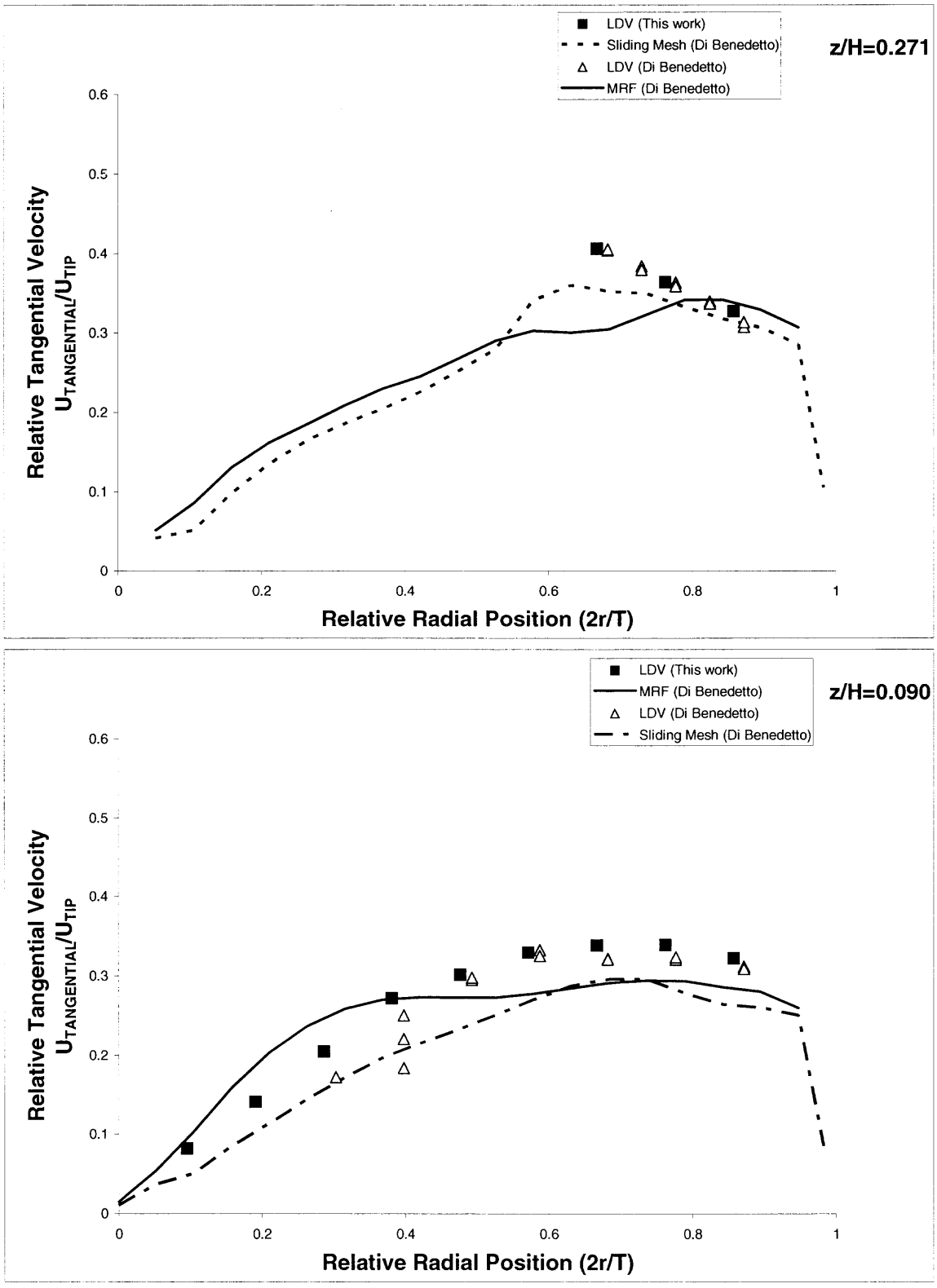

Figure B.2.1.3 Comparison between LDV data and CFD prediction for tangential velocities at iso-surfaces z=78mm and z=26mm in the baffled, flat-bottom tank

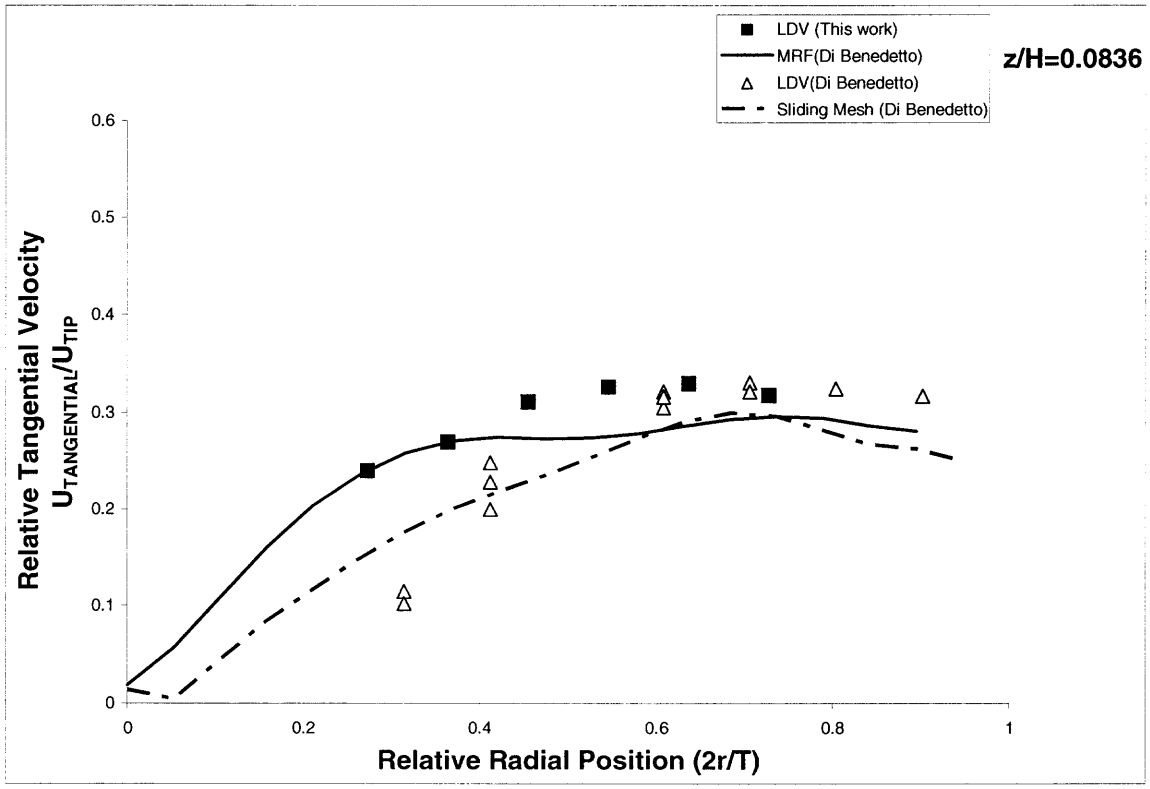

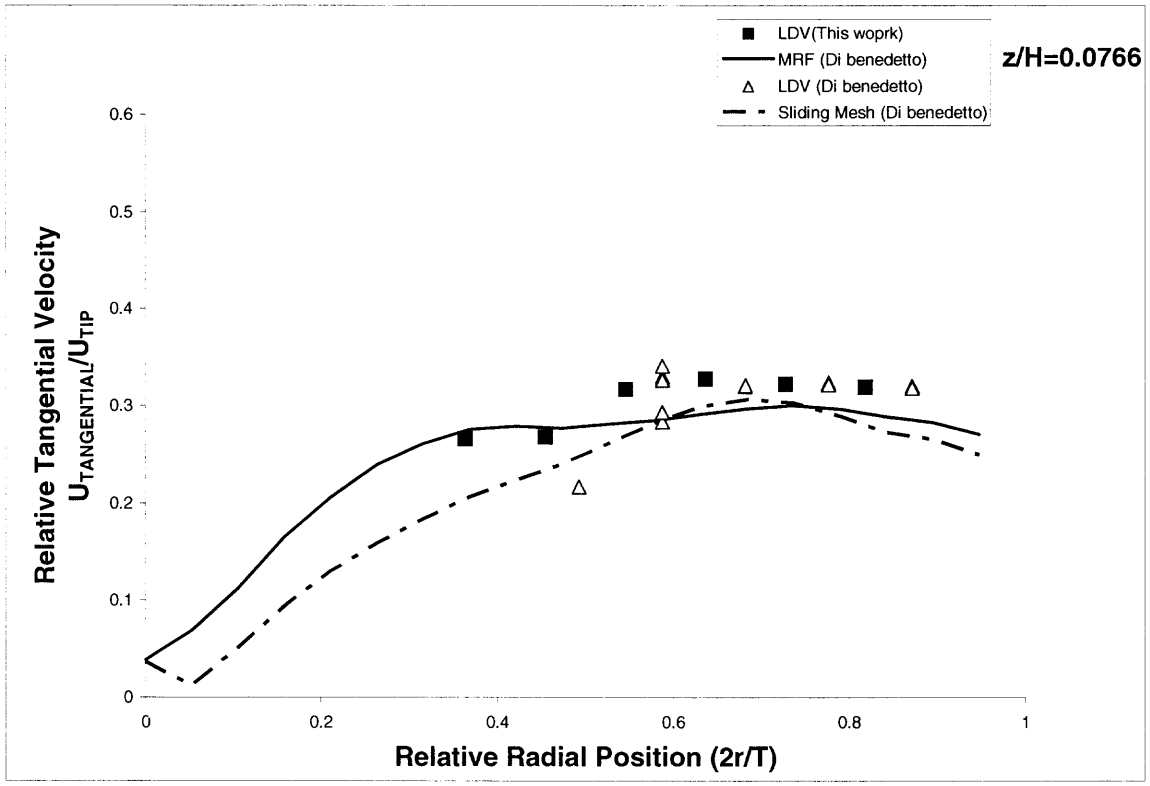

Figure B.2.1.4 Comparison between LDV data and CFD prediction for tangential velocities at iso-surfaces z=24mm and 22mm in the baffled, flat-bottom tank

B.2.2 Comparison between LDV data and CFD prediction for axial velocities

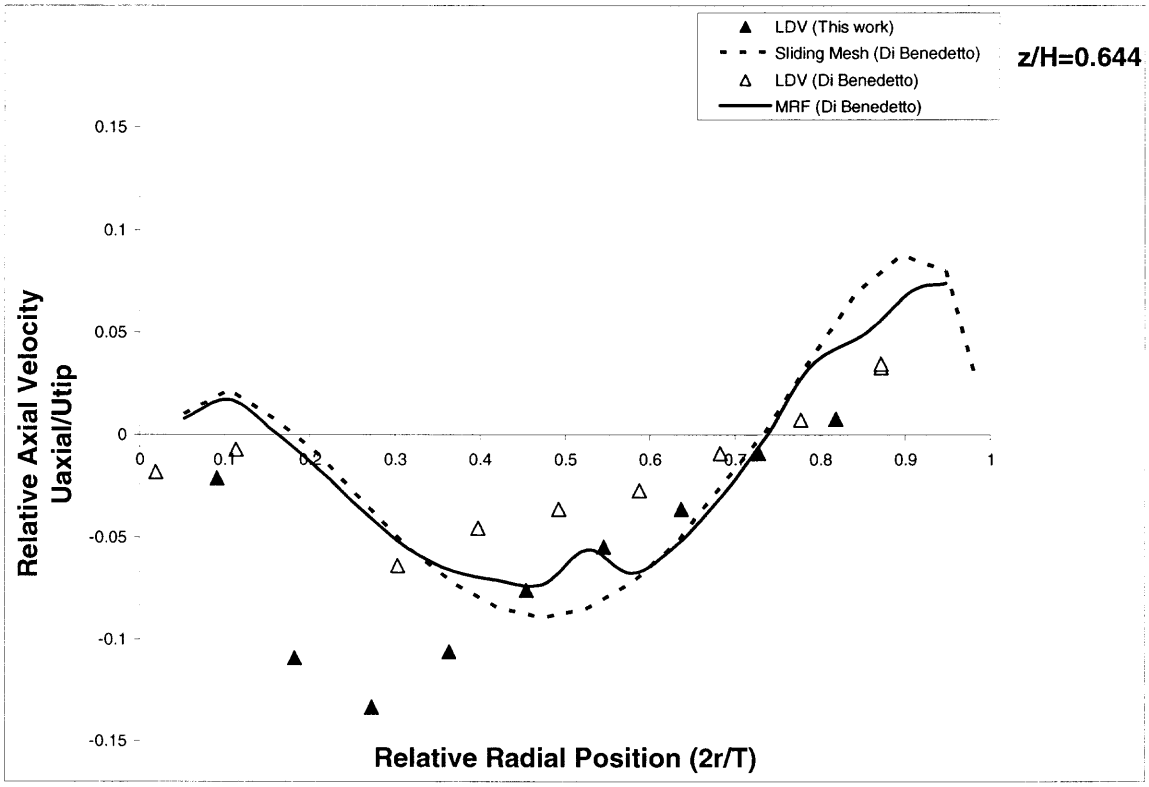

Figure B.2.2.1 Comparison between LDV data and CFD prediction for axial velocities at iso-surfaces z=185mm in the baffled, flat-bottom tank

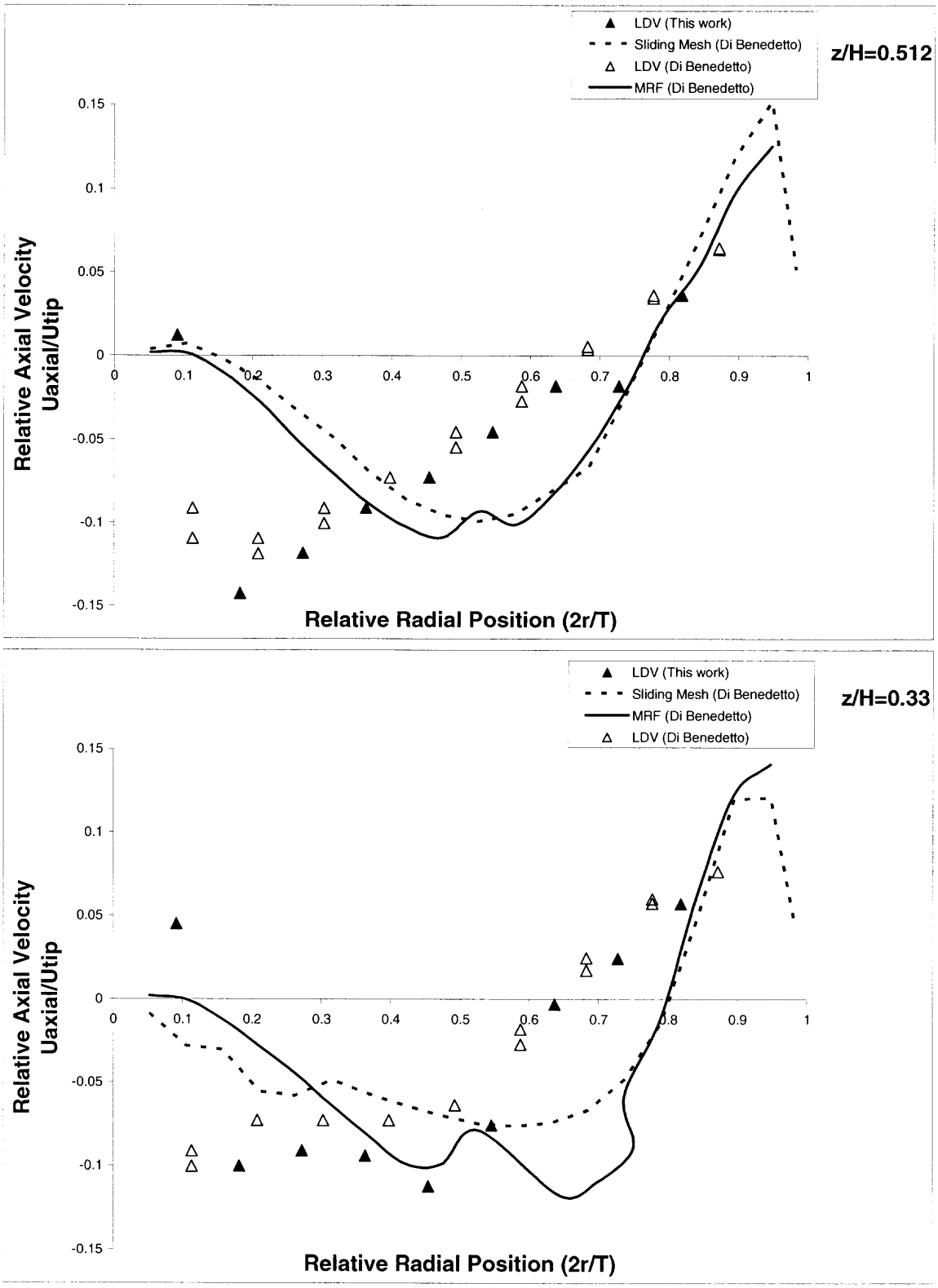

Figure B.2.2.2 Comparison between LDV data and CFD prediction for axial velocities at iso-surfaces z=147mm and z=96mm in the baffled, flat-bottom tank

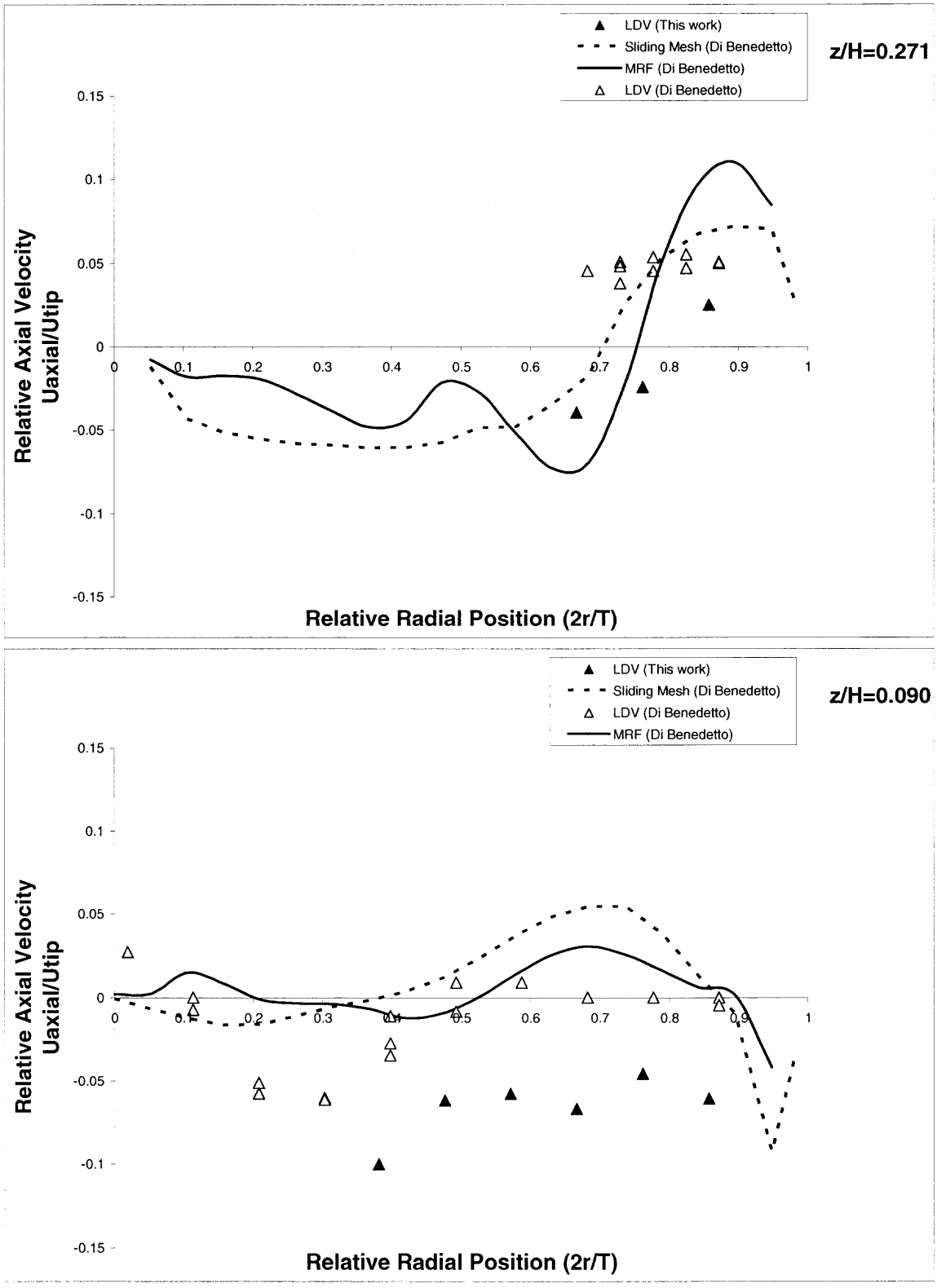

Figure B.2.2.3 Comparison between LDV data and CFD prediction for axial velocities at iso-surfaces z=78mm and z=26mm in the baffled, flat-bottom tank

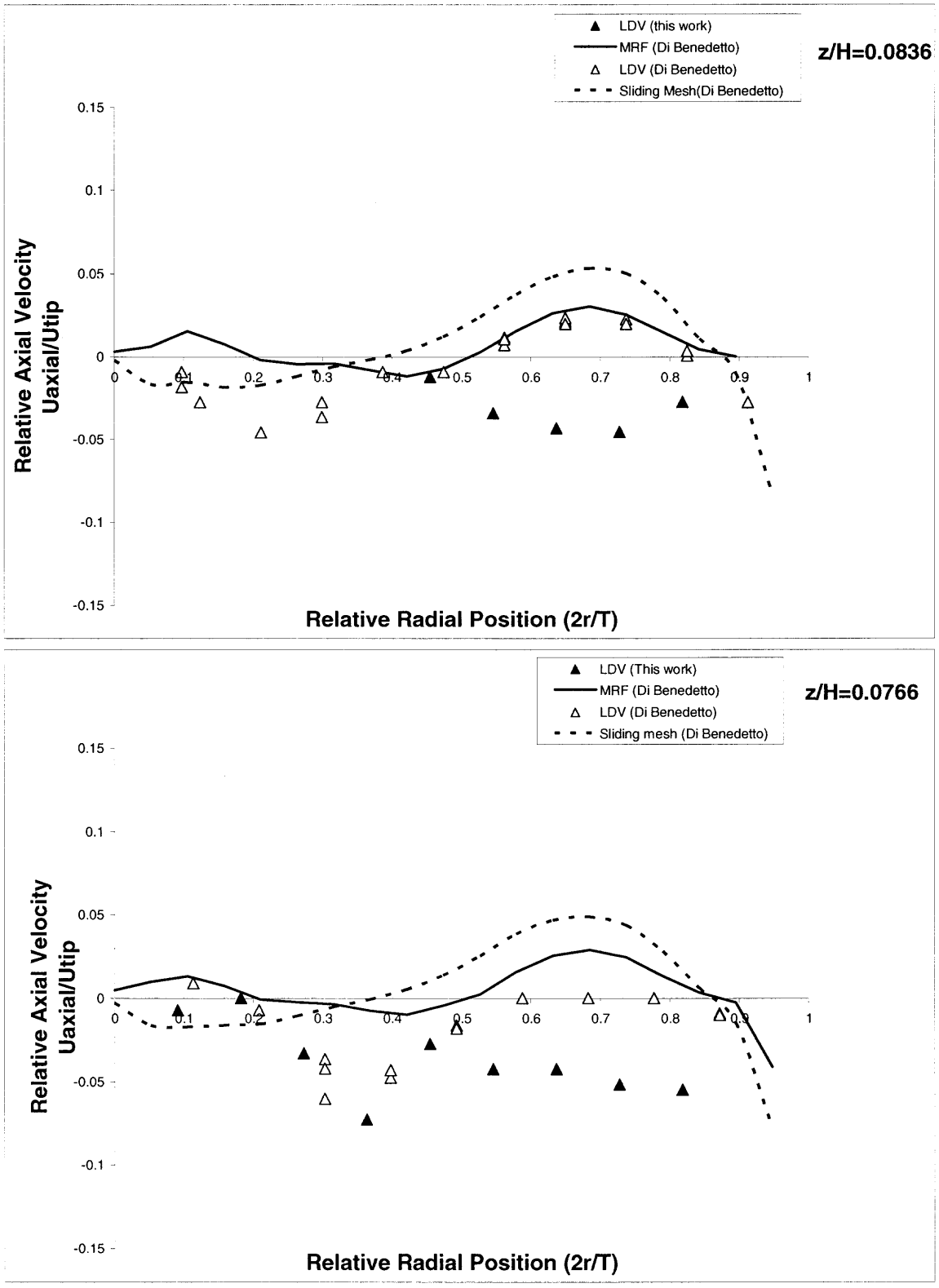

Figure B.2.2.4 Comparison between LDV data and CFD prediction for axial velocities at iso-surfaces z=24mm and z=22mm in the baffled, flat-bottom tank

B.2.3 Comparison between LDV data and CFD prediction for axial velocities

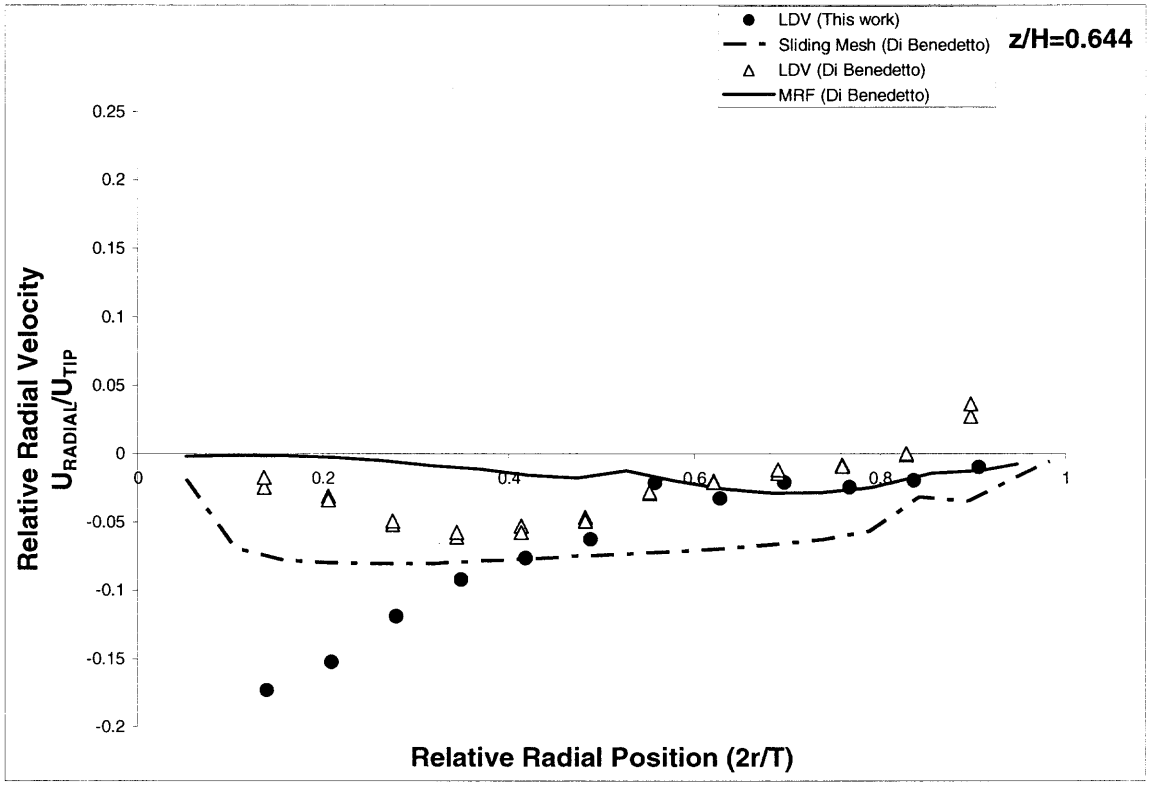

Figure B.2.3.1 Comparison between LDV data and CFD prediction for radial velocities at iso-surfaces z=185mm in the baffled, flat-bottom tank

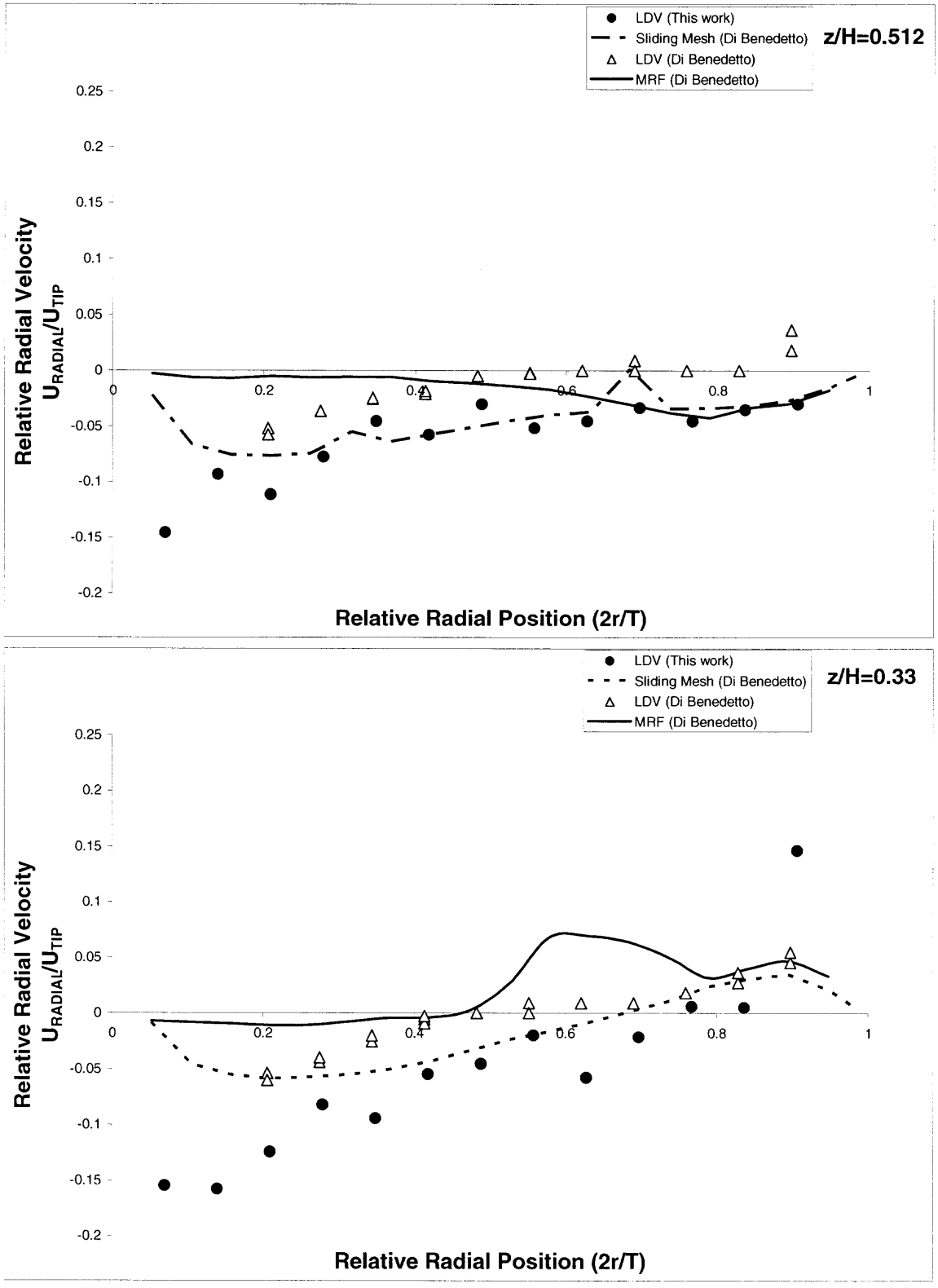

Figure B.2.3.2 Comparison between LDV data and CFD prediction for radial velocities at iso-surfaces z=147mm and z=96mm in the baffled, flat-bottom tank

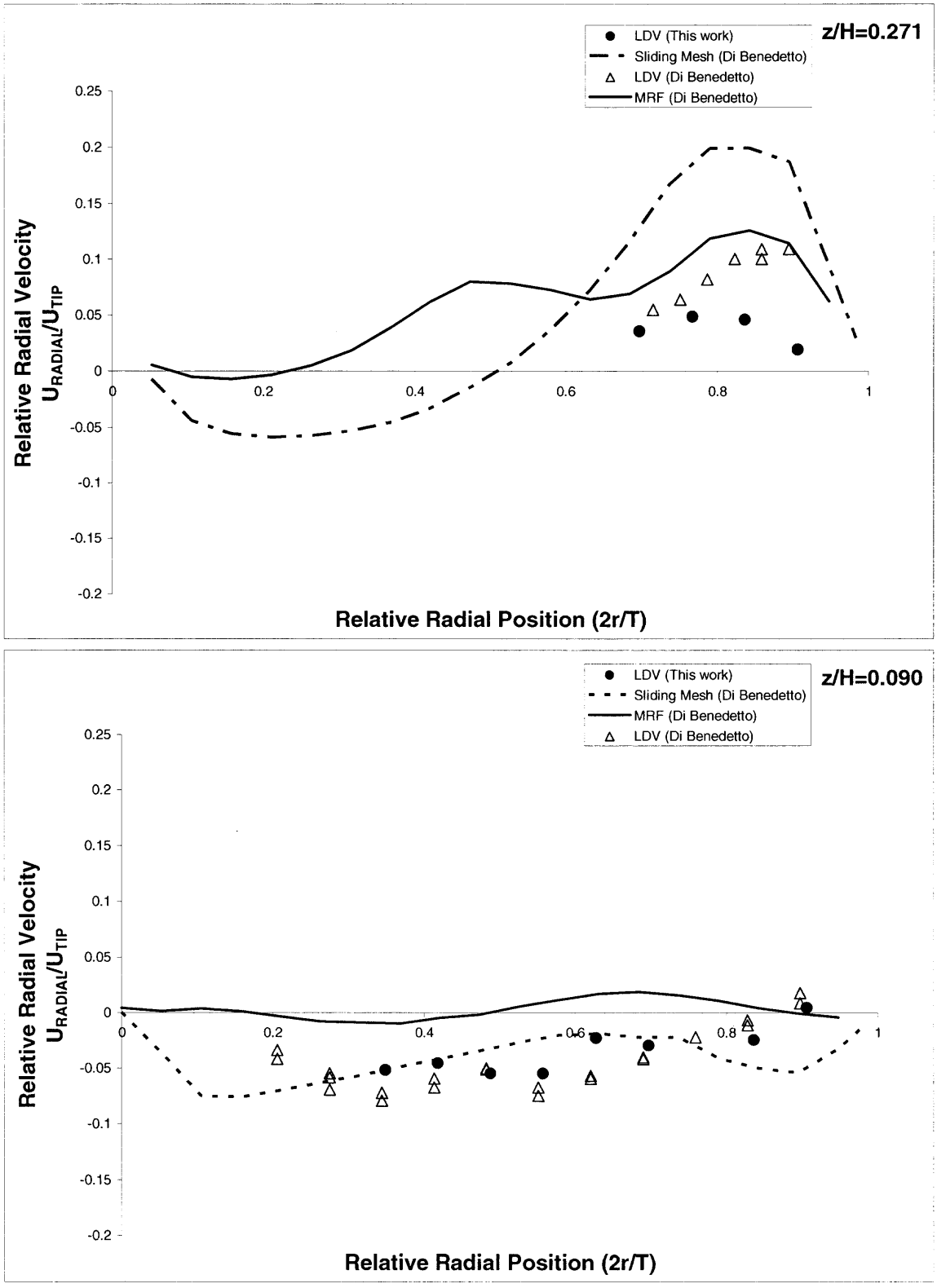

Figure B.2.3.3 Comparison between LDV data and CFD prediction for radial velocities at iso-surfaces z=96mm and z=26mm in the baffled, flat-bottom tank

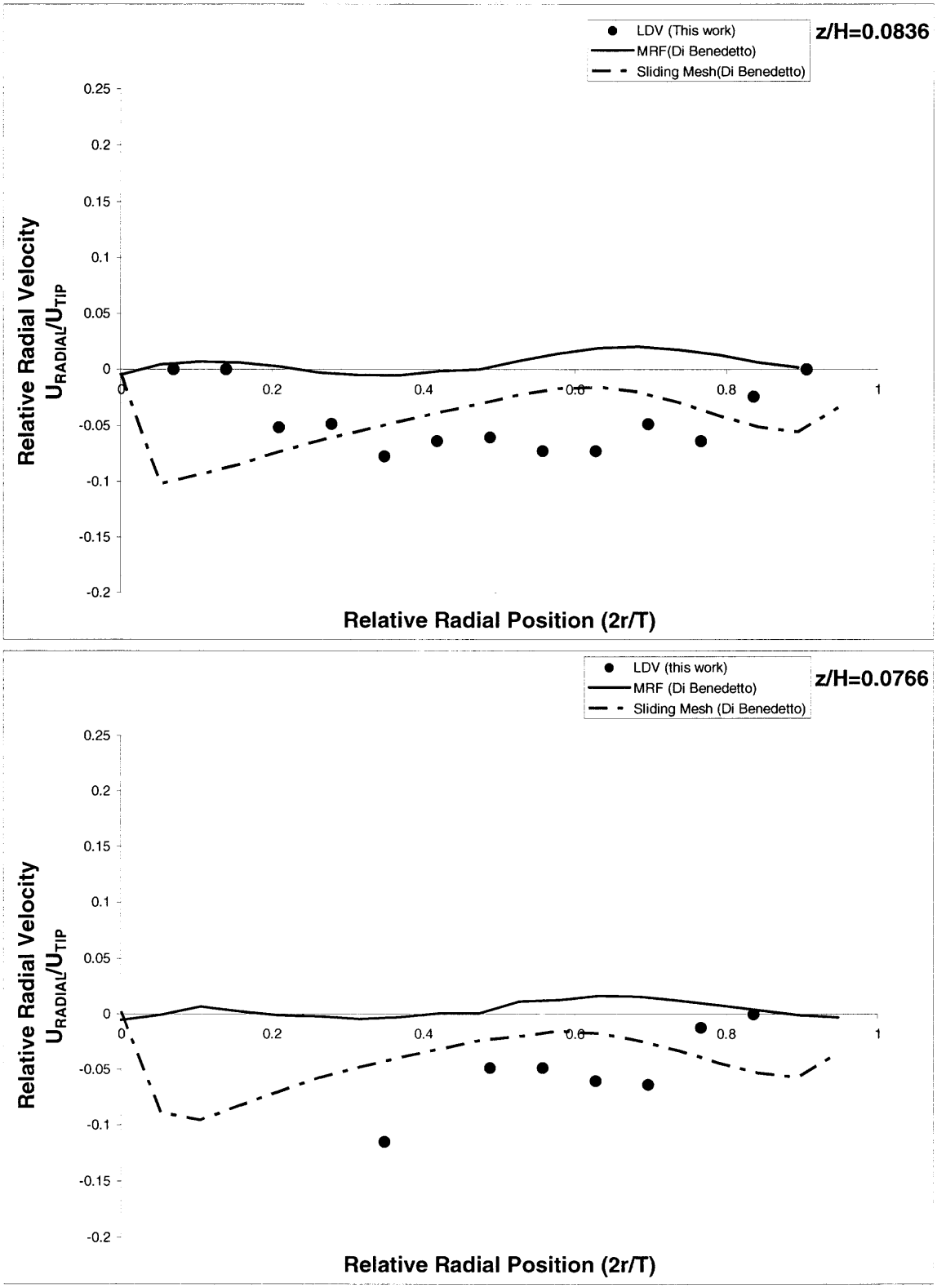

Figure B.2.3.4 Comparison between LDV data and CFD prediction for radial velocities at iso-surfaces z=24mm and z=22mm in the baffled, flat-bottom tank.

B.3 Comparison between LDV data and the CFD prediction in Unbaffled, Hemispherical-bottom tank.

B.3.1 Comparison between LDV data and CFD prediction for tangential velocities:

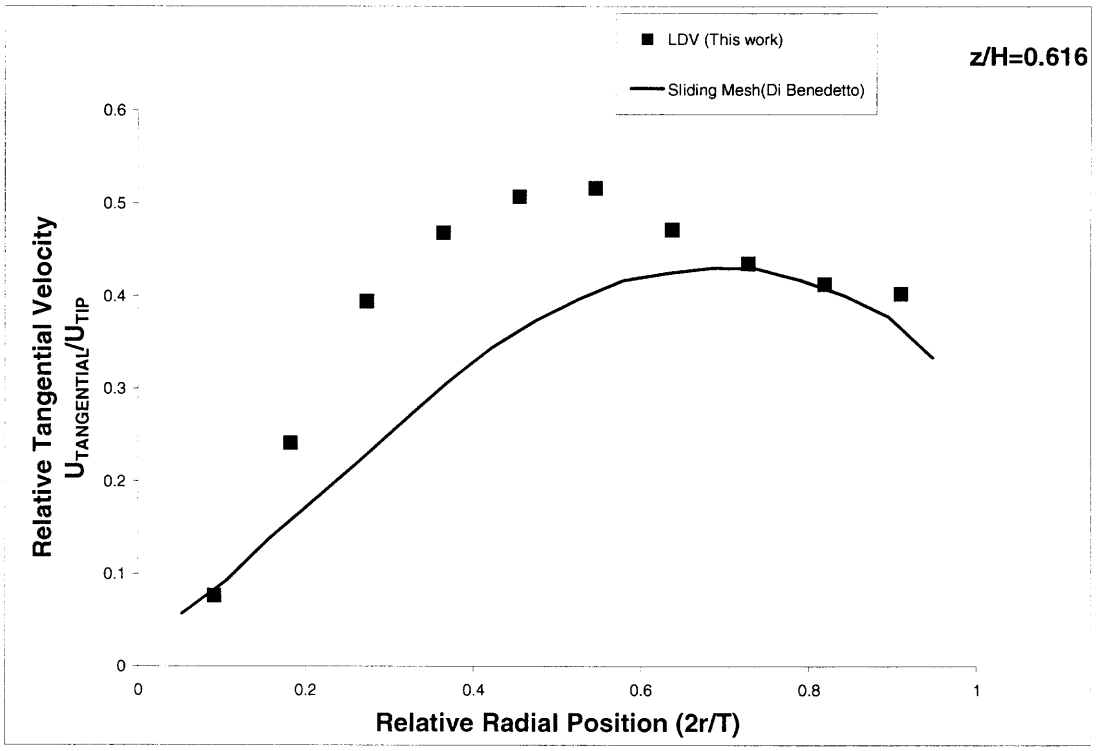

Figure B.3.1.1 Comparison between LDV data and CFD prediction for tangential velocities at iso-surfaces z=185mm in the unbaffled, hemispherical-bottom tank

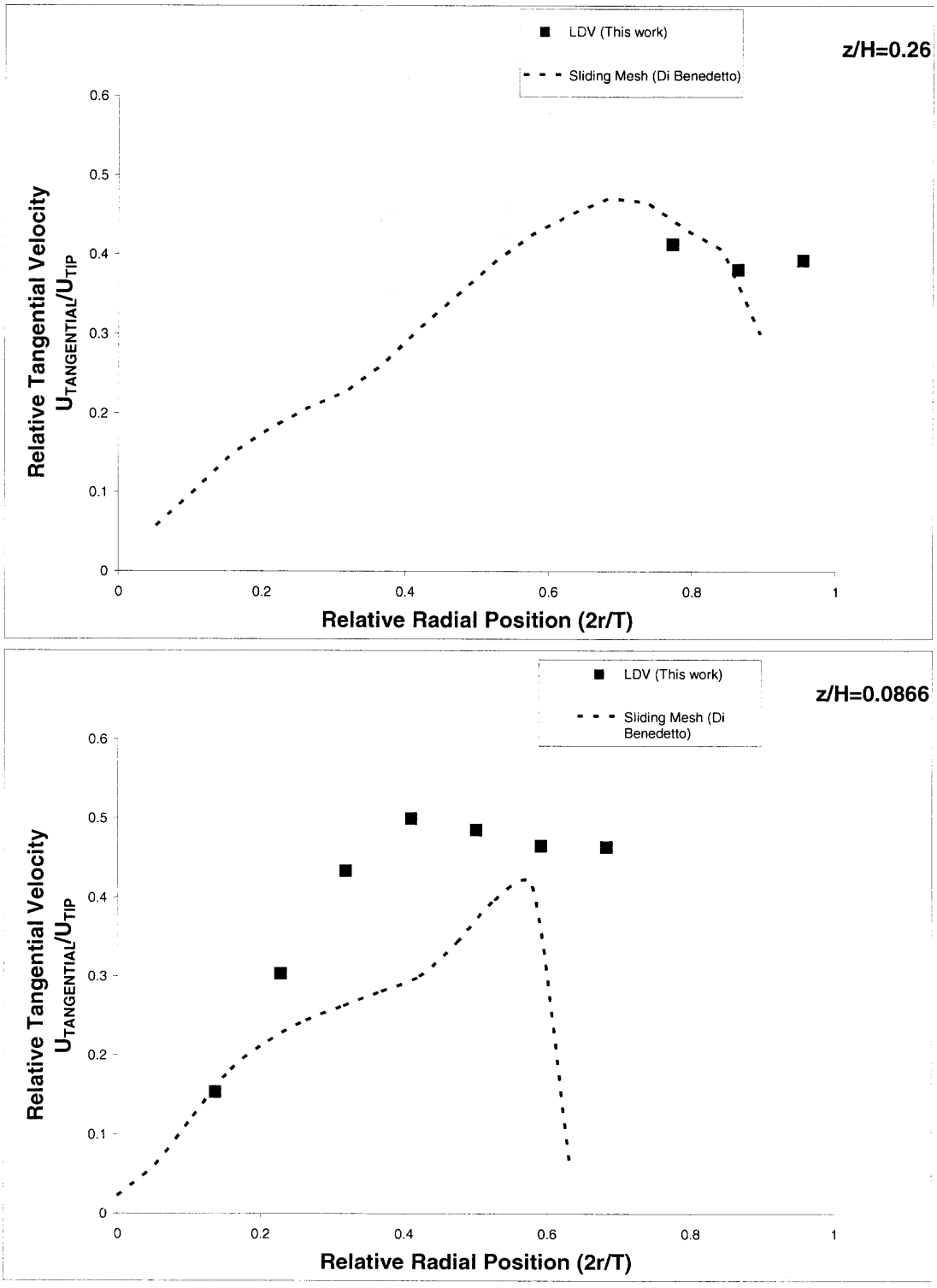

Figure B.3.1.2 Comparison between LDV data and CFD prediction for tangential velocities at iso-surfaces z=78mm and z=26mm in the unbaffled, hemispherical-bottom tank.

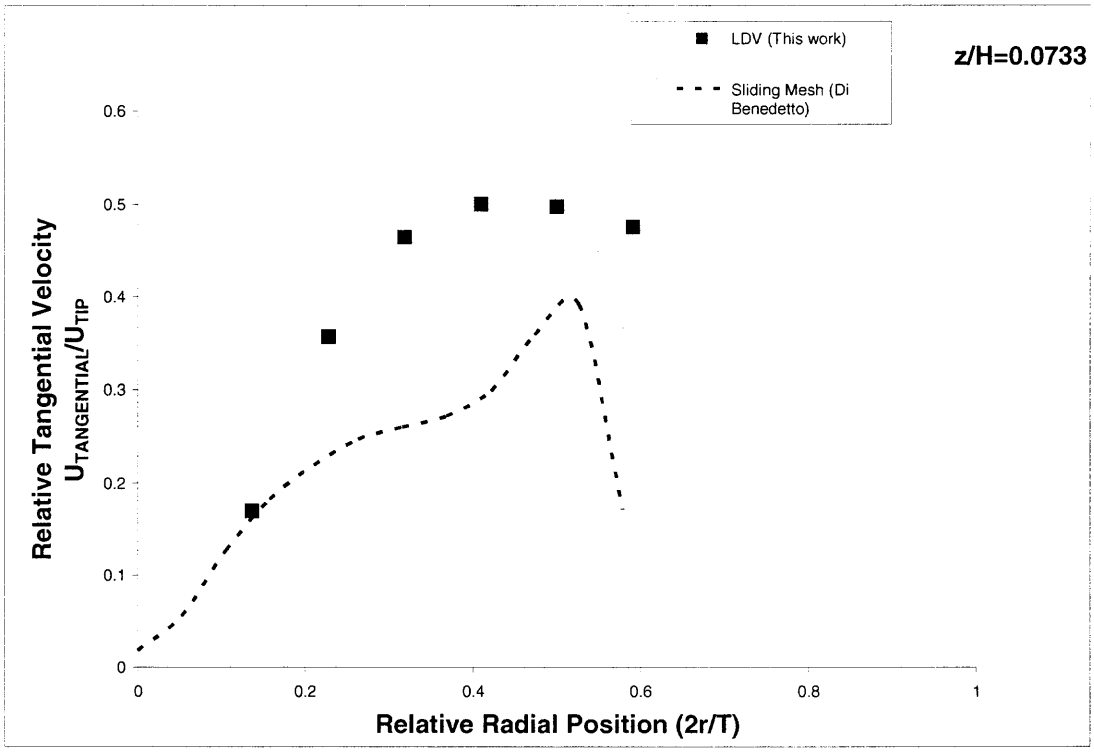

Figure B.3.1.3 Comparison between LDV data and CFD prediction for tangential velocities at iso-surfaces z=22mm in the unbaffled, hemispherical-bottom tank.

B.3.2 Comparison between LDV data and CFD prediction for axial velocities:

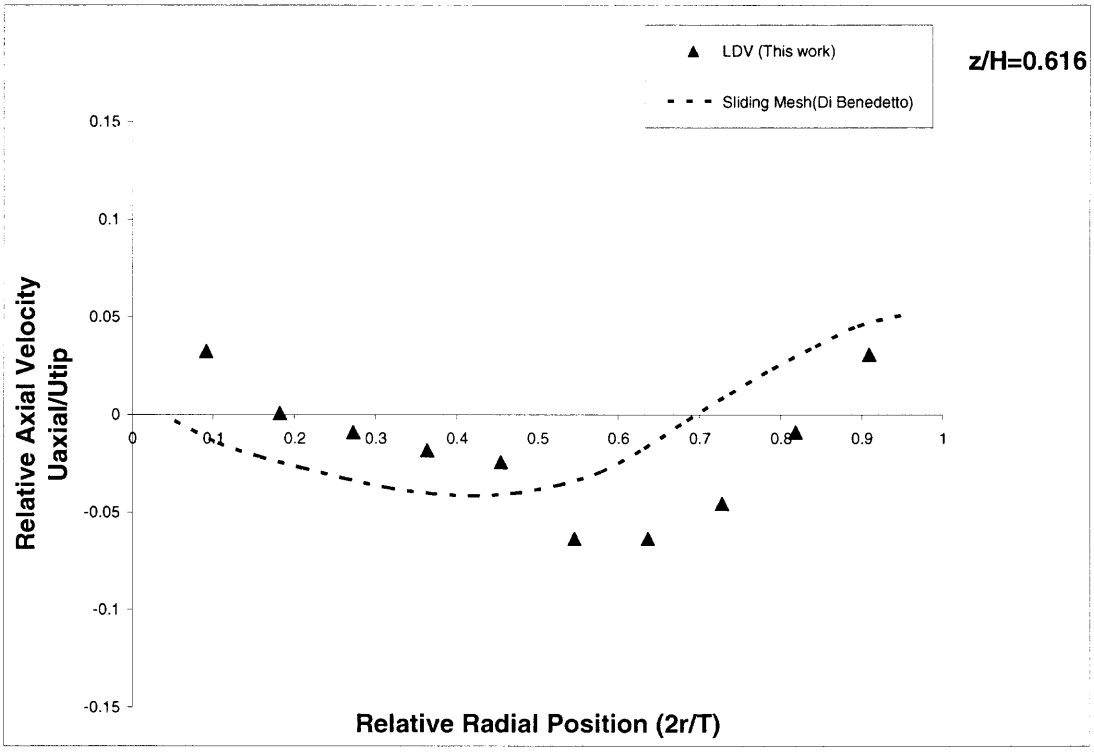

Figure B.3.2.1 Comparison between LDV data and CFD prediction for axial velocities at iso-surfaces z=185mm in the unbaffled, hemispherical-bottom tank

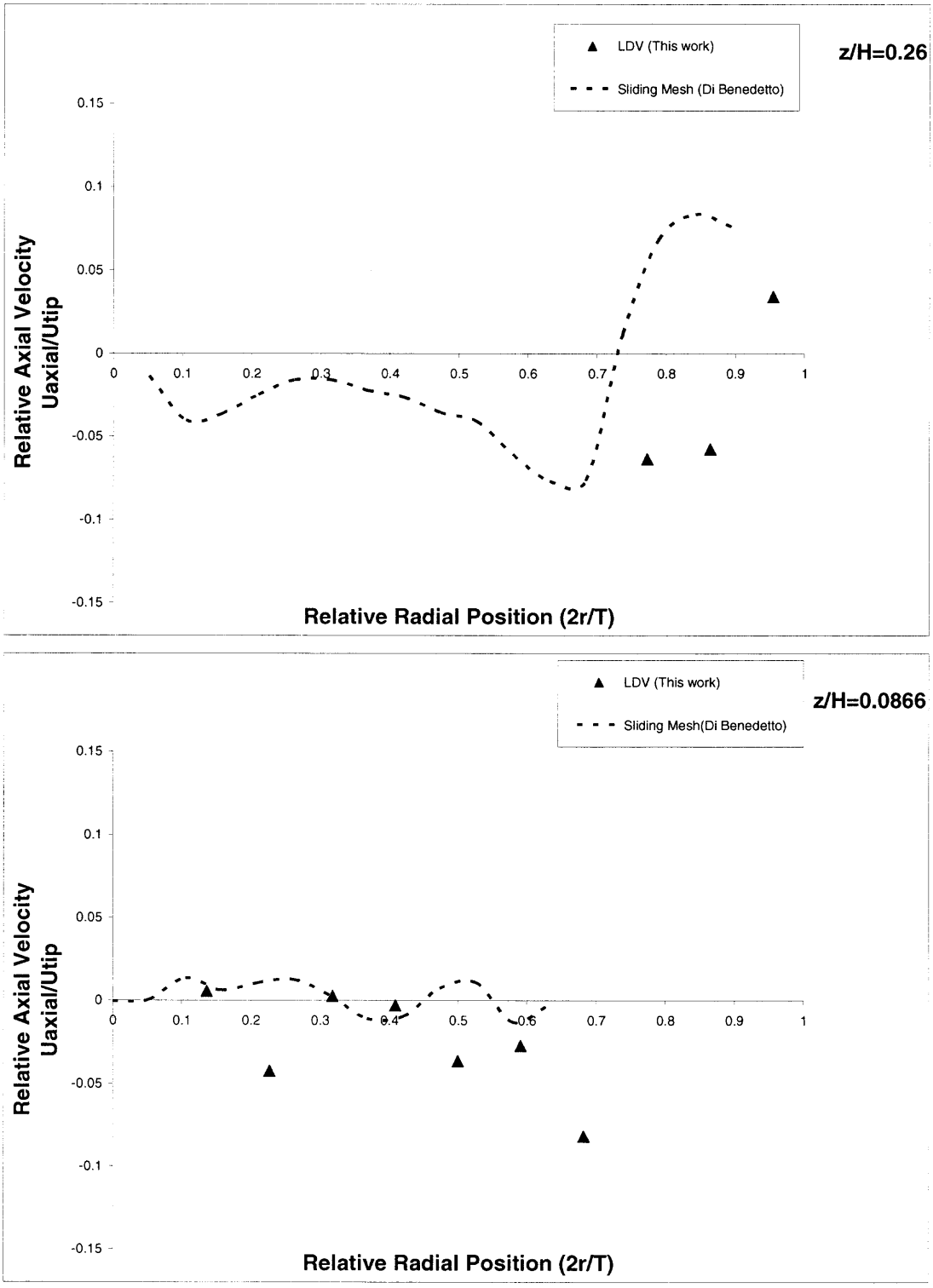

Figure B.3.2.2 Comparison between LDV data and CFD prediction for axial velocities at iso-surfaces z=78mm and z=26mm in the unbaffled, hemispherical-bottom tank

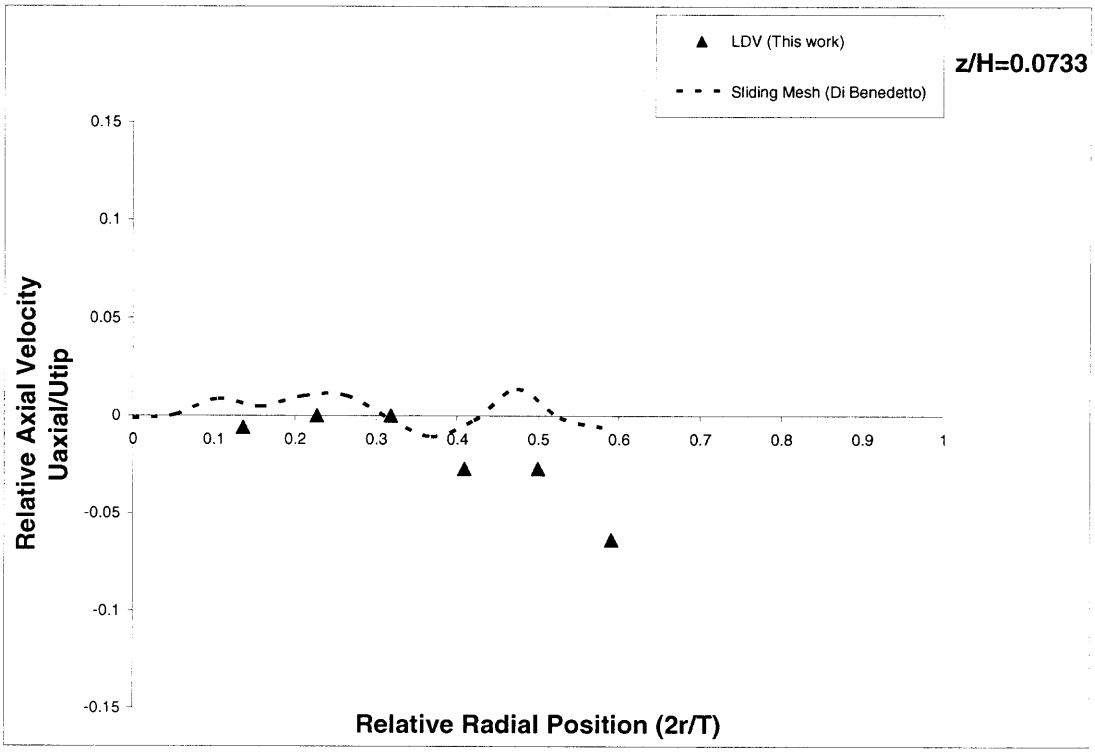

Figure B.3.2.3 Comparison between LDV data and CFD prediction for axial velocities at iso-surfaces z=22mm in the unbaffled, hemispherical-bottom tank.

B.4 Comparison between LDV data and the CFD prediction in baffled, Hemispherical-bottom tank.

B.4.1 Comparison between LDV data and CFD prediction for tangential velocities:

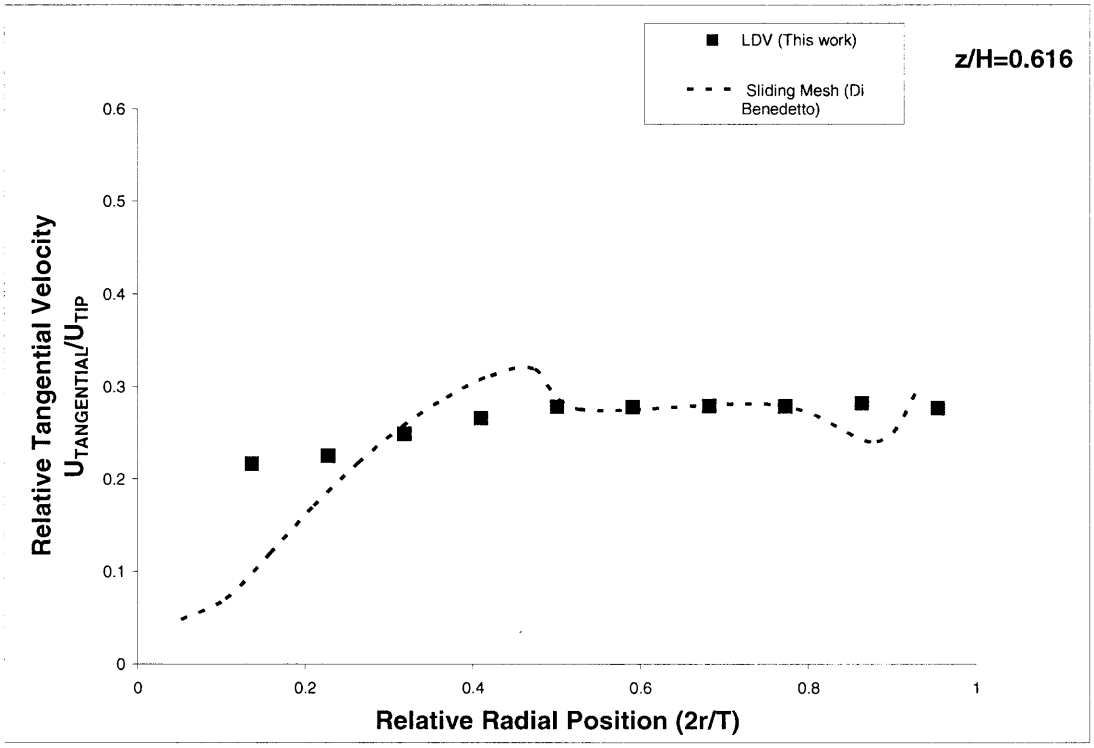

Figure B.4.1.1 Comparison between LDV data and CFD prediction for tangential velocities at iso-surfaces z=185mm in the baffled, hemispherical-bottom tank

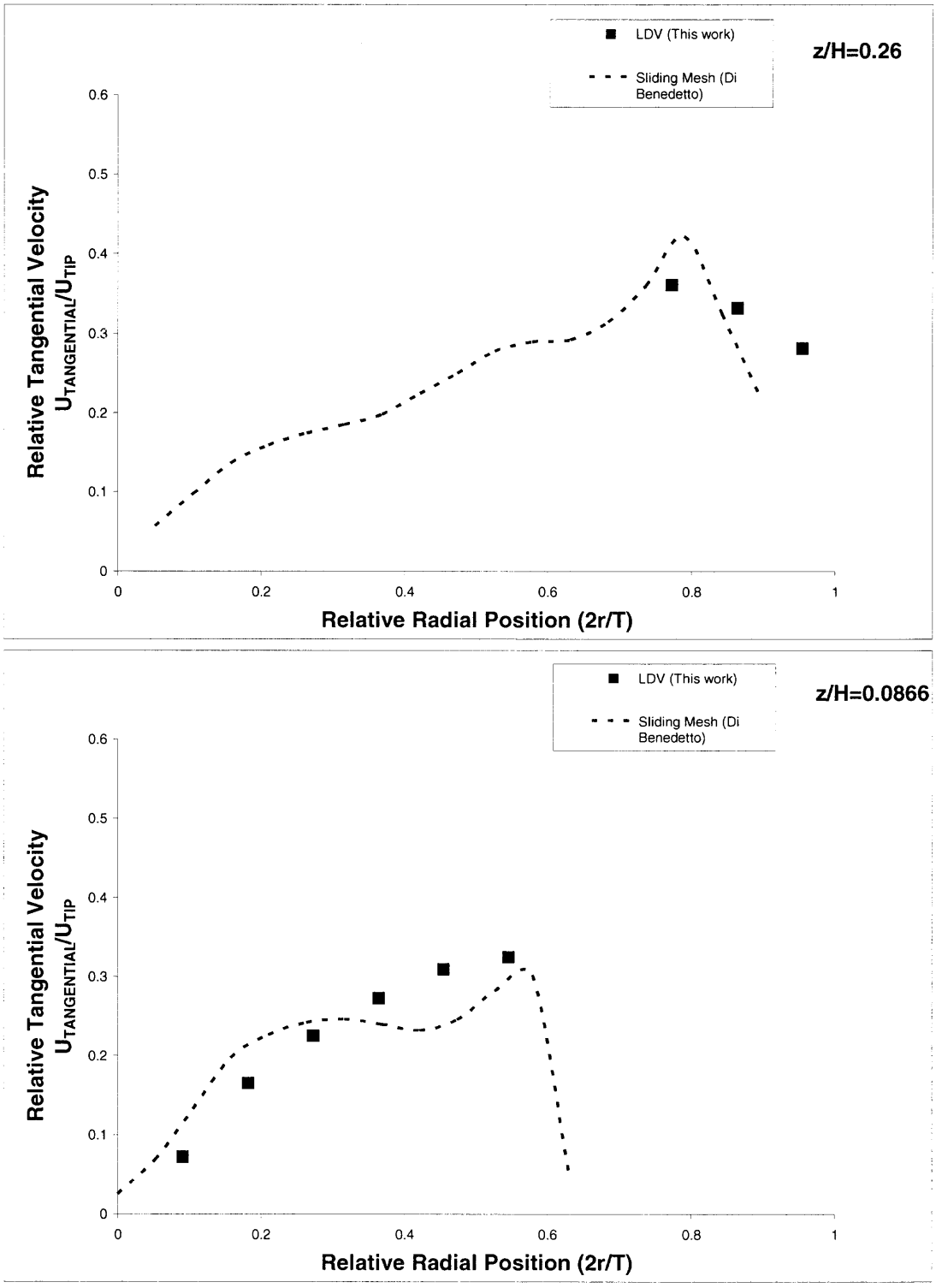

Figure B.4.1.2 Comparison between LDV data and CFD prediction for tangential velocities at iso-surfaces z=78mm and z=26mm in the baffled, hemispherical-bottom tank

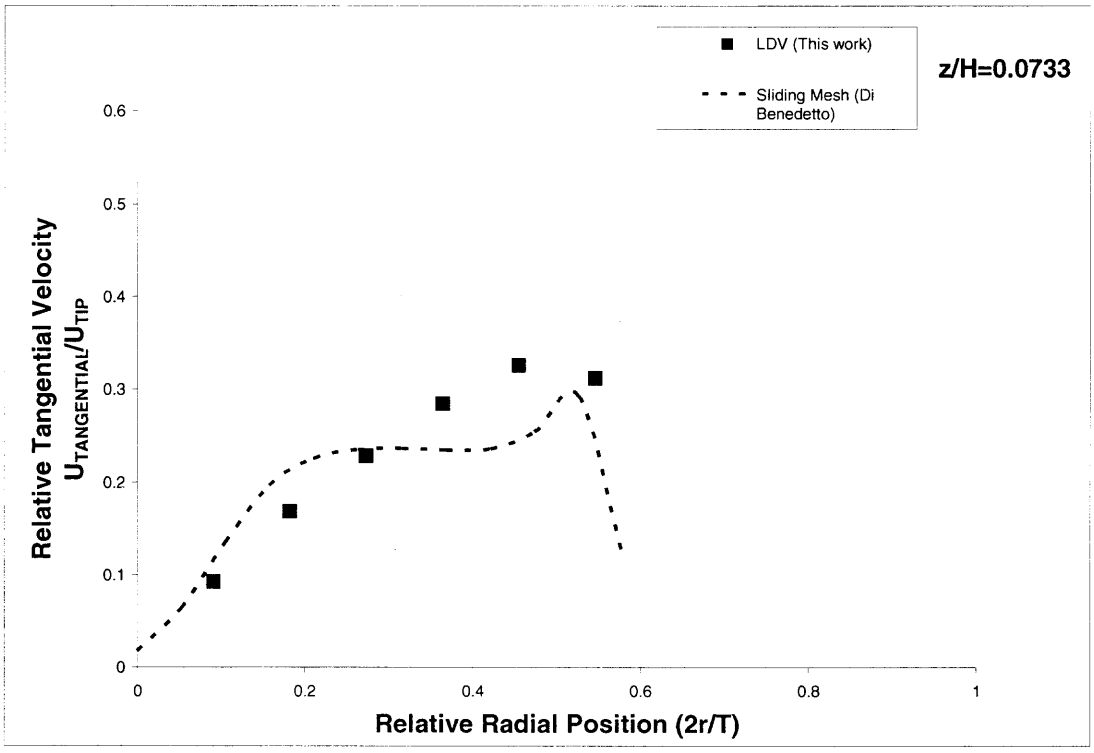

Figure B.4.1.3 Comparison between LDV data and CFD prediction for tangential velocities at iso-surfaces z=22mm in the baffled, hemispherical-bottom tank.

B.4.2 Comparison between LDV data and CFD prediction for axial velocities:

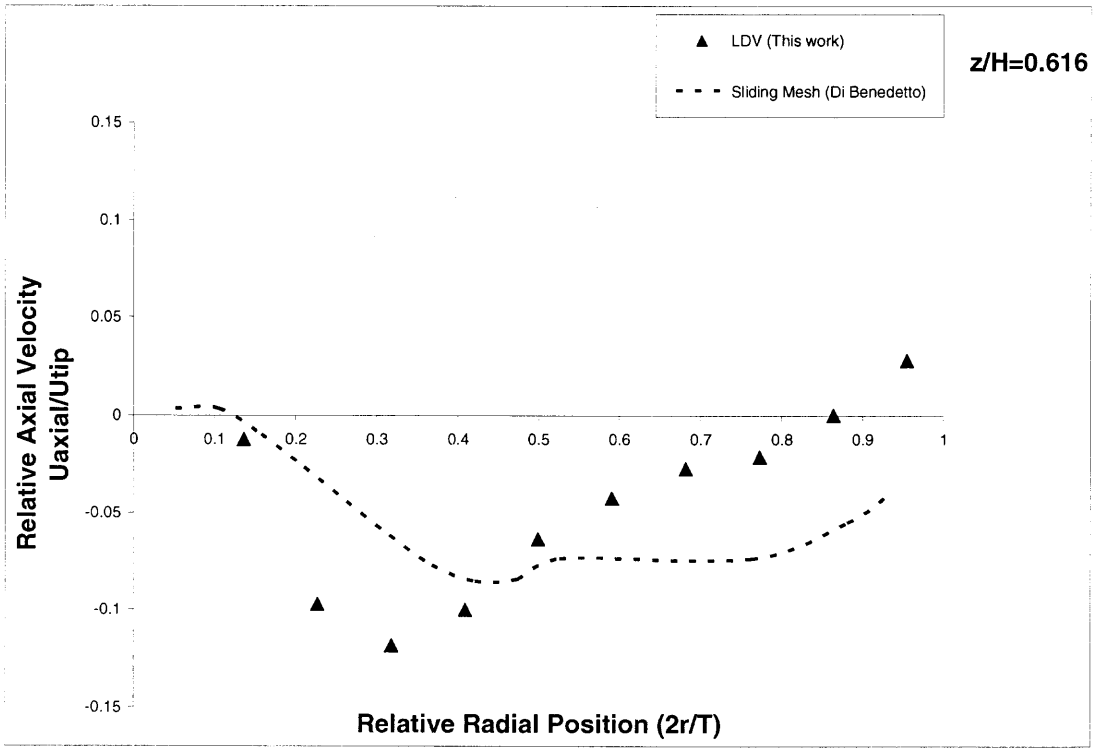

Figure B.4.2.1 Comparison between LDV data and CFD prediction for axial velocities at iso-surfaces z=185mm in the baffled, hemispherical-bottom tank

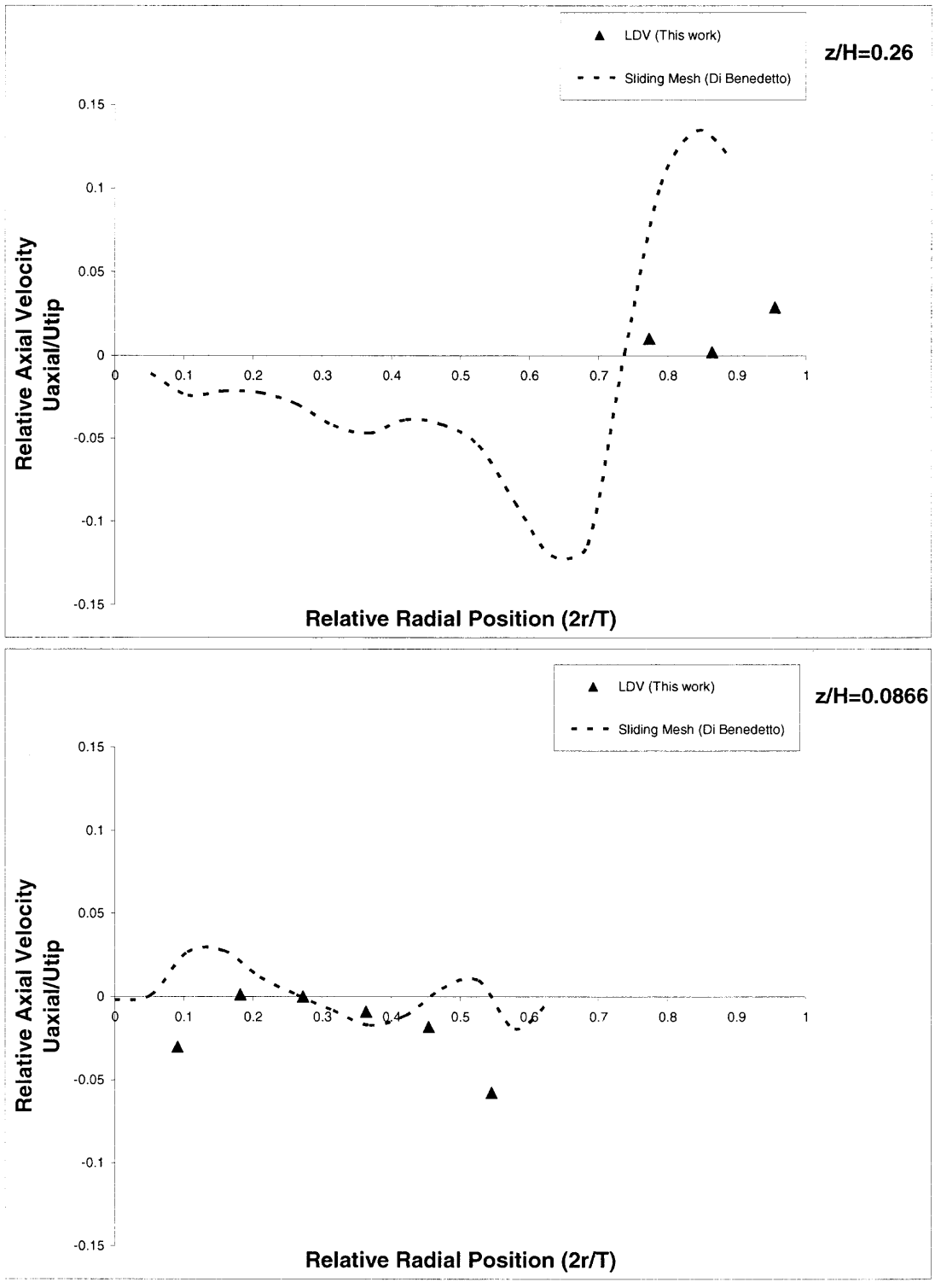

Figure B.4.2.2 Comparison between LDV data and CFD prediction for axial velocities at iso-surfaces z=78mm and z=26mm in the baffled, hemispherical-bottom tank

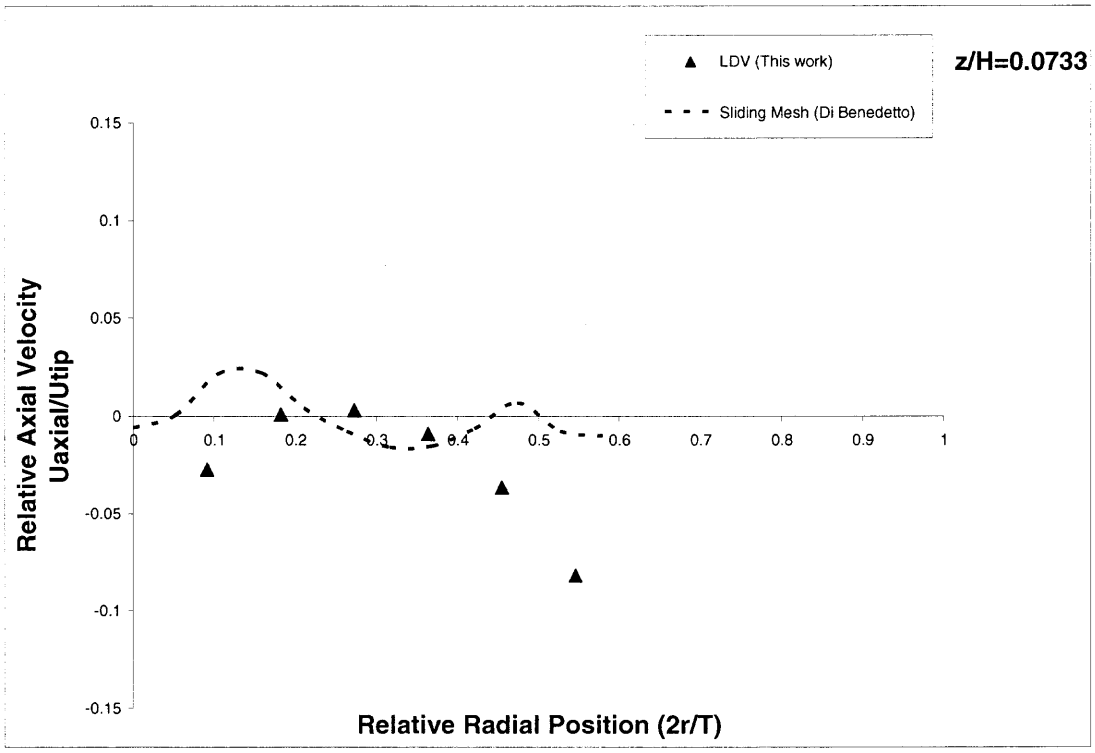

Figure B.4.2.3 Comparison between LDV data and CFD prediction for axial velocities at iso-surfaces z=22mm in the baffled, hemispherical-bottom tank.

REFERENCES

1. Campolo, M., Soldati, A. (2002). Appraisal of Fluid Dynamics Efficiency of Retreated-Blade and Turbofoil Impellers in Industrial-Size CSTRs. Ind. Eng. Chem, 41.1370-1377

2. Reilly, C.D, Habit, M. and Sherlock, J. P. (2007). Flow and Mixing Characteristics of a Retreat curve Impeller in a Conical-Based Vessel. Institution of Chemical Engineers85.0263-8762

3. Escudie, R., Line, A. (2003). Experimental Analysis of Hydrodynamics in a Radially Agitated Tank. AIChE Vol. 49, No.3

4. Li, M., White, G., Wilkinson, D., Kevin J. Roberts (2005). Scale up study of retreat curve impeller stirred tanks using LDA measurements and CFD simulation. Chemical Engineering Journal, 108, 81-90.

5. Harteveld, W.K., Mudde, R.F., Van den Akker, H.E.A. (2005). Estimation of turbulence power spectra for bubbly flows from Laser Doppler Anemometry signals. Chemical Engineering Science, 60, 6160-6168.

6. Akiti, O., Yeboah, A., Bai, G., Armenante, P.M. (2005). Hydrodynamic effects on mixing and competitive reactions in laboratory reactors. Chemical Engineering Science, 60, 2341-2354.

7. Kling, K., Mewes, D. (2004). Two-color laser induced fluorescence for the quantification of micro- and macro mixing in stirred vessels. Chemical Engineering Science, 59, 1523-1528.

8. Lamberto, D. J., Alvarez, M.M., Muzzio, F.J. (1999). Experimental and computational investigation of the laminar flow structure in a stirred tank. Chemical Engineering Science, 54, 919-942.

9. Lamberto, D. J., Alvarez, M. M., Muzzio, F. J. (2001). Computational analysis of regular and chaotic mixing in a stirred tank reactor. Chemical Engineering Science, 56, 4887-4899.

10. Rivera, C., Heniche, M., Ascanio, G., Tanguy, P. (2004). A virtual finite element model for centered and eccentric mixer configurations. Computers and Chemical Engineering, 28, 2459-2468.

11. Brucato, A., Ciofalo, M., Grisafi, F. and Micale, G. (98). Numerical prediction of flow fields in baffled stirred vessels: A comparison of alternative modeling approaches. PII: S0009-2509, 00149-3.

12. Harris, C.K., Roekaerts, D., Rosendal, F.J.J., Buitendijk, F.G.J., Daskopoulos, Ph. Vreenegoor, A.J.N. and Wang, H. (1996). Computational Fluid Dynamics for Chemical Reactor Engineering. S0009-2509, 00021-8.

13. Liang, K., White, G. and Wilkinson, D., Ford, L.J., and Roberts, K.J., Wood, W.M.L. (2004). Examination of the Process Scale Dependence of L-Glutamic Acid Batch Crystallized from Supersaturated Aqueous Solutions in Relation to Reactor Hydrodynamics. Ind. Eng. Chem. Res. 43, 1227-1234.

14. Montante, G., Lee, K. C., Brucato, A., Yianneskis, M. (2001). Numerical simulations of the dependency of flow pattern on impeller clearance in stirred vessels. Chemical Engineering Science, 56, 3751-3770.

15. Montante, G., Lee, K.C., Brucato, A., Yianneskis, M. (2001). Experiments and predictions of the transition of the flow pattern with impeller clearance in stirred tanks. Computers and Chemical Engineering, 25, 729-735.

16. Ranade, V.V., (97). An efficient computational model for simulating flow in stirred vessels: a case of Rushton turbine. PII: S0009-2509, 00292-3.

17. Li, M., White, G. and Wilkinson, D. (2004). LDA Measurements and CFD Modeling of a Stirred Vessel with a Retreat Curve Impeller. Ind. Eng. Chem. Res. 43, 6534-6547.

18. Serra, A., Campolo, M., Soldati, A. (2001). Time-dependent finite-volume simulation of the turbulent flow in a free-surface CSTR. Chemical Engineering Science, 56, 2715-2720.